Synthesis of Sequence-defined Glycooligomers for Studying Multivalent Interactions

Inaugural-Dissertation
to obtain the academic degree
Doctor rerum naturalium (Dr. rer. nat.)

submitted to the Department of Biology, Chemistry and Pharmacy
of Freie Universität Berlin

by
Daniela Ponader

Berlin, January 2014

The work presented in this thesis was accomplished in a period between July 2010 and December 2013 in the Department of Biomolecular Systems at the Max Planck Institute of Colloids and Interfaces and Free University of Berlin, Institute of Chemistry and Biochemistry under supervision of Dr. Laura Hartmann.

Date of defense: 14.03.2014

1st Reviewer: Dr. Laura Hartmann

2nd Reviewer: Prof. Dr. Beate Koksch

Table of Contents

Summary

Synthetic glycomimetics such as glycopolymers or glycodendrimers are considered as powerful tool to investigate and modulate the biological functions of natural sugar ligands and receptors. They have shown great potential in various applications, such as in drug delivery, inhibition therapy or vaccination but also for fundamental investigations of the principle of multivalency. However, most synthetic glycomimetics are still limited in terms of molecular and structural precision. On the one hand this hampers direct structure-property correlation studies and a more detailed understanding of their mode of action. On the other hand this limits the ability of glycomimetics to perform the comparably advanced tasks of their natural counterparts. This thesis therefore presents a novel synthetic approach towards sequence-defined, monodisperse glycooligomers employing solid phase polymer synthesis and their use as precision glycomimetics.

Solid phase assembly has been developed and successfully used for the synthesis of biopolymers such as peptides or oligonucleotides. The principle is based on the stepwise assembly of functional building blocks on a solid support thereby allowing for the control of the overall chain length as well as the positioning of building blocks within the chain. Recently this approach has also been applied for the synthesis of synthetic polymers and in this thesis will be further developed towards the synthesis of synthetic glycooligo- and polymers.

Therefore, in a first step, two sets of functional building blocks were introduced: First, a functional building block carrying an alkyne side chain allowing for the conjugation with sugar ligands via CuAAC reaction was designed. Secondly, spacer building blocks were synthesized enabling the incorporation of a desired distance between the sugar moieties and modulate polymer backbone properties such as hydrophobicity and flexibility (see Figure 1 a).

The building blocks developed in this thesis were then applied for solid phase synthesis of a) homomultivalent glycooligomers b) heteromultivalent glycooligomers, and c) photoswitchable glycooligomers with tunable backbone properties (see Figure 1 b). Homomultivalent glycooligomers were synthesized by simultaneous conjugation of the same type of sugar ligand after backbone assembly. Heteromultivalent glycooligomers were generated by a sequential coupling-conjugation protocol during backbone assembly. Photoswitchable glycooligomers were synthesized by using the synthetic approach of homomultivalent structures but using a different spacer building block.

A library of glycooligomers was synthesized varying specific parameters known to influence multivalent binding: Number and spacing of sugar ligands was varied for ten homomultivalent structures. Five heteromultivalent glycooligomers presenting combinations of mannose together

with galactose or glucose ligands displaying heterogeneity of sugar ligands were obtained. A change in backbone properties and spacing of sugar ligands was achieved by four photoswitchable structures incorporating a hydrophobic, stiff, azobenzene-moiety containing spacer in contrast to an ethyleneglycol based flexible, hydrophilic spacer used for the homo- and heteromultivalent glycooligomers.
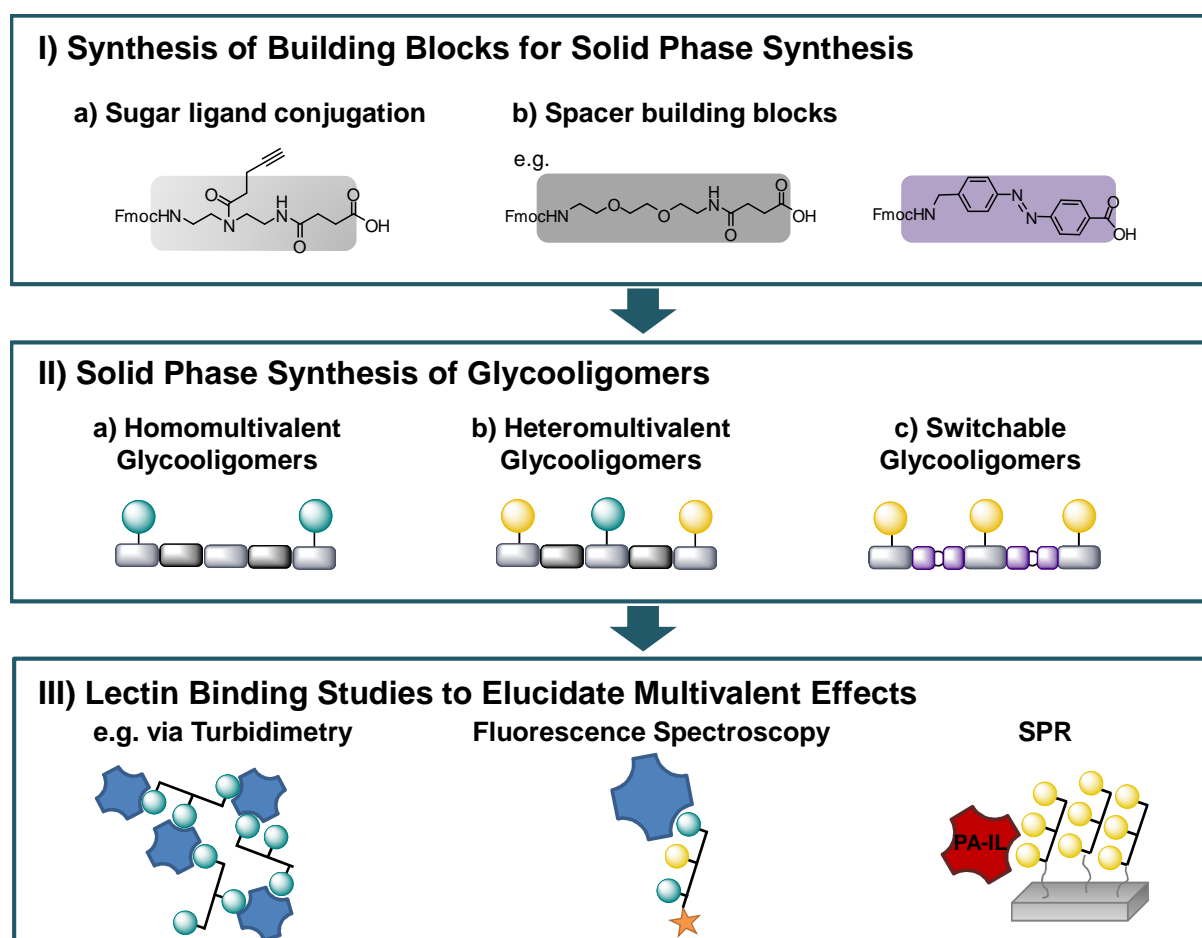
Figure 1: Schematic representation of the synthetic approach used in this thesis. After synthesis of functional building blocks (I), they are coupled on solid phase and conjugated to sugar ligands (II). The resulting library of sequence-defined, monodisperse glycooligomers is used for fundamental lectin binding studies using different binding assays to elucidate multivalent binding modes (III).

With this novel set of precision glycomimetics, fundamental investigations on multivalent ligand-receptor interactions were performed. Different binding assays were employed to study specific effects of multivalent binding (see Figure 1 c) towards sugar-recognizing lectin receptors Con A and PA-IL.

For homomultivalent glycooligomers, an increasing number of mannose ligands led to increased binding affinity to Con A determined by inhibition/competition assays. This was attributed to statistical rebinding. Interestingly, there is no linear correlation between an increasing number of binding ligands and the resulting binding affinity, indicating additional effects contributing to the binding of glycomimetics. A chelate effect could not be directly shown for any of the homomultivalent structures. The most efficient binder is a pentameric oligomer presenting three carbohydrate moieties, thus a rather small molecule with a low number of binding ligands in comparison to known polymeric glycomimetics presenting a similar affinity. Correlation fluorescence spectroscopy experiments showed that this structure is able to bind more than one Con A receptor leading to cluster formation which is positively contributing to the overall binding affinity.

Heteromultivalent structures presenting a combination of binding ligands (mannose) with less or non-binding ligands (glucose/galactose) showed surprisingly high binding affinities in inhibition/competition assay towards Con A. Similar binding affinities as measured for comparable structures presenting only binding ligands were measured, although less mannose units were present on the heteromultivalent glycooligomer. This binding enhancement could be attributed to a steric shielding of the non-binding sugar ligands preventing competitors from binding. This finding was supported by STD-NMR studies confirming a participation in binding of only the mannose ligands. Correlation fluorescence spectroscopy showed that heteromultivalent structures are not capable of cluster formation and thus their affinity can be mainly attributed to statistical and sterical effects.

In the third part of lectin binding studies, the previously employed hydrophilic spacer building blocks were exchanged towards stiffer and more hydrophobic AZO spacers. Latter can additionally be used to induce a conformational change of the oligomer backbone resulting in a changed spatial orientation of sugar ligands. Inhibition/competition assays measuring the affinity of galactose functionalized oligomers against PA-IL lectin receptor comparing directly between hydrophilic or AZO spaced oligomers showed that binding is enhanced for the flexible, hydrophilic spaced oligomers. This can be attributed to an entropic gain upon complex formation by the release of bound water from both, the ligand as well as the receptor. Inhibition/competition assay performed with both cis- and trans-isomers of glycooligomers showed enhanced binding of the trans configuration. Latter is attributed to a longer, more stretched backbone presenting the sugar ligands in a more accessible manner. Binding enhancement of trans-glycooligomers were even more pronounced in an additional surface based binding assay presenting the AZO-glycooligomers bound to a chip surface.

Overall, a straightforward synthetic approach towards highly defined glycooligomers was developed in this thesis based on the introduction of novel tailor-made building blocks and their assembly on solid phase. The obtained precision glycooligomers show a great potential as tool for fundamental studies on multivalency and to be applied as glycomimetics in biomedicine *e.g.* for targeted drug delivery or as bacterial anti-adhesins.

Zusammenfassung

Synthetische Glykomimetika, wie z.B. Glykopolymere oder Glykodendrimere, sind wichtige Modellsysteme, um die biologische Funktionsweise natürlicher Zuckerliganden und Rezeptoren zu verstehen und auch zu kontrollieren. Daher werden Glykomimetika bereits in verschiedenen Anwendungen eingesetzt, wie z.B. dem gerichteten Wirkstofftransport, als antibakterielle Wirkstoffe oder zur Entwicklung neuer Impfstoffe. In der Grundlagenforschung dienen Glykomimetika darüber hinaus zur Untersuchung der Multivalenz von Ligand-Rezeptor-Wechselwirkungen. Die bisherigen Glykomimetika haben aber auch eine wichtige Limitierung: es gibt kaum multivalente Glykomimetika, die sowohl strukturell definiert als auch mit struktureller Variabilität hergestellt werden können. Zum einen schränkt dies die Möglichkeit einer direkten Struktur-Wirkungsbeziehung ein und somit den Zugang zu einem genaueren Verständnis ihrer Wirkungsweise. Zum anderen sind aufgrund dieser Einschränkungen Glykomimetika bisher nicht geeignet, die komplexe Funktionsweise ihrer natürlichen Vorbilder vollständig nachzubilden und somit die nächste Generation der Glykomimetika zu entwickeln.

Diese Arbeit beschäftigte sich daher mit einem neuen Ansatz zur Synthese von sequenzdefinierten, monodispersen Glykooligomeren mit Hilfe der Festphasen-Polymersynthese sowie der Untersuchung der erhaltenen Makromoleküle als neuartige Glykomimetika.

Die Festphasensynthese wird bereits erfolgreich zur Synthese hochdefinierter Biopolymere wie den Peptiden und Oligonukleotiden eingesetzt. Das Prinzip basiert auf der schrittweisen Kupplung geeigneter Bausteine an einer Festphase. Durch die Kontrolle der einzelnen Additionsschritte werden so monodisperse Ketten erhalten und durch die Wahl der Bausteine die Positionierung funktioneller Gruppen in der Kette möglich. Dieses Prinzip wurde ebenfalls bereits für die Synthese monodisperser, sequenzdefinierter synthetischer Polymere angewandt und wird in dieser Arbeit nun für die Synthese von Glykooligomeren weiterentwickelt.

Im ersten Schritt wurden daher zunächst geeignete funktionelle Bausteine hergestellt: Zum einen wurde ein Baustein mit Alkinseitenkette entwickelt, der die Anbindung von Zuckerliganden mithilfe der CuAAC Reaktion ermöglicht. Zum anderen wurden *Spacer*-Bausteine hergestellt, die sowohl den Abstand der Zuckerliganden entlang der Kette kontrollieren als auch die Eigenschaften des Oligomerrückgrats, etwa Hydrophobizität und Flexibilität, beeinflussen (siehe Abbildung 1a).

Diese neu entwickelten Bausteine wurden dann in der Festphasensynthese eingesetzt zur Herstellung von a) homomultivalenten Glykooligomeren, b) heteromultivalenten Glykooligomeren und c) fotoschaltbaren Glykooligomeren mit veränderbaren Eigenschaften des Oligomerrückgrats (siehe Abbildung 1b).

Homomultivalente Glykooligomere wurden mithilfe einer simultanen Anbringung des gleichen Zuckerliganden im Anschluss an den Aufbau der Oligomerkette hergestellt. Heteromultivalente Glykooligomere wurden durch einen sequentiellen Kupplungs-Konjugations-Ansatz während der Festphasensynthese erzeugt. Fotoschaltbare Glykooligomere wurden durch den gleichen synthetischen Ansatz wie die homomultivalenten Glykooligomere hergestellt, aber unter Benutzung eines anderen Spacer-Bausteins.

Mit Hilfe dieser Syntheseplattform wurde dann eine Bibliothek von Glykooligomeren erzeugt und spezifische strukturelle Parameter variiert, von denen bekannt ist, dass sie multivalente Bindungen beeinflussen: Anzahl und Abstand der Zuckerliganden wurden bei zehn homomultivalenten Strukturen verändert. Fünf verschiedene heteromultivalente Glykooligomere präsentieren Kombinationen aus bindenden (Mannose) und nicht- bzw. schwächer bindenden Liganden (Galaktose- oder Glukoseliganden). Eine Veränderung der strukturellen Eigenschaften des Oligomerrückgrats und Abstand der Zuckerliganden wurde bei vier verschiedenen fotoschaltbaren Strukturen erzeugt durch den Einbau von hydrophoben, steifen AZO-Bausteinen anstelle der zuvor exklusiv verwendeten flexiblen, hydrophilen Ethylenglykol-Spacern.

Mit dieser ersten Bibliothek hoch-definierter Glykomimetika wurden dann Studien zur multivalenten Ligand-Rezeptor-Wechselwirkung durchgeführt. Hierzu wurden verschiedene Bindungsassays benutzt, um so spezifische Effekte multivalenter Bindung an Con A und PA-IL Lektinen zu erforschen (siehe Abbildung 1c).

Bei homomultivalenten Glykooligomeren führte eine Vermehrung der Anzahl an Mannoseliganden zu einer erhöhten Affinität gegenüber Con A, was mit Hilfe von Inhibitions-/Kompetitionsstudien nachgewiesen wurde. Dies wurde auf den multivalenten Effekt der statischen Rückbindung zurückgeführt. Interessanterweise gab es keine *lineare* Korrelation zwischen erhöhter Anzahl der Liganden und erhaltener Bindungsaffinität, was darauf hinweist, dass es zusätzliche Effekte gibt, die bei der Bindung von Glykomimetika eine Rolle spielen. Ein multivalenter Chelateffekt der homomultivalenten Strukturen konnte nicht direkt nachgewiesen werden. Der effizienteste Binder ist ein Pentamer mit drei Zuckereinheiten; also ein vergleichsweise kleines Molekül mit einer geringen Anzahl bindender Liganden im Vergleich zu literaturbekannten makromolekularen Glykomimetika mit ähnlicher Affinität. Mit Hilfe der Fluoreszenz-Korrelations-Spektroskopie wurde festgestellt, dass dieses Pentamer in der Lage ist, mehr als einen Con A Rezeptor zu binden. Diese intermolekulare Komplex- oder Clusterbildung von zwei Rezeptor Molekülen an einem Glykooligomer trägt somit positiv zur Bindungsaffinität bei.
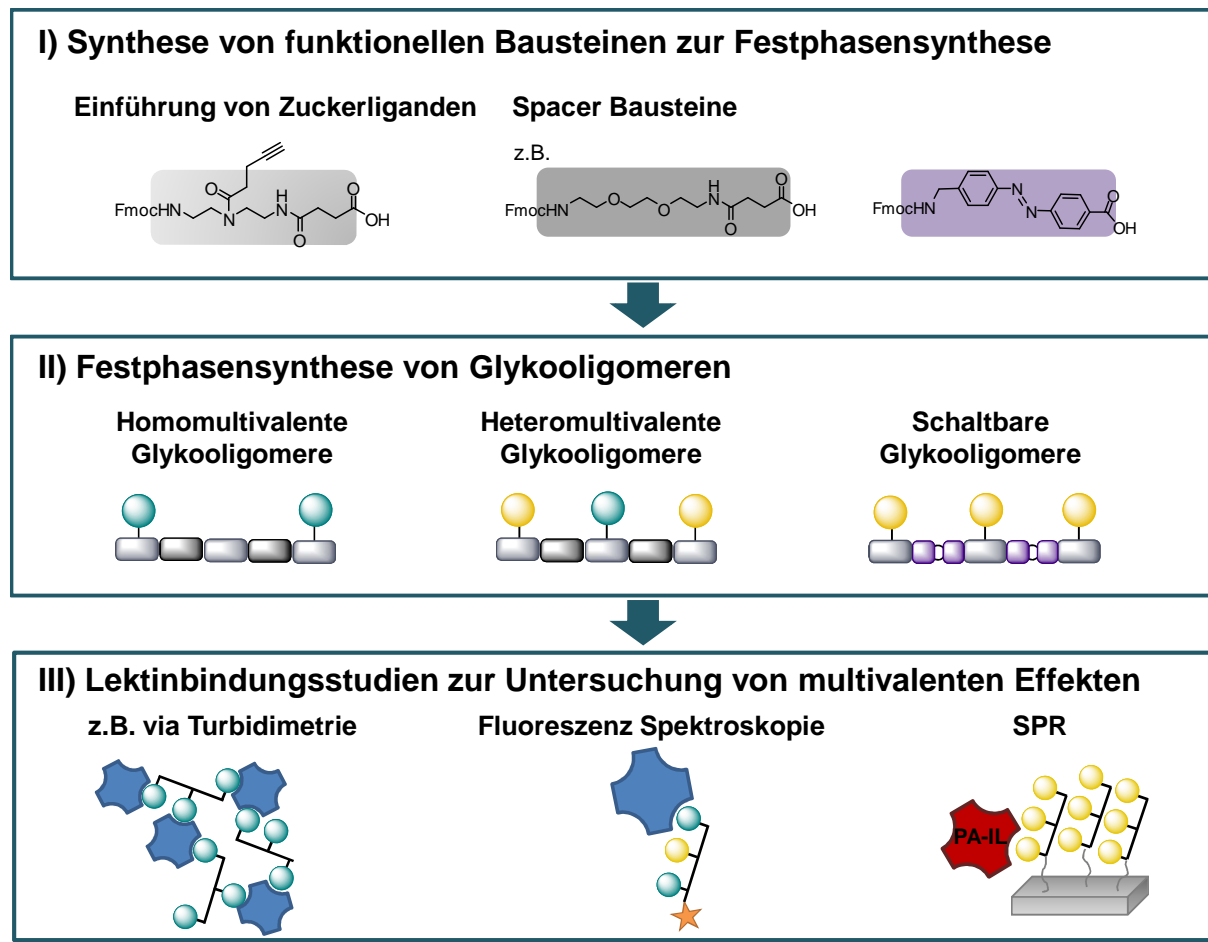
Abbildung 1: Schema des synthetischen Ansatzes dieser Arbeit: I) Zunächst wurden in Lösung funktionelle Bausteine hergestellt. II) Diese wurden dann an der Festphase gekuppelt und mit Zuckerliganden konjugiert. III) Es wurde eine Bibliothek aus sequenz-definierten, monodispersen Glykooligomeren hergestellt welche zur Studie von multivalenten Ligand-Rezeptor-Wechselwirkungen benutzt wurde. Um die verschiedenen Bindungsmodi aufzuklären wurden verschiedene Bindungsassays benutzt.

Heteromultivalente Glykooligomere mit einer Kombination aus bindenden (Mannose) und schwach bzw. nicht-bindenden Zuckerliganden (Glukose/Galaktose) zeigten überraschend hohe Bindungsaffinitäten zu Con A in Inhibitions-/Kompetitionsstudien. Ähnlich hohe Affinitäten, wie bei vergleichbaren Studien mit reinen Mannose-Oligomeren, wurden gemessen, obwohl insgesamt weniger bindende Liganden auf dem heteromultivalenten Glykooligomer präsentiert wurden. Diese Erhöhung in der Bindungsaffinität wurde auf eine sterische Abschirmung der nichtbindenden Zucker zurückgeführt und somit eine verringerte Kompetition anderer Liganden um die gleiche Bindungsstelle. Dieses Ergebnis wurde ebenfalls durch STD-NMR Studien bestätigt und zeigte, dass nur die bindenden Mannose Liganden an der Komplexbildung teilnehmen. Mit Hilfe der Fluoreszenz-Korrelations-Spektroskopie konnte zudem gezeigt werden, dass heteromultivalente Strukturen keine Cluster ausbilden können und deshalb die Affinitätserhöhung vor allem auf statistische und sterische Effekte zurückzuführen ist.

Im dritten Teil der Lektinbindungsstudien wurde der bisher eingesetzte hydrophile Spacer-Baustein ausgetauscht gegen einen steiferen, hydrophoberen AZO-Baustein. Dieser kann zusätzlich dazu benutzt werden, eine Konformationsänderung des Oligomer Rückgrats durch Lichteinstrahlung herbeizuführen und so die räumliche Anordnung der Zuckerliganden ändern. Mit Hilfe von Inhibitions-/Kompetitionsstudien wurde die Affinität der fotoschaltbaren Galaktose-Oligomere an PA-IL Rezeptoren gemessen und direkt zwischen hydrophilen und AZO-Oligomeren verglichen. Hierbei zeigten die flexibleren hydrophilen Oligomere eine erhöhte Affinität im Vergleich zu den fotoschaltbaren Strukturen. Dies wird auf die Freisetzung von Wassermolekülen bei der Bindung zwischen Ligand und Rezeptor zurückgeführt, was zu einer Erhöhung der Entropie und somit einer Erhöhung der Affinität führt. Darüber hinaus wurden Inhibitions-/Kompetitionsstudien mit den cis und trans Isomeren der fotoschaltbaren Glykooligomere durchgeführt und eine erhöhte Affinität der trans-Konfiguration gezeigt. Dies wird auf die bessere Zugänglichkeit der Zuckerliganden in der längeren, gestreckteren Konfiguration zurückgeführt. Diese Bindungserhöhung war noch deutlicher in einem zusätzlichen, oberflächenbasierten Affinitätsassay, bei dem die AZO-Glykooligomere auf die Oberfläche gebunden waren.

Zusammenfassend wurde in dieser Arbeit ein neuer Ansatz zur Herstellung von hoch-definierten Glykooligomeren mit Hilfe maßgeschneiderter Bausteine und deren Festphasenkupplung entwickelt. Diese erhaltenen Glykooligomere wurden auf ihre Eignung als Glykomimetika getestet und zeigen ein großes Potenzial zum einen als Modellsysteme für die Erforschung von Multivalenzeffekten und zum anderen für die Biomedizin.

1. General Introduction

1.1. Sugar Ligands and Lectin Receptors

Carbohydrates along with peptides/proteins and DNA represent one of the three major classes of biopolymers. Basic structural features of carbohydrates were discovered by Emil Fischer in the late 19th century. Later, the function of carbohydrates was mostly determined as storage and energy supply. It was not until 1988 when glycobiology, a term created by Dwek et al.[1], became a major research topic combining carbohydrate chemistry and biochemistry. Glycobiology deals with the function of sugars in biological systems. Carbohydrate structures are mostly part of glycoproteins and glycolipids. They are essential for numerous biological processes such as inflammation and immune response, viral and bacterial infection or fertilization.[2]
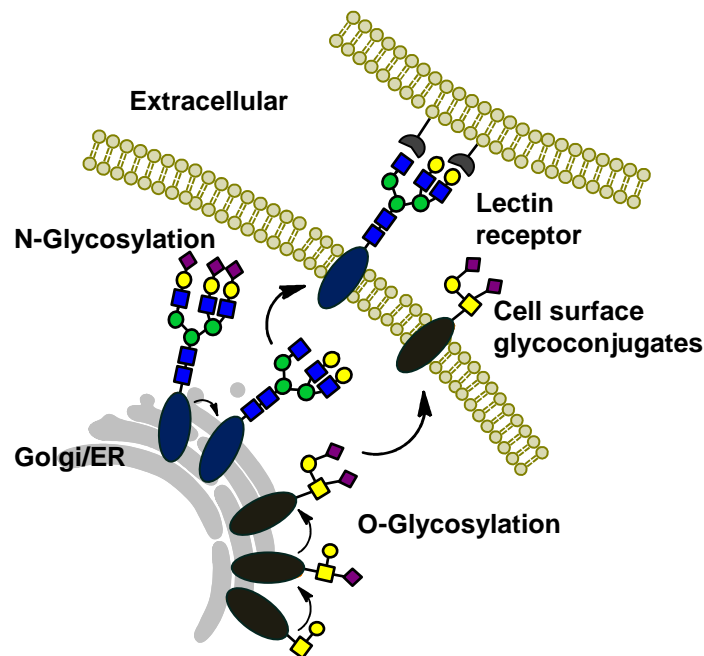

Figure 2: Schematic representation of glycoproteins and -lipids in the cell membrane. (Adapted from [3])

Glycosylation

Glycoproteins are synthesized by attachment of carbohydrates to the protein in a posttranslational modification.[4,5] Conjugation of sugars to proteins occurs with a known total of 13 different monosaccharide structures and 8 amino acids. [6] The two most common linkages between protein and carbohydrates are N- and O-glycosylation. O-linked oligosaccharides are linked to the hydroxyl group of serine or threonine via N-acetyl-galactosamine (GalNac) or (in collagens) to the hydroxyl group of hydroxylysine via galactose. They are generally short, often

containing only one to four sugar residues. O-linked oligosaccharides are formed by the sequential addition of sugars in the endoplasmatic reticulum and Golgi apparatus.[7]

In all N-linked oligosaccharides, N-acetylglucosamine (GlcNAc) is bound to the amide nitrogen of asparagine. Formation of N-linked oligosaccharides begins with the assembly of an ubiquitous 14-sugar residue, $Glc_3Man_9(GlcNAc)_2$. Enzymes localized in the endoplasmatic reticulum or Golgi cisternae remove or add sugar residues to the high-mannose precursor yielding a final N-linked oligosaccharide. Differences in processing different proteins, as well as in different cell types and species, produce N-linked oligosaccharides with a large variety of structures.[7]

Among many other functions, glycoproteins and glycolipids are part of the cell membrane, whose hydrophilic part –the sugar moiety-, points out of the cell surface. (see Figure 2). The oligosaccharide presenting cell surface serves as docking site for carbohydrate specific recognition proteins, the so called lectins, which interact with sugars through carbohydrate specific recognition domains. The term 'lectin' refers to the Latin word meaning 'to pick out'. This group of proteins is devoid of any catalytic, enzyme-like activities and antibody-like roles.[8]

Classification of Lectins

Lectins are classified regarding the monosaccharide to which they exhibit the highest affinity. Despite numerous naturally occurring sugars, only six, namely N-acetyl-neuraminic acid (a sialic acid), N-acetyl-glucosamine, N-acetyl-galactosamine, fucose, galactose and mannose, are typical constituents of surfaces of eukaryotic cells. However, despite their classification concerning monosaccharides, oligosaccharides are their natural ligands exhibiting much higher binding affinities (association constants 1000-fold higher compared to monosaccharide).[9] Lectins are found in most organisms, ranging from viruses and bacteria to plants and animals each dividing into several subgroups which will be discussed in the following:[9]
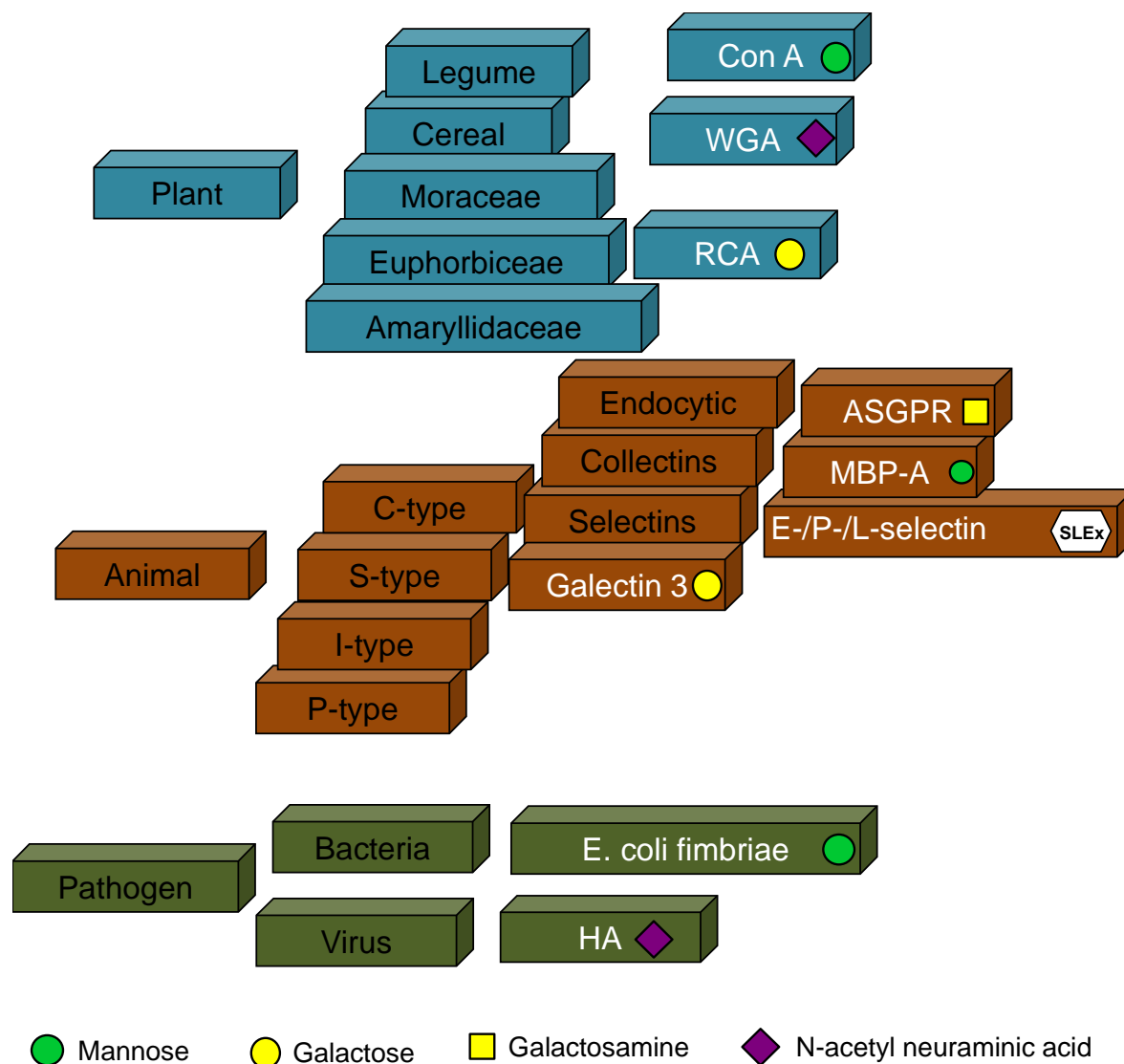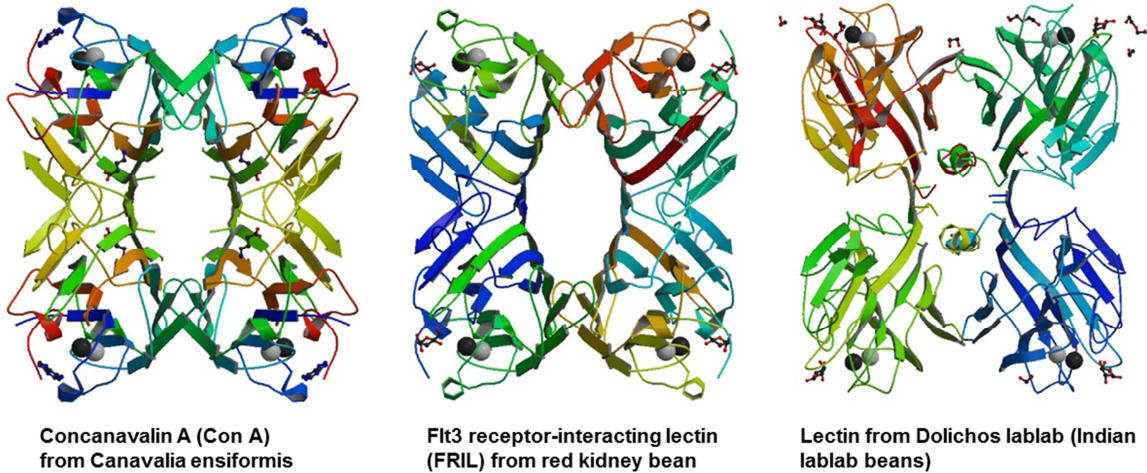
Figure 3: Overview of the three main classes of lectins and their subclasses ordered by organism. Specific lectin examples, also mentioned in the main text, are written in white letters. Their main binding sugar is depicted by standardized symbols from glycobiology.[10]

Legume lectins form the major class of plant lectins. They all share a structural homology consisting of two or four identical subunits (di- or tetramers). Each is built up of app. 250 amino acids, often carrying one or two N-linked oligosaccharides, having a molecular weight of app-25-30 kDa. One subunit presents one carbohydrate binding pocket and two divalent cations (Ca^{2+} and a transition metal such as Mn^{2+}) required for carbohydrate binding.[11] The function of plant lectins is not yet fully understood. However, it is most likely that they act as defense agents.[12,13] One of the most prominent members of this lectin class is the mannose and glucose specific Concanavalin A (Con A), being the first isolated lectin in 1919 (from canavalia ensiformis, jack bean) and still today one of the most studied lectins.[9] Typical other examples are galactose specific ricinus communis agglutinin (RCA) and GlcNAc binding wheat germ

agglutinin (WGA).

Legume lectins

Concanavalin A (Con A)
from Canavalia ensiformis

Flt3 receptor-interacting lectin
(FRIL) from red kidney bean

Lectin from Dolichos lablab (Indian lablab beans)

Figure 4: Examples of different legume lectins demonstrating the high structural similarity of this class. (PDB codes 4I30, 1QMO and 3UJQ).

Animal lectins can be classified in P-, I- , S- and C- type lectins. The latter two are most abundant and important in mammalians and will be described further.

S-type lectins (Galectins) share the above described topology of legume lectins but consist of a different amino acid sequence. Galectins occur in mammals but not in plants. They are soluble and do not require metal ions for binding.[14,15] Furthermore they are galactoside specific lectins binding to lactose and N-acetyl-lactosamine.[15,16] Galectins are a large family of receptors with relatively broad specificity such as adhesion, cell growth and cell differentiation as well as diseases (e.g. galectin 1 is highly expressed in early embryos[17], galectin 3 is present on cancer cells.[18]).

C-type lectins are named for their requirement of Ca^{2+} for activity.[19] They often consist of one membrane embedded subunit (115-130 amino acids in total, 14 invariant, 18 highly conserved) presenting one carbohydrate binding site.[9] This class is divided into three families sharing a common overall architecture: Endocytic lectins, selectins and collectins.

C-type lectins
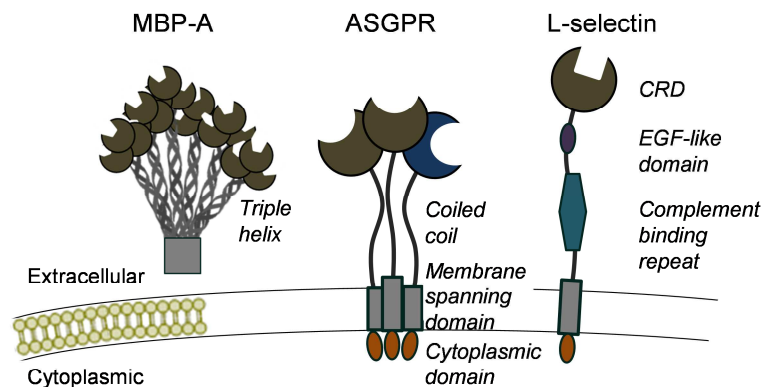
Figure 5: Schematic representation of examples for lectins belonging to the class of C-type lectins and their subclasses described here: collectins, endocytic lectins and selectins.(Adapted from [9])

A well-known example for endocytic lectins is the hepatic asialoglycoprotein receptor (ASGR) which was the first described mammalian lectin in 1971 [20–22] They are type II transmembrane proteins consisting of a terminal carbohydrate recognition domain (CRD) bound to a hydrophobic anchor in the membrane and a short domain in the cytoplasm. This subunit is often presented in bundles of two or three (see Figure 5).

The collectins family is made of soluble proteins composed of a CRD bound to a helical neck region, a number of collagen like repeats and a cysteine rich domain (see Figure 5). The best studied examples are mannose binding proteins (MBP). They circulate in the sera of mammals in tri- or hexameric units (650 kDa) being part of innate immune system. MBP bind to oligomannosides of infectious microorganisms (e.g. salmonella, listeria) activating the complement system which is followed by lysis of the pathogens.

The third family belonging to C-type lectins is the selectins. This group consists of E-, P and L-selectins, membrane bound proteins. [23–25] They mediate selective contacts between cells. Selectins consist of the CRD linked to an epidermal growth factor-like (EGF) domain, several short repeating units related to complement-binding protein, the membrane spanning region and the cytoplasmic domain (see Figure 5). Selectins bind specifically to sialyl Lewis x requiring fucose and sialic acid for binding. Latter can be replaced by another negatively charged group such as a sulfate.[9]

Selectins mediate the adhesion of circulating leukocytes to endothelial cells of blood vessels, a prerequisite for the exit of the former cells from the circulation and their migration into tissues. Thus they control leukocyte trafficking to sites of inflammation and the migration of

5

lymphocytes to specific lymphoid organs.[24,25]

The last class of lectins consists of viral and bacterial lectins. Viral and microbial lectins mediate the adhesion of the pathogens to the host cell being a prerequisite for infection.[26,27]
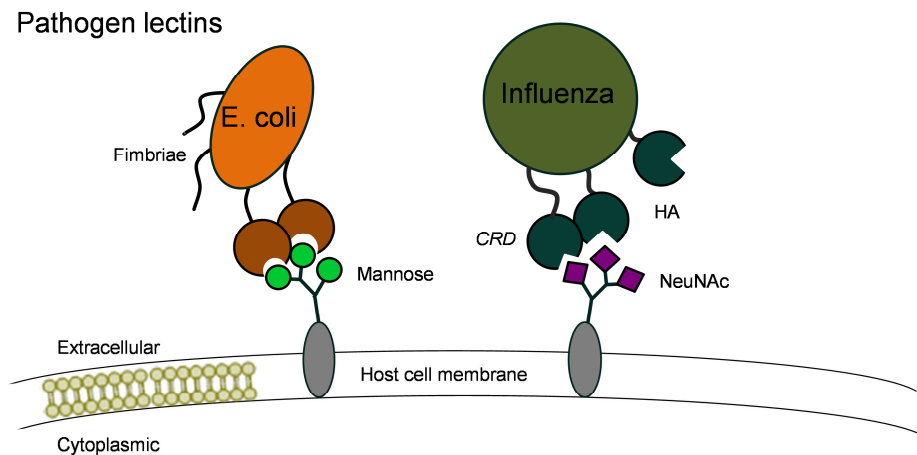
Figure 6: Schematic overview of pathogen lectins interacting with a cell surface.

The most studied examples are hemagglutinin, a N-acetyl-neuraminic acid specific lectin present on influenza viruses.[28,29] It consists of two disulfide bound peptides namely HA1 (36 kDA) and HA2 (26 kDa).

In bacteria, lectins are usually present part of the fimbriae, filamentous heteropolymeric organelles present on the surface of the bacteria. They are 3-7 nm in diameter and 100 to 200 nm in length, consisting of helically arranged subunits (pilins) of several different types, assembled in a well-defined order[27,30] (Figure 26). Only one of the subunits, usually a minor component of the fimbriae, possesses a carbohydrate combining site and is responsible for the binding activity and sugar specificity of the fimbriae, e.g. for mannose in E. coli bacteria.

Structural Basis of Lectin Recognition

The recognition between lectins and carbohydrates is based on several structural features (see Figure 7).[6,19]
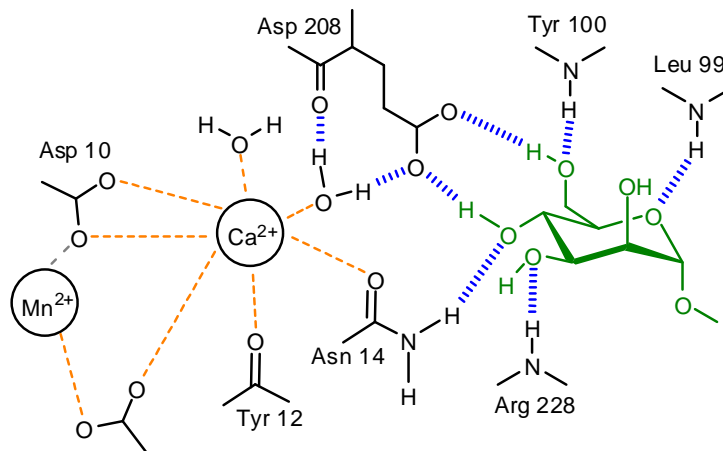
Figure 7: Binding interactions between α-methyl mannose and specific residues on Con A lectin. The carbohydrate is depicted in green, hydrogen bonds in blue and donor bonds to metal ions in orange. (Adapted from [9])

The most important recognition elements are hydrogen bonds between specific hydroxyl groups present on the sugar and amino acids in the lectin. In case of legume lectins, despite their carbohydrate specificity, three invariant amino acids are involved: aspartic acid, asparagine, an aromatic amino acid (e.g. Tyr) or leucin (see Figure 7). The carbohydrate OH- acts as hydrogen bond acceptor to acidic side chains and as donor to amide main chain moieties.

Despite of hydrogen bonding, the apolar carbon-containing hexose rings interacts with the aromatic side chain in so called nonpolar interactions.

Divalent cations, such as Ca^{2+} or Mn^{2+}, either stabilize the binding site or coordinate directly with two OH- groups of the carbohydrate.

1.2. Multivalent Carbohydrate Mimetics

The recognition and binding between lectins presenting multiple carbohydrate recognition sites and glycoproteins presenting (multiple) oligosaccharides, as described in the section above, is based on multivalent interactions. Investigation of the molecular basis of lectin-receptor binding is of high importance for the design and development of novel ligands for biomedical applications. One impeding factor for research is the limited access to isolate natural oligosaccharide structures. In order to overcome this limitation, synthetic oligosaccharide and glycoprotein mimetics have become an important tool for investigation of receptor-lectin binding. Improved accessibility of these structures compared to their natural analogues but also their capability of gaining higher or modulated affinity than using their corresponding natural ligands led to successful use of mimetic structures.[3,31] Since single carbohydrate-protein interactions are weak, multiple presentation of sugar ligands is a key factor for these structures to exploit and study multivalent binding effects.

Several multivalent binding effects have been recognized so far and will be presented in the following chapter. This is followed by a chapter presenting examples for synthetic glycomimetics used in lectin-binding studies.
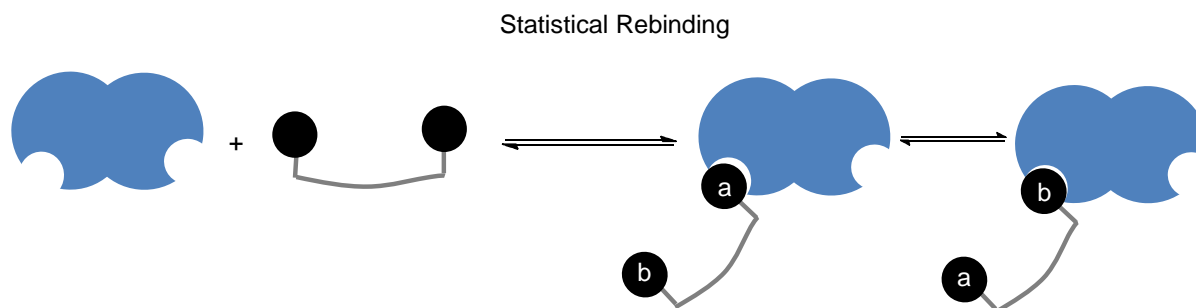
1.2.1. Multivalent Binding Effects

Multivalency is a fundamental principle underlying carbohydrate ligand-receptor interactions. Monovalent carbohydrates bind to protein receptors only weakly, showing association constants of about 10^3 M^{-1}.[9] By the display of multiple entities of sugars on one scaffold, multiple interactions with one or several receptor units are possible. Such multivalent effects are usually stronger than the corresponding monovalent interactions. By definition, a multivalent effect is observed when the measured binding value of a multivalent structure presenting x ligands is more than x times the binding of a monovalent analogue.[32] The binding enhancement can be caused by different effects occurring either simultaneously or independently depending on both the structure of the lectin and the multivalent ligand.[33] These multivalent binding effects will be described in detail in the following:
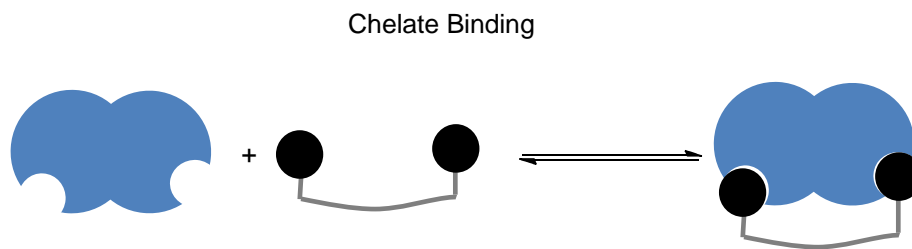
Chelate Binding

Figure 8: Schematic representation of chelate binding. A receptor with two binding sites is bound simultaneously by a multivalent structure presenting two ligands.

Chelate binding refers to the binding of at least two ligands, connected by a linker, over at least two binding sites of a receptor unit (see Figure 8). Binding is enhanced because translational and rotational entropic penalties were already brought up by the first binding event and need to be paid only once.[34,35] This effect was shown to strongly enhance binding activity in comparison to the monovalent binding of a single ligand from three up to five orders of magnitude.[31,36,37] Many studies examining this phenomenon were reported using divalent structures reaching activity gains up to 6000-fold compared to the monovalent reference structures.[36–40] The highest gain in affinity so far known is the inhibition of pentameric AB_5 toxins with star shaped polymers showing 10^6 affinity enhancements.[31] Chelate binding strongly depends on the nature of the linker connecting the multiple binding ligands. On the one hand, the distance between the presented binding ligands has to match exactly the distance between the binding pockets. [36,37] It has been shown that differences in structure as small as one ether bond led to a six-fold drop in affinity.[37] On the other hand, stiffness/flexibility influences the ability of the multivalent structure to adapt a suitable conformation that matches the distance between two binding sites. In general, flexible linkers, such as ethylene glycol, are considered to be advantageous.[41,42] However, also stiff linking units were shown to lead to dramatic potency enhancement when distancing between sugar ligands fit to the binding sites of the receptor.[36,43]

The second very widely recognized multivalent effect has been termed statistical rebinding.

Statistical Rebinding

Figure 9: Schematic representation of the multivalent effect of statistical rebinding.

Binding between a single carbohydrate ligand and protein receptor can be described as equilibrium between a bound and unbound state due to the weak binding affinity of a single unit (see Figure 9). By multivalent presentation of several ligands on one scaffold, a dynamic process between bound and unbound ligands occurs. In the event of release of a binding ligand, another ligand in proximity can take its place.[34,44] This also called bind-and-slide-effect[8,44] was shown to result in one to two orders (e.g. up to 200-fold described by Cloninger et al.[39]) of magnitude gain in affinity.[39]

The next multivalent effect to be discussed is intermolecular aggregation (see Figure 10).
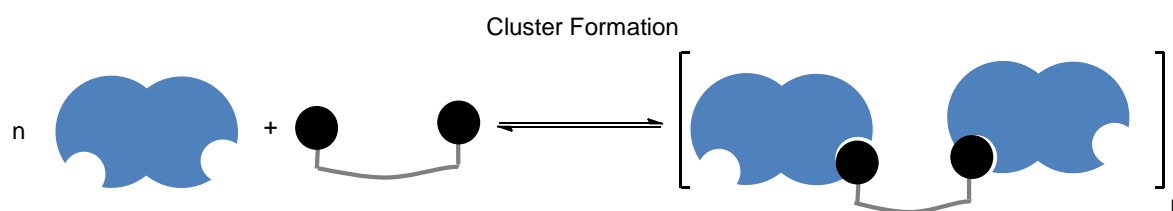
Figure 10: Schematic representation of the multivalent effect of cluster formation.

This process refers to the complexation of multiple *receptor* units to a multivalent structure. This effect can either occur in solution or on surfaces, e.g. cell surfaces, representing an important trigger for signal transduction.[45] Depending on the concentration of glycostructure as well as lectin, formation of soluble clusters or cross-linked lattices, being able to precipitate from solution, occurs. Intermolecular binding is energetically favored as it does not involve major contributions of linkers and scaffolds.[8,46,47] It is known that aggregation occurs in many multivalent structure binding events but the extent of enhancement of solemnly this effect has not been evaluated yet due to the difficult differentiation from other multivalent effects.[34]

Steric shielding refers to the role of non-binding ligands as part of multivalent structures preventing
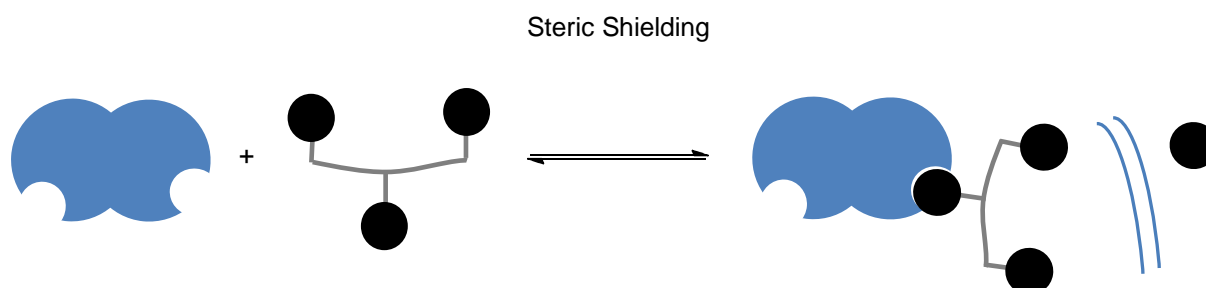
Figure 11: Schematic representation of the multivalent effect of steric shielding.

competing ligands from binding to the receptor (see Figure 11). This results in a stabilization of the ligand/receptor complex.[48,49] This effect has been observed by Whitesides et al. [87,88] (for detailed discussion see the next chapter 1.2.2). However, besides Whitesides' studies, no detailed investigation of this effect has been carried out so far.

Another important contribution in multivalent lectin-receptor binding is the involvement of water. Carbohydrates displaying several polar hydroxyl groups and polar group-abundant lectin binding sites are highly hydrated in aqueous environment. Thus, displacement of the water molecule becomes an important event during the complexation.[50] Water molecules from hydrated shells are released to the bulk which provides an increase in entropy.[51] In addition to that polar interactions mediated by hydrogen- bonding and van der Waals interactions result in favorable enthalpy changes.[52]

The last known effect influencing ligand-receptor binding is the so called subsite binding.

Recognition via an extended binding site was shown for some lectins[9]. Additional sugars of an oligosaccharide apart from the main binding sugar ligand interact with positions on the lectin adjacent to the binding site. One example is the extended binding site of Con A.[53,54] Naismith et al. recognized the natural trisaccharide Manα6-(Manα3)Man ligand binding not only to the recognition domain (formed by Tyr100, Leu99, Arg 228, Asn 14 and Asp 208, see Figure 7) but also to adjacent amino acids (Tyr 12, Thr 15, Asp 16). The resulting enhancement in binding has been termed subsite multivalency.[55]

In general, the described binding modes cannot be clearly differentiated for multivalent ligands but contribute simultaneously to the overall increase in affinity, e.g. by a combination of statistical effect and cluster formation. Thus, it is highly important to investigate and understand the interplay of the different binding modes in dependence of the chemical structure of the multivalent glycoligand and to potentially derive general design rules for the design of novel glycomimetics.

1.2.2.<u>Carbohydrate Presenting Scaffolds for Investigations on Multivalency</u>

Natural carbohydrate binding occurs between lectins and glycoproteins presenting *oligosaccharide* structures. The terminal sugar units of oligosaccharides represent the primary recognition ligands that undergo lectin binding. This implies that the internal portions of the glycoprotein and oligosaccharide might not be involved in binding and therefore can be replaced with scaffolds that do not interfere with the ligand–lectin binding.[8,56] Following this assumption, synthetic carbohydrate presenting scaffolds are used as oligosaccharide mimetics.

$Man_9GlcNAc_2$

Synthetic mannose presenting scaffold
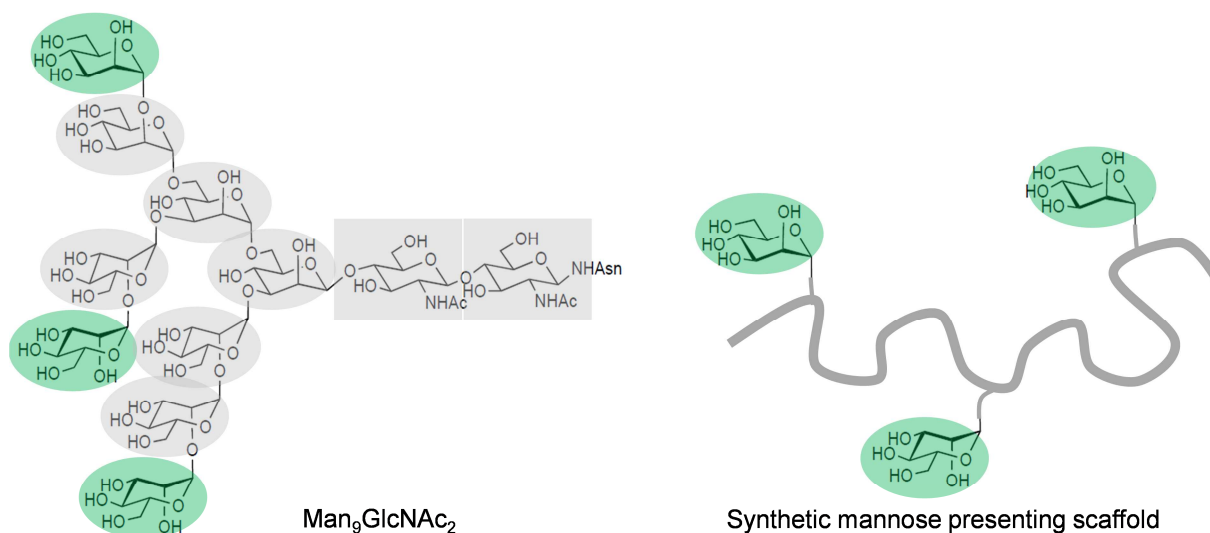
Figure 12: Resemblance between high mannose multiantennary glycan (Man9GlcNAc2Asn) and a synthetic carbohydrate presenting scaffold. (Adapted from [56]**)**

A plethora of different types of scaffolds presenting carbohydrate ligands were reported so far in literature including liposomes, micelles, vesicles, proteins, hard surfaces, cyclodextrins, calixarenes, nanoparticles, peptides, dendrimers and polymers.[8] The following chapter will focus on peptides, dendrimers and polymers due to their structural and synthetic similarity compared to the glycooligomers presented in this thesis.

Glycopeptides

Glycopeptides consist of amino-acid based backbones presenting sugar ligands in the side chain. They are synthesized by solid phase synthesis (SPS) leading to sequence-defined, monodisperse structures. Sugar ligands can either be introduced using glycosylated amino acids in SPS[57–59] or in a concerted functionalization step after assembly of the scaffold.[60,61] Typical conjugation of sugar moieties proceeds via functionalization of side chain amino acids (e.g. lysine, aspartic acid).[62] The introduction of non-natural amino acids with functional side chains for specific conjugations (e.g. azido-modified amino acid for click chemistry or Staudinger Ligation) has also been shown in many examples.[63,64] Regarding the shape of glycopeptides, they are often linear or cyclic. Additionally, it is possible to generate defined spatial orientations by using amino acids inducing typical secondary structure motifs such as helices or ß-sheets.[65]
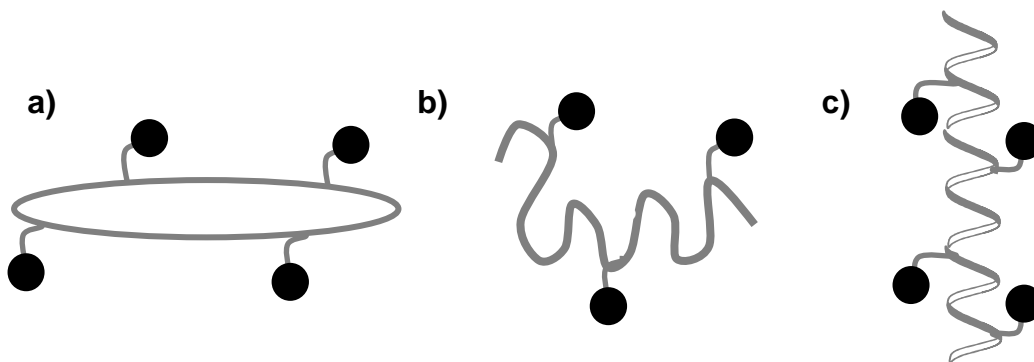
Figure 13: Schematic representation of typical structures of glycopeptides: a) presentation of sugar ligands on a cyclic scaffold, b) presentation of sugar ligands on a linear scaffold and c) presentation of sugar ligands on a helical scaffold.

Glycopeptides have been widely used as oligosaccharide mimetics in biological studies. Investigations of hepatic lectins by Lee at al. showed that such structures do not only present several ligands in a clustered manner but also vary the inter-sugar distances that are required to optimize the lectin binding efficiencies.[8,66].

Van Berkel et al. showed increasing affinity of mannose presenting lysine scaffolds towards human mannose binding receptor with increasing number of sugar ligands.[67] Peptide scaffolds presenting sialyl Lewis x were used in selectin binding studies. The study showed that not only multiple ligand presentation was required in order to achieve nanomolar inhibition potencies, but also optimal ligand densities were necessary.[68]

Dumy et al. synthesized cyclic peptides functionalized with four to 16 mannose units. Latter showed high binding affinities in nanomolar range of Con A potentially caused by multivalent

chelate binding.[69]

Toone et al carried out a systematic study regarding multivalent effects of trisaccharide presenting glycopeptides binding to Shiga like toxin binding subunit. They concluded that binding enhancement depended not only on carbohydrate presentation but also on the nature of the linkers and their interaction at the lectin binding sites.[70]

However one limitation of peptides as carbohydrate presenting scaffolds is their inherent potential toxicity and immunogenicity caused by the amino acid backbone which can be recognized by the mammalian immune system. In order to avoid this, biocompatible carbohydrate presenting structures are highly desired. One class of synthetic oligosaccharide mimetics fulfilling this requirement are the glycodendrimers.

Glycodendrimers

Glycodendrimer structures used for biological applications often consist of biocompatible materials such as poly(amidoamine) (PAMAM), polyglycerol (PG) or poly(propylene imine) (PPI). [56,71,72]
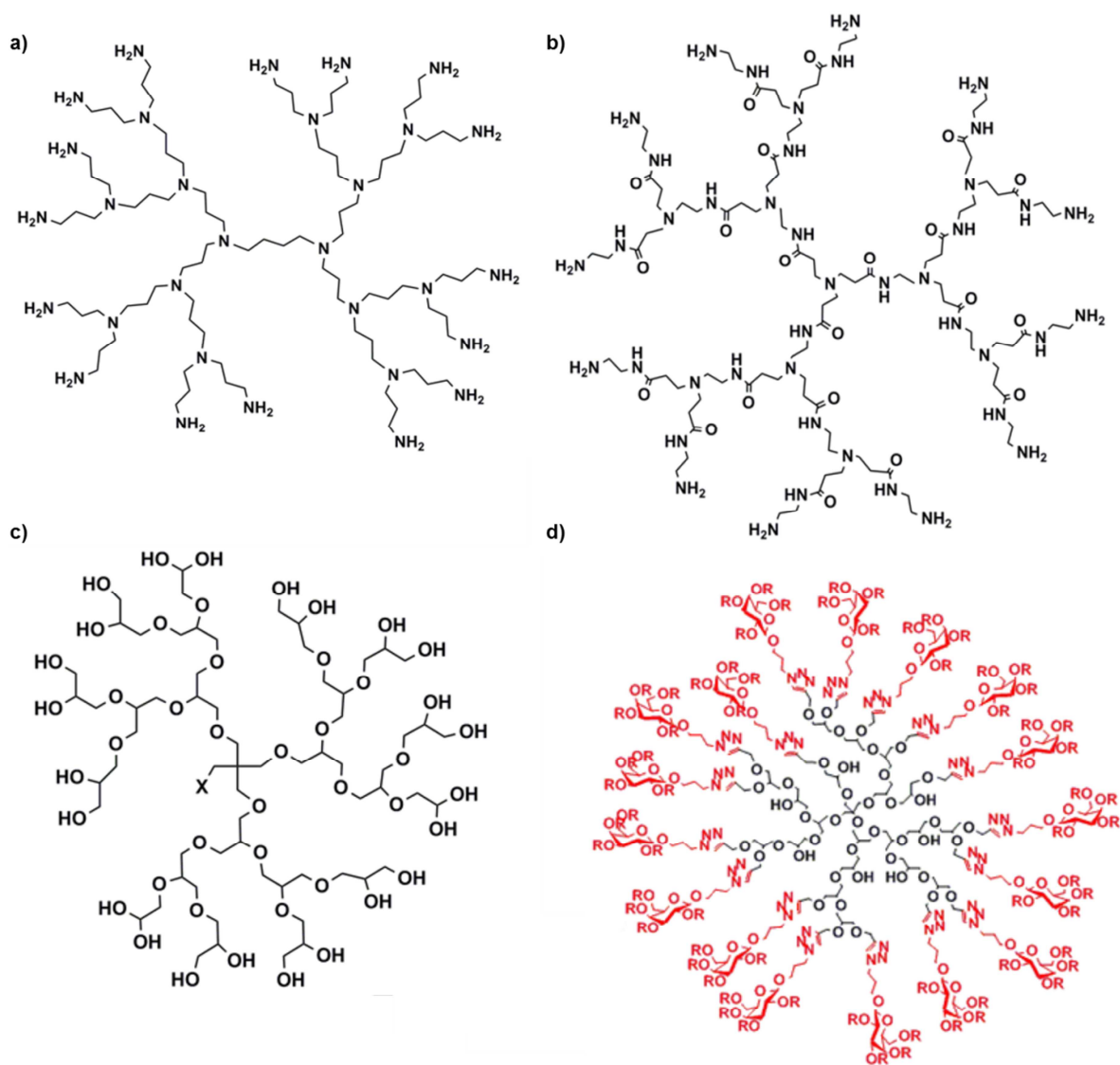
Figure 14: Typical structures of biocompatible dendrimers. a) poly(propylene imine) (PPI), b) poly(amidoamine) (PAMAM), polyglycerol (PG) and d) carbohydrate presenting polyglycerol dendrimer.

Glycodendrimers are monodisperse, tree-like molecules built in a generation-wise manner consisting of a series of branches emerging from a central core.[73] They can be synthesized either starting from the core and working out toward the periphery (divergent synthesis) or in a top-down approach starting from the outermost residues (convergent synthesis).[73] The size is

typically in the range of several nanometers.[56] In general, the carbohydrate ligands are found at the periphery of the macromolecules. Efficient conjugation reactions are required for complete substitutions such as amidation, use of thioureas or click chemistry.

Glycodendrimers have been widely studied in many biologically related applications such as selectin binding[74], hepatic lectin binding[75], inhibition of E. coli[76], etc. Glycodendrimers were also used in studies investigating specifically multivalent binding effects often using Con A as model lectin.

Many studies were carried out investigating dendrimers with a different *number* of mannose ligands. As described above for glycopeptides, binding affinity increases for structures with increasing number of presented sugar ligands. Interestingly, for dendrimers capable of presenting up to hundreds of carbohydrate moieties, a certain limitation in the number of ligands for efficient binding seems to exist. One example is a study carried out by Ashton et al who examined 3- to 36-valent mannosylated dendrimers. A nonavalent structure showed the best inhibition in ELLA.[77] A similar finding was observed by Roy et al. who reported tetra- to 32-valent PAMAM dendrimers with a nonavalent structure having the highest affinity.

In order to separate the relative contributions of chelation and statistical rebinding effects Cloninger et al studied monomeric and dimeric versions of Con A instead of the usual tetramer. It was shown that the statistical rebinding effect can be close to a factor of 200 for a dendrimer containing 172 end groups.[39]

Cluster formation was shown by Toone et al. with low valency (up to hexavalent) dendrimers.[46]

Also density of sugar ligands plays a role in multivalent binding. Tetra- to 178-valent PAMAM dendrimers yielded enhancements of up to 600-fold per sugar in a hemagglutination inhibition assay. The maximum effect was reached when only 50% of available linkage sites were functionalized with mannose.[78]

This example and the findings of Roy et al. and Ashton et al. imply that dendrimer structures might be not well accessible for efficient binding. This could be caused by the inherent globular shape of these structures. In order to overcome this, linear structures which can adapt their conformation to match to the binding sites of a lectin are desirable. One important example of such linear scaffolds are synthetic polymers.

Glycopolymers

Linear glycopolymers are synthetic macromolecules with sugar moieties as pendant groups.[79] These structures are either synthesized by polymerization of sugar units with polymerizable endgroups or by the postmodification of polymers with pendant functional groups. Latter was demonstrated, among others, with examples such as the Cu(I) catalyzed alkyne and azide 1,3-dipolar click cycloaddition (CuAAC), which uses azide containing carbohydrates to react to a polymer backbone[80] or thiol-ene click reaction, which utilizes polymers with pendant vinyl functionalities and glucothiose.[81] Modern polymerization techniques like RAFT (Reversible Addition–Fragmentation chain Transfer) or ATRP (Atom Transfer Radical Polymerization) and forms of ring opening polymerization (ROMP) are employed.[82] These techniques allow the control over the molecular weight, thus resulting in narrow molecular size distributions. Introduction of different saccharides is possible but only in a statistical or strongly alternating manner.[83]

Glycopolymers have been used as ligands for many biological applications: Kopecek et al reported the use of galactose-functionalized N-(2-hydroxypropyl)methacrylamide (HMPA) to successfully bind to hepatic lectin (ASGPR).[84] Poly(N-glycosyl 1,2,3-triazole) glycopolymers reported by Haddleton et al., were used to bind to DC-SIGN, a C-type lectin expressed on dendritic cells of the immune systems.[85,86]

In addition to that, also a plethora of studies especially focusing on multivalent binding modes have been carried out. Whitesides et al. studied inhibition of viral hemagglutinin binding to erythrocytes by poly(acrylamide) bearing sialosides. The effective inhibition was rationalized by an effect termed steric shielding. It describes a shielding of the influence virus between the non-binding carbohydrate moieties on the glycopolymer and the oligosaccharides present on the viral cells. This effect hinders the virus from binding to erythrocytes and consequently leads to increased binding of the glycopolymer to the virus.[87,88]

Davis et al. used poly(methacrylate) polymers functionalized with galactopyranoside for binding to peanut agglutinin. Thermodynamic studies showed that the affinity enhancements for its interaction with lectin were primarily due to cross-linked complex formation.[89] Kobayashi et al. compared binding of rigid helical poly(glycosyl phenyl isocyanide)s with flexible phenylacrylamide glycopolymers to Con A and RCA. The compatibility of orientation and spacing of clustering saccharide chains were found to be essential for specific molecular multivalent recognition by lectin.[90]

Kiessling et al. examined different linear mannose functionalized neoglycopolymers in binding to Con A and could show that there is a direct correlation between the number of active groups
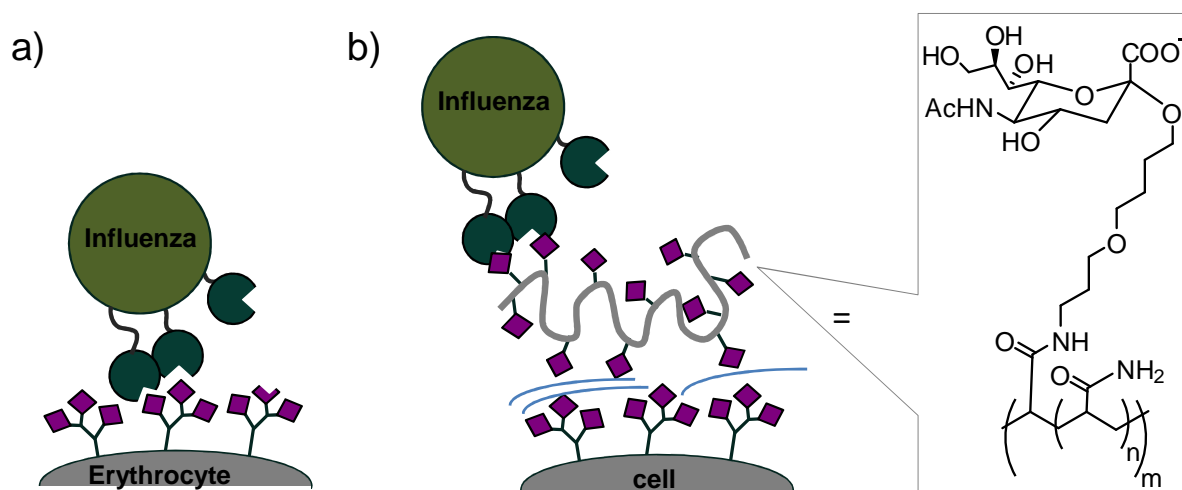
Figure 15: Schematic represention of a) binding of Hemagglutinin lectin present on influence virus to erythrocyte. b) Inhibition of binding by poly(acrylamide) bearing sialosides caused by steric shielding. (adapted from [87]**)**

per polymer molecule and the resulting binding affinity to a receptor.[45] This effect was attributed in part to chelation that is possible for the longer systems, along with statistical effects.

These are just a few examples from a large number of studies on glycopolymer synthesis and lectin-binding described in literature. In summary, the following factors are known to influence the binding of glycopolymers to lectin receptors: Number and distance of sugar ligands, density and accessibility as well as the nature of the linking moiety. Most studies report only their observation and variation of one single structural parameter. This might be due to the fact that for the literature-known systems variation of individual parameters is not possible or synthetically challenging (e.g. dendrimers always present a globular shape restricting the spatial presentation of carbohydrate ligands). Therefore a technique giving access to easily variable, monodisperse, biocompatible glycomimetics is highly desired and would further promote the fundamental understanding of multivalent interactions.

1.3. CuAAC Reaction

The introduction of functional groups such as sugar ligands to a macromolecular scaffold has to be effective and work with high yields. One important synthetic strategy for the introduction of saccharides to polymeric structures is the use of click reactions.[79,80,91]

The term click chemistry was introduced by Berry Sharpless in 2001. It stands for a set of powerful, highly reliable, and selective reactions which enable the rapid synthesis of new compounds through heteroatom links (C-X-C). By definition, such reactions have strong driving forces that ensure the reaction to be efficient, quick, reliable and without creation of unwanted by-products.[92]

The most potential and widely used click reaction is the copper catalyzed 1,3-dipolar cycloaddition of alkynes and azides yielding triazoles (CuAAC). Its non-catalyzed predecessor was introduced by Huisgen in 1957.[93] 1,3-dipole means a structure consisting of three atoms, **a-b-c**, in which **a** possesses an electron sextet and therefore is formally positively charged. Atom **c** has an unshared electron and is negatively charged. The dipole reacts with a dipolarophile, structures presenting double or triple bonds.[93]

Azides and alkynes are easy-to-introduce functionalities and do not require additional protecting groups in most reactions. Although they are among the most energetic species known, they are also among the least reactive functional groups. This stability has a kinetic origin and is responsible for the slow nature of the cycloaddition.[94] With a suitable catalyst, this low reaction rate can be improved. In 2002, Sharpless and Tornøe and Meldal independantly introduced a copper(I) catalyzed variant of this reaction with a $\sim 10^{-7}$-fold accelerated reaction rate.[63,95] Another advantage is the improved regioselectivity to form the 1,4-disubstituted triazole exclusively (see Figure 16), which was confirmed by NOE measurements and x-ray crystallography.[95]
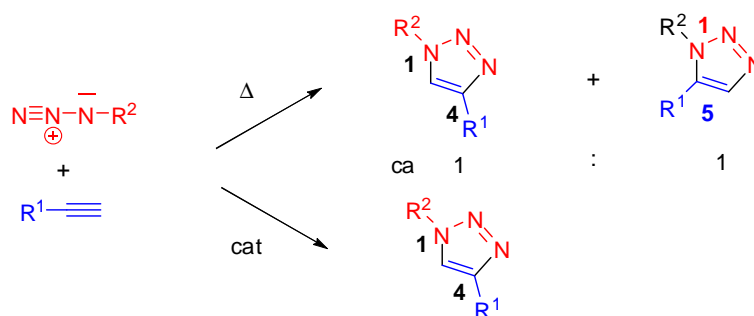

Figure 16: Regioselectivity of 1-3 dipolar azide alkyne reaction.(Adapted from [95])

The copper(I) catalyst can either be added from various copper(I) sources (CuI, CuOTf·C$_6$H$_6$, [Cu(NCCH$_3$)][PF$_6$]) or generated in situ by reduction of Cu(II) salts. The mostly employed redox system is Cu(II)SO$_4$ and ascorbate [94,96]. The reaction proceeds in a variety of solvents, including water, at pH values ranging from approximately 4 to 12, in 6 to 36 hours.[94]

Catalytic Mechanism and Triazole Properties

The catalytic mechanism of the CuAAC reaction has been subject to many studies in the past few years.[95,96] Recently, Fokin et al. proposed a revised catalytic cycle in which two copper atoms take part (Figure 17).[97]

The first step is the π–attraction of the alkyne triple bond to the copper metal. Then, a second copper atom is σ-bound to the acetylide accompanied by proton abstraction. This is followed by a reversible coordination of the organic azide. Nucleophilic attack at N-3 of the azide by the β-carbon of the acetylide forms the first covalent C-N bond. By release of one copper atom a triazole-copper heterocycle is formed. This is converted by reprotonation into the final product.[97]
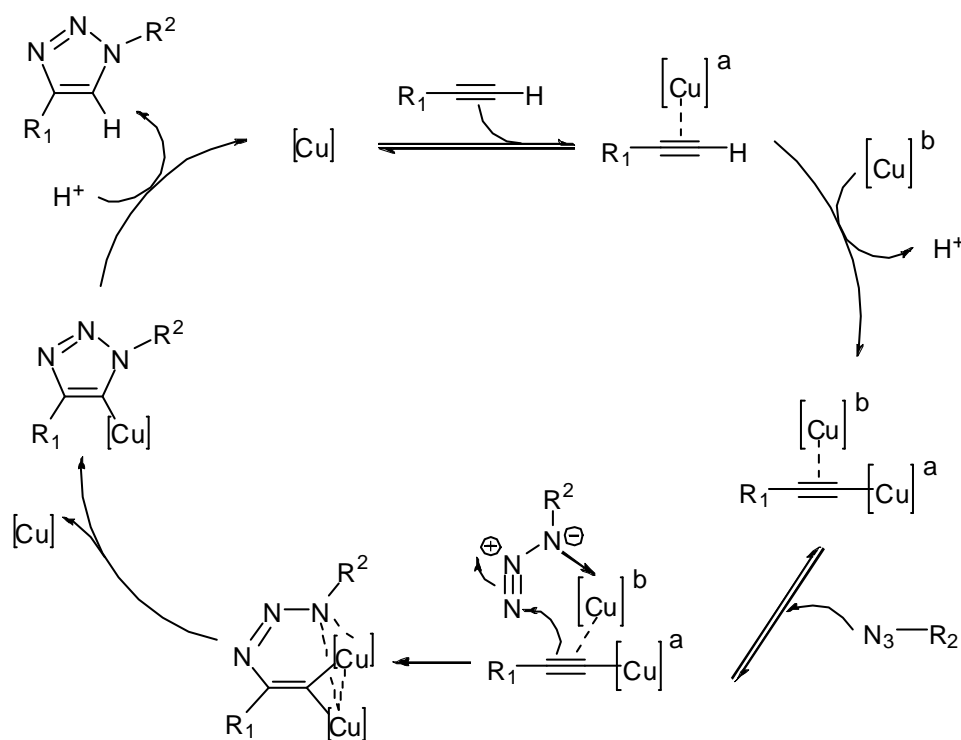
Figure 17: Catalytic mechanism of copper catalyzed azide alkyne reactions. (Adapted from [97])

Further interest in CuAAC reaction comes from the biological activity of 1,2,3-triazoles. These heterocycles function as rigid linking units that can mimic the atom placement and electronic properties of a peptide bond without the same susceptibility to hydrolytic cleavage.

R^1 to R^2 distance: 3.9 Å R^1 to R^2 distance: 5.0 Å
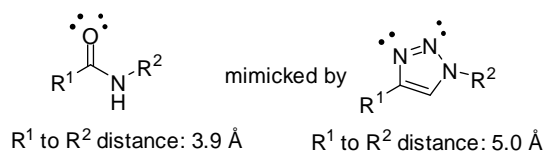
Figure 18: Similarities between amide bond and triazole.

In addition to the possibility of both, the N(2) and N(3) triazole atoms acting as hydrogen-bond acceptors, the strong dipole may polarize the C(5) proton to such a degree that it can function as a hydrogen-bond donor, similar to the amide proton. Partly due to their ability to mimic certain aspects of a peptide bond, many known 1,2,3-triazoles possess biological activity, including *anti*-HIV, *anti*-bacterial and *anti*-histamine activity.[98–100]

The Huisgen 1,3-dipolar cycloaddition reaction of organic azides and alkynes had a tremendous impact in recent years due to the introduction of Cu(I) catalysis leading to a major improvement in both, rate and regioselectivity. Many applications in biochemical synthesis, such as conjugations with biological materials like proteins, DNA, and viruses are known. Also in material science, the CuAAC reaction had an important impact. Examples are the synthesis of neoglycoconjugates, nanostructures or ligations in polymers. For further information the following reviews can be recommended. [94,101,102]

Due to the wide spread applications and reliability of the CuAAC reaction, it was chosen to be a key step in sugar ligand functionalization of the oligomer structures in this thesis.
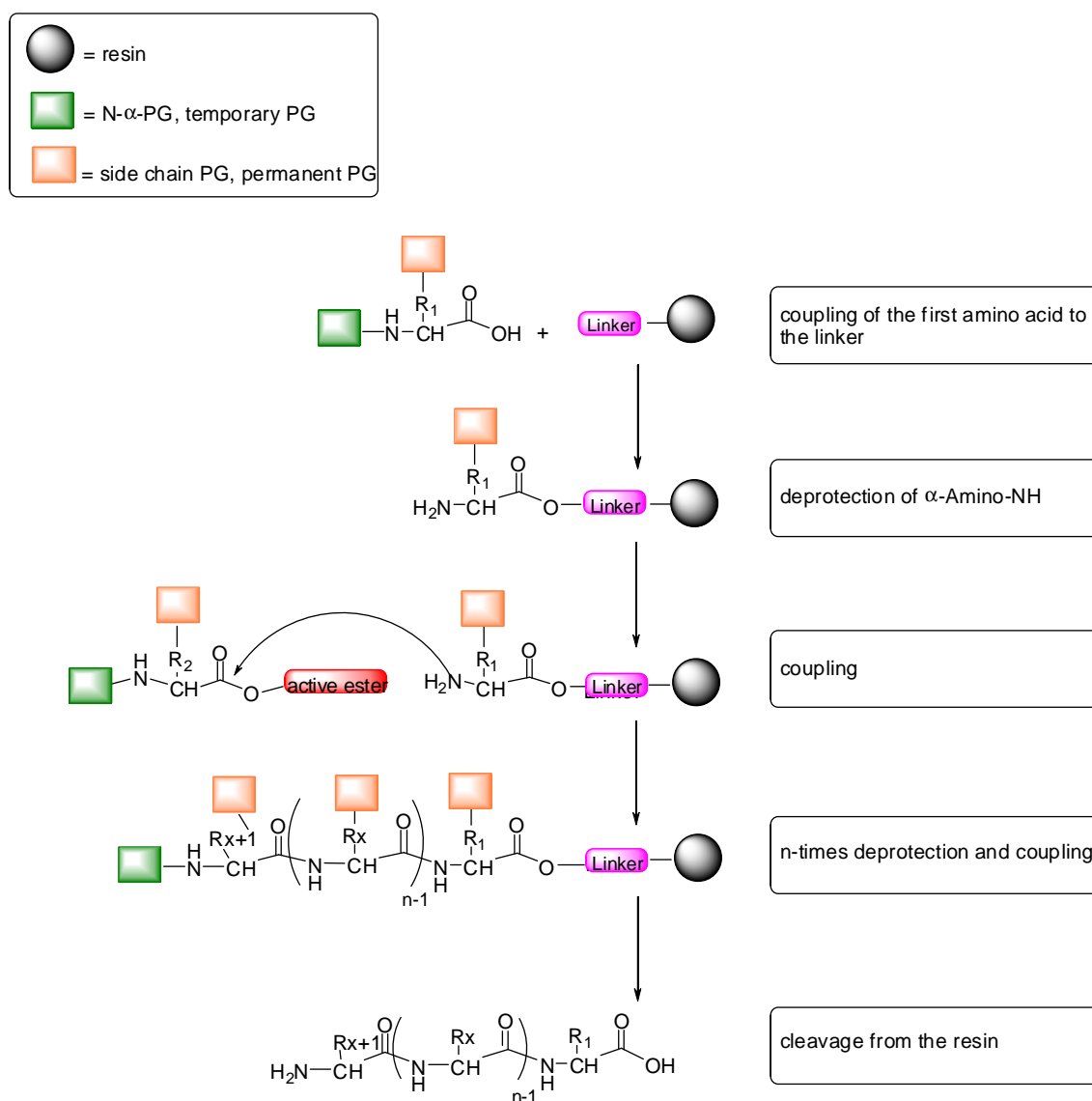
1.4. Solid Phase Synthesis

Origin and General Principle

Solid phase peptide synthesis (SPPS), developed by R.B. Merrifield in 1963 [103] is the first example for solid phase synthesis and presents the standard method for peptide synthesis today. It is based on the stepwise addition of α-amino- and side chain protected amino acids, in which the first amino acid is covalently bound to a polymer resin insoluble in the used solvent. After addition of the last amino acid to the desired peptide chain, the peptide can be cleaved off

the resin and isolated as a pure product ideally without the need for further purification. Before Merrifield's invention, peptides were synthesized in solution, which is only possible to a certain length, due to emerging problems with solubility and purification. One big advantage of solid phase synthesis is the possibility to use reagents in excess, to obtain quantitative reactions, followed by simple washing off the unreacted reagent.[103]

Figure 19: Principle of standard Fmoc peptide solid phase synthesis.

Figure 19 shows the basic principle of SPPS including protecting group strategy. Beginning from the C-terminus to the N-terminus, repeating amide bonds are formed. The first step is to couple the carboxyl group of the first amino acid to a linker covalently attached to the resin. During this addition of the first amino acid, the amine function is protected, in order to prevent

polycondensation and to generate selectivity. After a complete addition, this temporary protecting group can be removed in order to liberate a "new" primary amine function, at which further condensation may take place. Additionally the amino acid side chains must be protected, in a so-called permanent manner. Those functions most often are simultaneously deprotected during the cleavage from the solid support. In the early beginnings, tert-butoxycarbonyl (BOC) was used for temporary protection of the amine function and benzyl based groups as permantent protecting groups, followed by the cleavage from the chloromethyl polystyrene resin and temporary masking with anhydrous hydrogen fluoride.[104] However, this technique is nowadays mostly replaced by the utilization of an orthogonal protecting group strategy using the base labile N-Fmoc (fluorenylmethoxycarbonyl) group to protect the alpha-amino acid term, and the acid labile BOC as permanent protecting group. Fmoc is readily removed under basic conditions (e.g. piperidine, DBU) and is stable during standard coupling conditions. Another advantage of Fmoc protection is the possibility to detect and quantify its UV-signal during cleavage and thus an internal quality control of each coupling step.[104]

Activation Reagents

As solid phase synthesis always is a multi-step procedure, every step should obtain near quantitative conversions, because even conversion of 95% would lead to only 60% product after 10 steps. In order to maximize conversions, excess of the amino acid is applied. Un-reacted material can easily be removed from the reaction media by washing the solid phase resin. Additionally, the carboxylic acid function is converted into highly reactive species to facilitate amide bond formation. Today, a large variety of special activation reagents is commercially available.

One important class of activation reagents uses O-acylisourea generating carbodiimides. Examples are dicyclohexycarbodiimide (DCC), diisopropycarbodiimide (DIC) or 1-ethyl-3-(3'-dimethylamino)carbodiimide hydrochloride salt (EDC). However, only DIC and EDC are practical for solid phase synthesis, as they generate dichloromethane or water soluble urea derivates.

Another class of activation reagents are phosphonium salts belonging to the benzotriazol compound class. The first representative of that class was benzotriazol-1-yl-oxy-tris-(dimethylamino)-phosphoniumhexafluorophosphate, also called BOP or Castro's reagent.[105] During the reaction a very toxic phosphoniumoxide is generated. Therefore BOP was substituted by PyBOP. This reacts following the same reaction mechanism but presents the less toxic N-cyclopentane rest. Today PyBOP is one of the mostly used activation reagents in solid phase peptide synthesis.
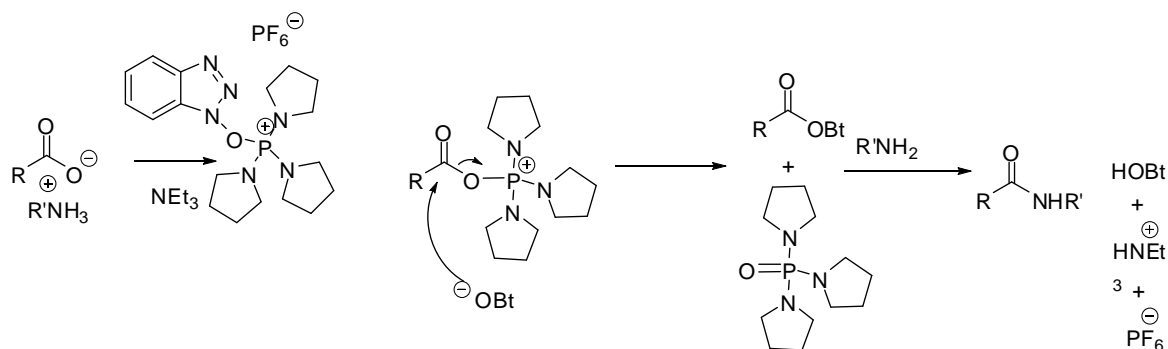
Figure 20: Reaction mechanism of PyBOP.

The one-pot coupling is performed by mixing the desired acid and amine in the presence of PyBOP and a non-nucleophilic base like triethylamine or Hünig's base (see Figure 20). The deprotonated acid first reacts with PyBOP to generate both, an activated acylphosphonium species and HOBt. HOBt readily reacts with the activated acid to produce a reactive Bt ester, which finally undergoes aminolysis. The driving force of this phosphonium-based reaction is the formation of the corresponding phosphoniumoxide.[106]

Another family of reagents has been developed around uronium species such as O-(1H-benzotriazol-1-yl)-N,N,N′,N′-tetramethyluronium hexafluorophosphate (HBTU).[107] In crystalline form, HBTU is usually the guanidinium form. In solution there is equilibrium between this form and the uronium form (Figure 21) [95].
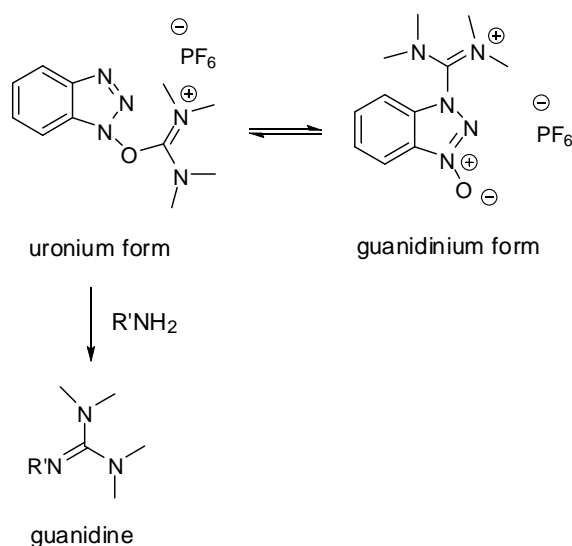
Figure 21: Equilibrium between uronium form and guanidinium form of HBTU and the potential by product formation of guanidine.

The coupling mechanism proceeds in a similar way to that shown for the phosphonium salts. In this case, the driving force is the generation of the urea by-product (Figure 22).[106]
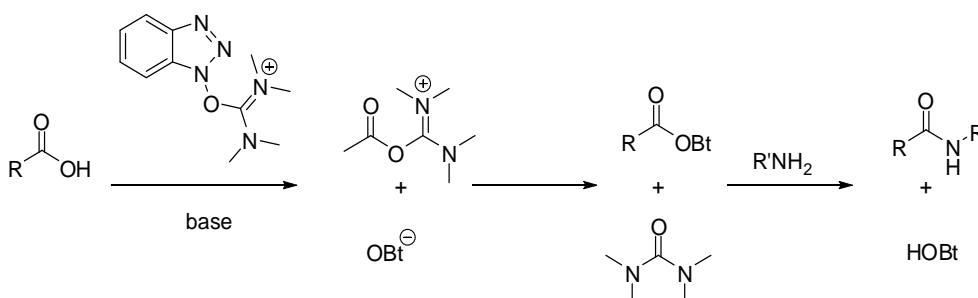
Figure 22: Reaction mechanism of HBTU.[106]

HATU, a derivate of HBTU with a phenyl ring -instead of the pyridine ring, has been proven to be very efficient in difficult, sterically hindered couplings and usually gives a minimal level of racemisation. It involves the formation of 7-azabenzotriazol-1-yl esters, very highly reactive species towards amines, probably due to intramolecular base catalysis.[106]

Solid Support/Resin

The solid support plays a very important role in solid phase synthesis. It can be considered as important as the choice of solvent for chemical reactions in solution. It is the environment in which two reactants collide and therefore has a profound influence on how fast they will react.[108] The polymeric support used by Merrifield, polystyrene cross-linked with divinyl benzene having pendant chloromethyl groups as points of attachment, has come to be known simply as Merrifield resin. It is to this day the most commonly employed resin.[109] Before the reaction takes place, the resins have to swell because most sites of attachment of solid-phase resins are inside the swollen beads.[110] As the reaction takes place in a heterogeneous medium, reaction rates are not only dependent on concentration and temperature but also on diffusion of the reagent into and out of the resin. Reaction rates are in general slower compared to solution, dependent on the swelling properties and the structure of the resin.[111] Swelling of classical polystyrene resins only takes place in apolar solvents. This drawback has been overcome with the modification of polystyrene with hydrophilic poly(ethylene glycol) (PEG) chains (Tentagel, Agrogel) and now also allows for solid phase synthesis using water or other polar solvents.

Linkers

The linker is the bridging molecule between the solid support and the first amino acid/building block of the growing chain. It is of high importance, because it has to be stable against all reaction conditions employed during elongation. After cleavage, i.e. the break of the bond between linker and resin, it determines the end group of the liberated molecule.
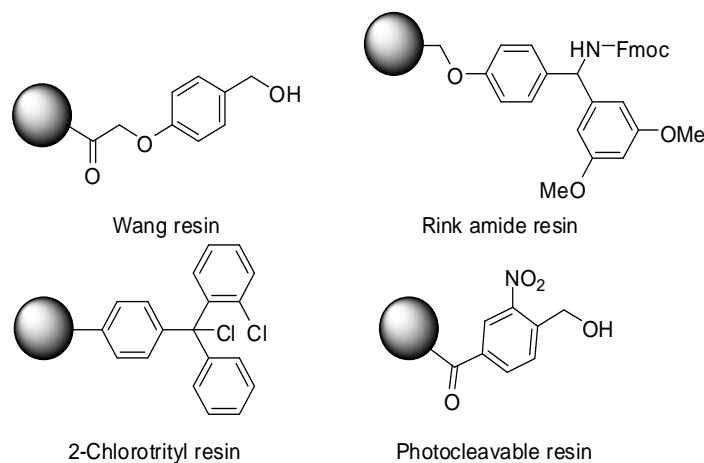
Figure 23: Examples for popular resins with linkers.

Many different examples are known; therefore here only the main classes are mentioned (see Figure 23). The most common linkers are acid labile linkers, due to their orthogonality to the base labile Fmoc chemistry. Examples are the 3-chlorotrityl-linked resin, wang-linked resin or Rink amide resins. Another class are photolabile linkers. For example 3-nitro-4-hydroxymethyl benzoyl linkers are cleaved at absorption of ultraviolet radiation with 350 nm for 24 h.[104] Safety catch linkers are stable during synthesis and become only labile after a specific activation. Traceless linkers do not leave any functional group and release the free C-terminus of the first amino acid after cleavage. These linkers are usually substituted by a hydrogen atom during cleavage.[111]

1.4.1.Solid Phase Synthesis beyond Peptides

Early on, the potential of solid phase synthesis for the synthesis of other molecules besides peptides was recognized. One important example is oligonucleotide synthesis. In this case, a nucleic acid is bound to a controlled pore glass solid phase. The phosphate group of the nucleic acid is, for instance, converted into a phosphoramidite and then coupled to a 5'-hydroxyl function of the solid bound growing chain.[112]

Solid phase synthesis also plays an important role in combinatorial chemistry.[111] This field of chemistry deals with the rapid synthesis of a large number of different but structurally related molecules, creating so called substance libraries. So far, many classical organic and metallorganic reactions could be transferred to solid support. Examples are aromatic substitutions, cycloadditions, olefinations, grignard reagents, nucleophilic substitutions and many more.[113]

Also in the synthesis of oligosaccharides, solid phase synthesis plays a very important role. Fréchet and Schuerch in the early 1970s carried out the first studies concerning the solid phase synthesis of oligosaccharides.[114] In 2001 the first automated synthesizer for solid phase oligosaccharide assembly was introduced by Seeberger et al.[115] Linkage to the solid support is for example given by octene diol linkers. Connection to the solid support is possible via the glycosyl acceptor or the anomeric leaving group (glycosyl donor) of a sugar monomer. The acceptor bound solution is nowadays preferred because the glycosylating agent, the reactive species, can be used in excess to drive the glycosidic bond forming reaction to completion.

After binding the glycosyl acceptor to the resin the temporary C2 protection group is removed (see Figure 24). Glycosylation is performed by installing a leaving group, like glycosyl trichloroacetimidates or glycosyl phosphate followed by the activation with trimethylsilyl trifluoromethanesulfonate (TMSOTf) and addition of the building block, forming an O-glycosidic linkage. After assembly of the oligosaccharide, it is cleaved off the resin followed by purification with HPLC.
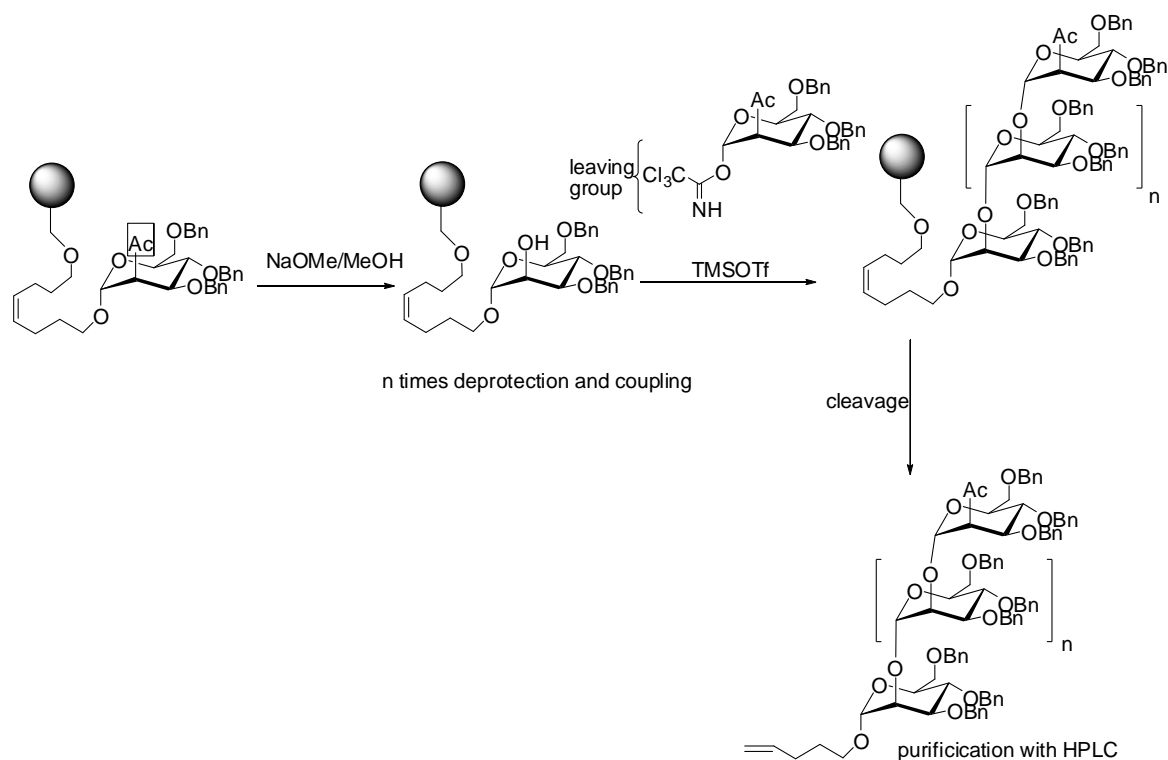
Figure 24:Formation of oligosaccharides in automated solid phase synthesis.[116,117]

Solid Phase Synthesis of Poly(amidoamines)

Solid phase polymer synthesis of poly(amidoamines) (PAAs) was introduced by Hartmann et al. in 2006.[118] Its main principle is the repetitive alternate coupling of diamines and diacids under the formation of multiple amide bonds (see Figure 25).
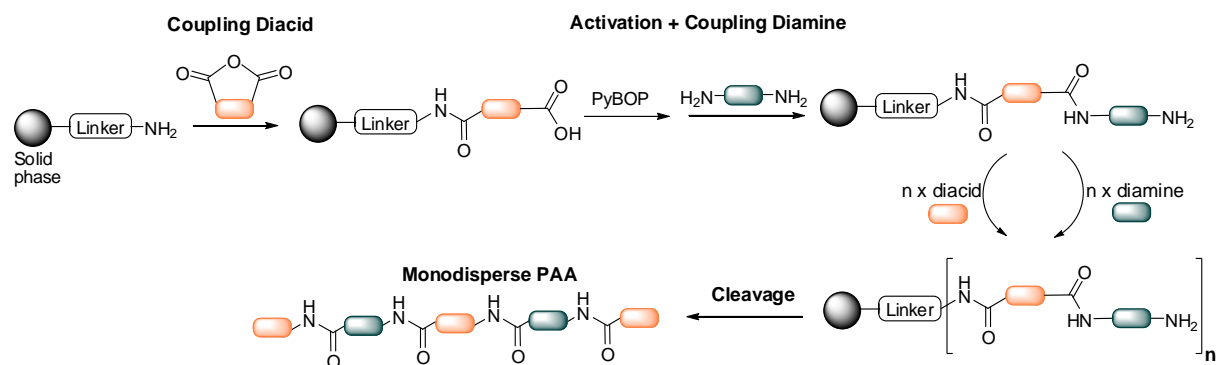

Figure 25: Schematic overview of the formation of linear poly(amidoamines) (PAA) on solid phase. A cyclic diacid is coupled to a free primary amine present on solid phase resin. The created carboxy function is then on-resin activated by PyBOP followed by coupling of a diamine. These two steps can be performed repeatedly until the desired length of the PAA which is released after cleavage from resin. (Adapted from [118]**)**

The first step is the coupling of a diacid to a resin linked amine functionality. This reaction proceeds via a preactivated acid anhydride which readily reacts with the primary amine to form an amide bond and a free carboxy group. In contrast to standard SPPS procedures, in which the

amino acid activation occurs in solution, the resin-bound carboxyl moieties have to be activated. This was achieved with PyBOP and HOBT. However, no temperoray protecting groups are required during chain elongation. The two coupling steps can now be repeated until the desired length of the PAA backbone is reached and is followed by cleavage of the final polymer from the resin. The synthesis was performed on a standard peptide synthesizer allowing for the full automation of the procedure.[118]

Several monomer building blocks were shown to be suitable for the synthesis of PAAs including natural occurring diamines and diacids, such as spermine, spermidine, tartaric acid, and aspartic acid (see Figure 26).
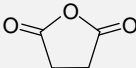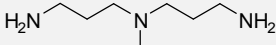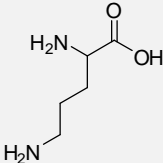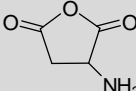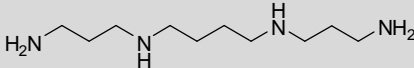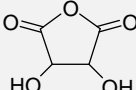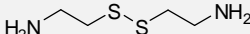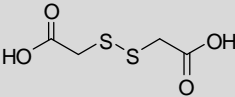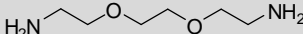
Diacids	Diamines	Amino acids
		all amino acids

Figure 26: Library of building blocks for solid phase supported synthesis of PAA. (Adapted from [119]**)**

In this thesis, a combination of Fmoc based solid phase peptide synthesis and solid phase PAA synthesis will be described. The diamine/diacid coupling approach employed in solid phase PAA synthesis was extended to functional building blocks that allow for the introduction of sugar ligands. Moreover, the functional diamine unit is Fmoc-protected and coupled to the diacid unit in solution leading to so called dimer building blocks. These dimer building blocks can then be coupled according to solid phase peptide protocols.

2. Aims and Outline

Carbohydrates play a key role in all organisms in nature. Apart from use as energy supply, carbohydrates are involved in signaling events, cell-cell communication, targeting and host-pathogen interactions.[9,120] Although underlying many important processes in biology, the fundamental mechanisms involving carbohydrate recognition are still barely understood. One reason for that are the scarce possibilities to isolate or synthesize natural occurring complex oligosaccharides. Due to this limitation, more easily accessible carbohydrate mimetics have been demonstrated to be a valuable tool for the investigation of carbohydrate-receptor interactions.[48,121,122] Apart from the facilitated access to such synthetic structures they are also capable of gaining higher affinities than their natural analogues.[31] Especially synthetic *multivalent* scaffolds presenting multiple copies of carbohydrates are used to enhance binding affinity and specificity since interactions between monovalent ligand and receptor are too weak. Thus understanding multivalent binding interactions as key feature in carbohydrate-receptor interactions is also crucial for the development of novel sugar-based therapeutics.[123,124]

For the investigation of multivalent interactions many different carbohydrate presenting scaffolds have been described previously.[8,65] Among others, glycopeptides, glycodendrimers and glycopolymers play an important role. However, each of these systems has its specific advantages and disadvantages: Glycopeptides have the advantage of being monodisperse and therefore allowing for a direct structure-activity correlation. However, they exhibit an increased risk of toxicity and immunogenicity. While being mostly biocompatible, glycodendrimers are limited in their shape and number of functional groups strongly depending on the synthetic route. Glycopolymers overcome these limitations but lack of structural definition, as they are inherently polydisperse.

In order to overcome these limitations and to combine the positive features of the existing scaffolds, a new class of precision glycooligomers for the investigation of multivalent ligand-receptor binding will be presented in this thesis. These glycomimetic ligands are biocompatible, monodisperse and sequence-defined, enabling for a direct correlation between their chemical structure and resulting biological function, specifically their receptor binding affinity.

The synthetic strategy towards monodisperse, sequence-defined glycooligomers is based on the solid phase polymer synthesis of poly(amidoamines) introduced earlier by Hartmann et al.[118] In this thesis, this approach is extended towards the synthesis of sugar functionalized oligoamides. Therefore, as a first step, functional building blocks have to be developed that are suitable for the use in solid phase coupling. On the one hand, they are intended for the use in Fmoc solid

phase synthesis. Thus a carboxyl and Fmoc protected amine moiety have to be present on the building block. On the other hand, they serve as carbohydrate conjugation site. Consequently, a side chain functional group has to be incorporated. In addition, a second set of building blocks is required to adjust both, the distance between the sugar ligands and the oligomer backbone properties such as flexibility or hydrophobicity. Copper catalyzed 1,3-dipolar cycloaddition (CuAAC) will be exploited as conjugation strategy for sugar ligands due to its compatibility building block design and solid phase coupling strategy.

The resulting building blocks will then be applied for solid phase synthesis. Here, different coupling strategies are possible: First, oligomers presenting multiple copies of the *same* sugar ligand, so called homomultivalent structures will be synthesized. This will be carried out by a simultaneous coupling of carbohydrate azides to the multiple alkyne presenting backbone obtained after solid phase assembly. Alternatively, a sequential solid phase coupling and conjugation protocol will be explored, enabling the functionalization of the scaffolds with *different* sugars leading to so called heteromultivalent structures. In a third set of glycooligomers, a light switchable, hydrophobic, spacer moiety will be introduced allowing for a switch in conformation of the oligomer backbone upon irradiation.

Following these different strategies, a set of precision glycooligomers will be obtained varying individual parameters known to influence multivalent receptor-interactions. Consequently, these glycooligomers will be used to study their ability to bind to lectin receptors and derive new insights into the design and binding mechanisms of multivalent glycomimetics. Different binding assays such as surface plasmon resonance, NMR and correlation fluorescence spectroscopy will be used to enlighten specific aspects of multivalent binding effects.

All in all, this thesis aims to develop a new class of synthetic glycomimetics for investigation of ligand-receptor binding and their underlying multivalent interactions. It is intended to develop a fundamental understanding of multivalent recognition between glycooligomers and protein receptors at a molecular level that will help to design novel glycomimetics for biomedical applications.

3. Results and Discussion

The aim of this thesis is to develop monodisperse, sequence-defined glycooligomers for the investigation of multivalent carbohydrate-receptor interactions. Therefore, first a novel synthetic approach towards monodisperse, sequence-defined oligoamides was developed. Solid phase synthesis was applied as a well-established synthetic approach to access monodisperse, sequence-defined macromolecules such as peptides or oligonucleotides. In order to use Fmoc-based solid phase protocols, novel functional building blocks were developed. Their synthesis will be presented in the first part of this thesis. The second section then describes the assembly of the building blocks on solid phase as well as the conjugation of sugar ligands to these oligomers. In the third and final section, the obtained glycooligomers are used for fundamental studies regarding ligand-receptor binding. Multivalent binding with two different lectins, mannose binding Con A and galactose binding PA-IL, will be investigated by different binding assays. Special focus will be devoted to the effect of number and spacing of sugar ligands presented on homomultivalent glycooligomers. Heteromultivalent structures presenting different types of sugars on one scaffold will be used to determine the effect of heterogeneity on multivalent binding. Moreover, the effect of a change in backbone hydrophobicity and spatial distribution of sugar ligands will be examined by glycooligomers consisting of light switchable AZO spacers inducing a conformational change in the scaffold.
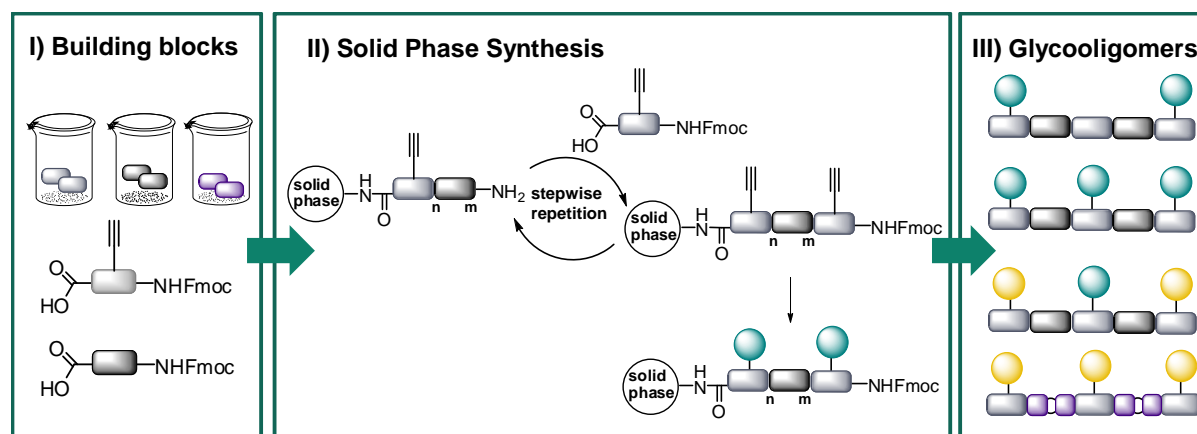
Figure 27: Schematic overview of the synthesis of sequence-defined, monodisperse glycooligomers. I) At first functional building block applicable in solid phase synthesis were synthesized in solution. II) Then, solid phase synthesis was carried followed by conjugation of sugar ligands out. This led to III) monodisperse, sequence defined glycooligomers.

3.1. Synthesis of Building Blocks

The synthesis of sequence-defined, monodisperse oligoamides is based on standard solid phase peptide chemistry (SPPS), specifically on Fmoc coupling protocols. This highly advanced synthetic method allows for efficient coupling, easy scale-up and automation. However peptides are not used as carbohydrate presenting scaffolds in this thesis due to their potential toxicity and immunogenicity. Oligoamide structures are preferred, because of their known biocompatibility[118,125] and reduced immunogenicity[56]. Therefore, non-amino acid based novel functional building blocks will be employed in solid phase synthesis.

In order to be suitable for standard Fmoc coupling SPPS protocols, the building blocks have to fulfill certain criteria: They have to be soluble in DMF or NMP being standard solvents used in SPPS. Permanent protective groups and side chain functionalizations have to be stable under typical SPPS conditions such as use of piperidine or TFA. It is of great importance that the building blocks have a high purity; e.g. 5% impurity of building block would leads to at least 23% impurity for a final pentamer. Another important prerequisite is the use of several equivalents of building block during solid phase synthesis, therefore high quantities are needed. Hence, a protocol has to be developed which allows for straightforward and upscalable synthesis of the desired building blocks. Moreover, for variation of oligoamides structures, the building block synthesis has to be easily adaptable for the synthesis of different building blocks.

For the design of multivalent glycooligomers, two classes of building blocks were envisioned: functional building blocks allowing for the introduction of sugar ligands in the side chain and spacer building blocks allowing for a controlled spacing of sugar ligands as well as the variability of backbone properties such as hydrophilicity and flexibility.

The following chapter will therefore present the design and synthesis of seven different building blocks with a major focus on two of them: The alkyne presenting building block which serves as side chain conjugation site for the sugar ligands via CuAAC reaction and a hydrophilic, flexible ethylene glycol based spacer unit.
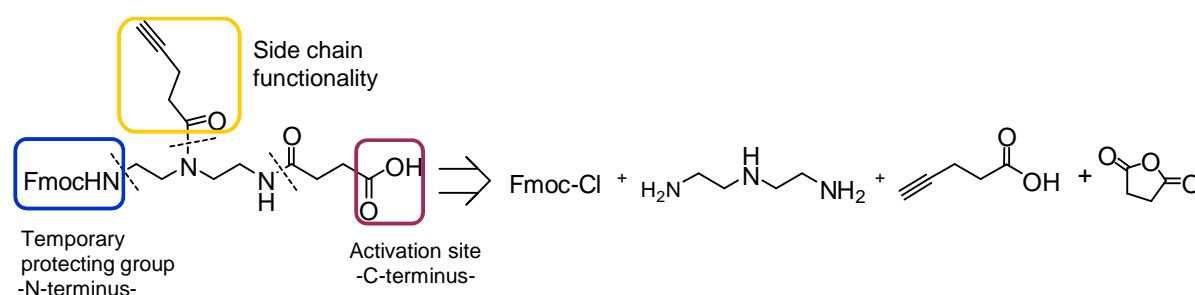
3.1.1. Alkyne Building Block

The first building block should allow for the introduction of sugar ligands in the side chain. Thus, besides the free carboxy and Fmoc-protected amine group to form the oligoamide backbone, a third functional group needs to be incorporated into the building block design. Ideally this group allows for a selective and highly efficient coupling of sugar ligands that is orthogonal to the chemistry used for main chain elongation and final cleavage. Furthermore, this functional group should not require additional protection groups during solid phase synthesis but still be

compatible with standard solid phase chemistry. These requirements are met by the CuAAC reaction, a well-established conjugation method as discussed in Chapter 1. Consequently, an alkyne moiety was incorporated in the side chain of the building block and sugar azides can be used for the introduction of sugar ligands.

Diethylenetriamine was chosen as starting material for the synthesis of the alkyne building block. On the one hand, this precursor presents three amine functionalities that allow for the introduction of the three required groups: carboxy-, Fmoc-protected amine and alkyne group (see Figure 28). On the other hand, it is commercially available and cost efficient starting material. Additionally, the ethylenediamine unit has previously been shown to be biocompatible and non-toxic, another important prerequisite for the targeted scaffolds and their potential applications in biomedicine.[118]

Figure 28: Structural requirements of the alkyne building block and its precursors.

The overall building block synthesis is based on a five step procedure. Figure 29 shows the synthesis of the **T**riple bond functionalized building block (**TDS**) with a **S**uccinyl rest synthesized starting from **D**iethylenetriamine.
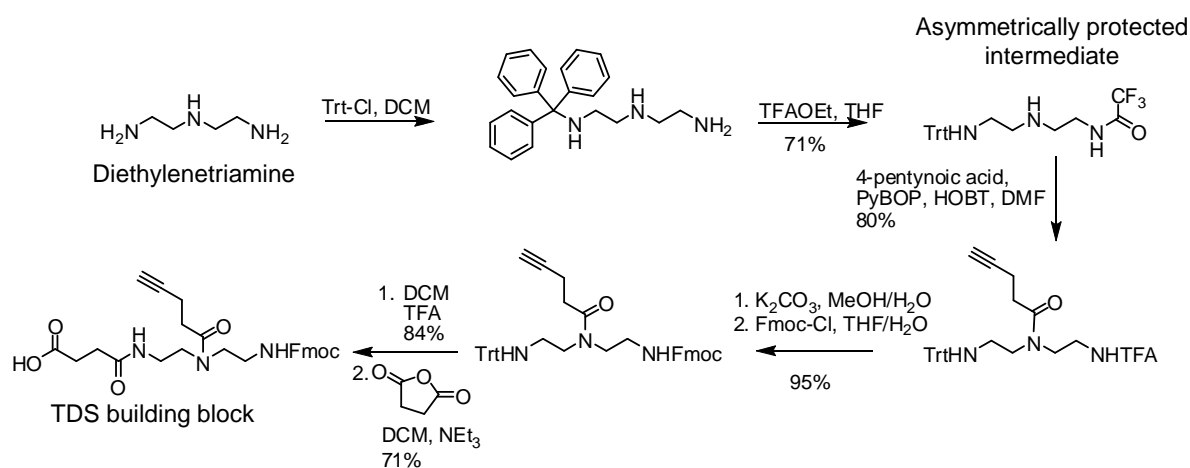
Figure 29: Synthesis of TDS building block.

In a first step, the two primary amines had to be orthogonally protected to allow for the introduction of the alkyne moiety on the secondary amine. Trityl (Trt) and triflouracetyl (NHTFA) protecting groups are known to be selective for primary amines in presence of a secondary amine.[126,127] The symmetrical amine was monoprotected with a trityl protecting group using excess of commercially available diethylenetriamine in high dilution. This was followed by protection of the second primary amine with ethyl trifluoroacetate (TFAOEt). The asymmetrically protected intermediate was recrystallized from toluene. Such desymmetrization reactions are usually of low yield. However, here it was possible to obtain 71% of crystalline product after two steps on large scale of up to 23 g.

In order to introduce the alkyne moiety for later CuAAC reaction, the asymmetrically protected intermediate was then coupled with 4-pentynoic acid at the secondary amine. Two different activation reagents for this amidation reaction were examined. At first, EDC was used because the urea derivates formed by this activation reagent are known to be water soluble. Therefore, the resulting product was considered to be purified easily by aqueous extraction. However, this reaction resulted in low yields. PyBOP together with HOBt and DIPEA as base in DMF showed better results, giving 80% crude product which was used in the next step without further purification. Then, the trifluoracetyl protecting group (NHTFA) was removed and exchanged towards the final Fmoc-moiety. As NHTFA can be cleaved in aqueous basic solution and Fmoc can be attached with the same conditions, a one-pot reaction was used for these two transformations. Potassium carbonate in methanol and, as second step, exchange of methanol to tetrahydrofurane together with the addition of Fmoc chloride gave the Fmoc-trityl compound with a yield of 95%. The crude product was used in the next step without further purification. The trityl protecting group was removed by adding 30% TFA in DCM. After coevaporation with toluene to remove TFA, the resulting intermediate was purified by precipitation in Et_2O giving 84% yield. The carboxyl-unit was attached in the final step by coupling with succinic anhydride in basic DCM. The complete synthesis of TDS was carried out on large scale resulting up to 8 g of final building block with a total yield of 32%. TDS building block was characterized by NMR (see Figure 30) and ESI-MS. The purity of the final compound was determined by RP-HPLC giving a purity of above 99%.
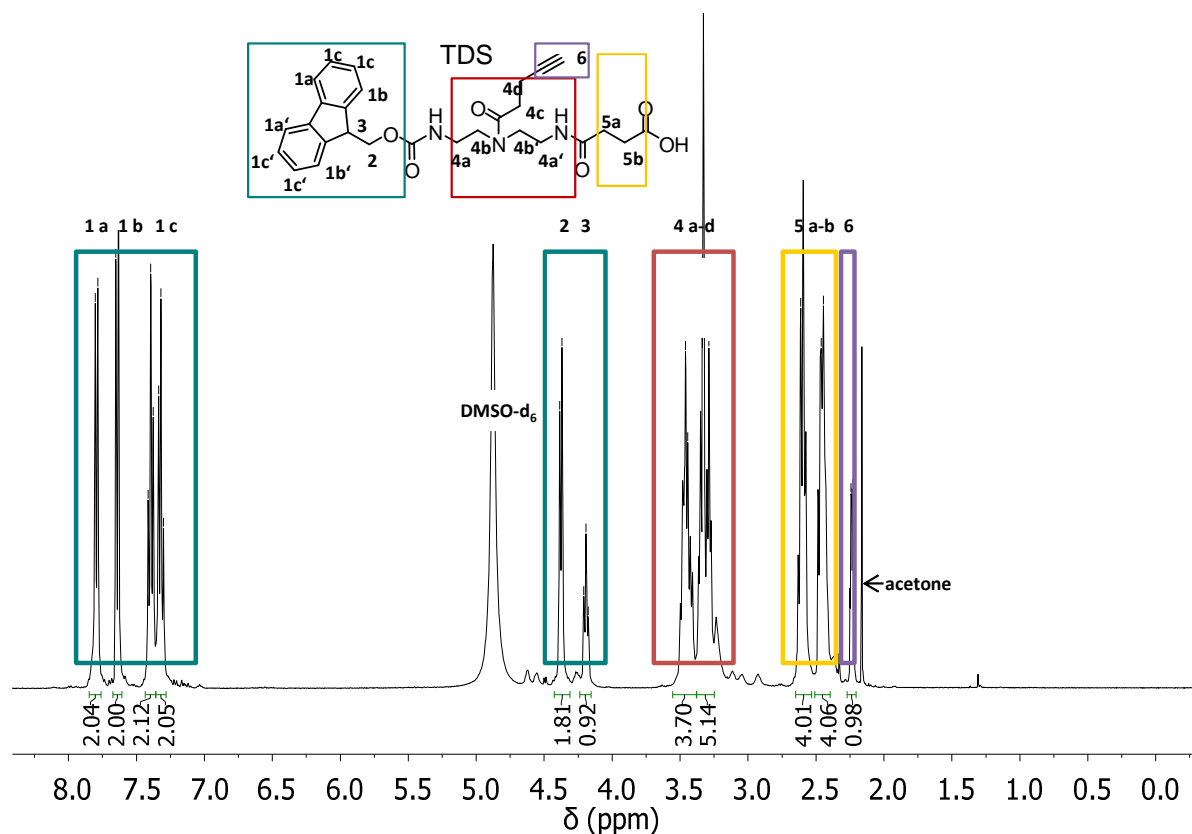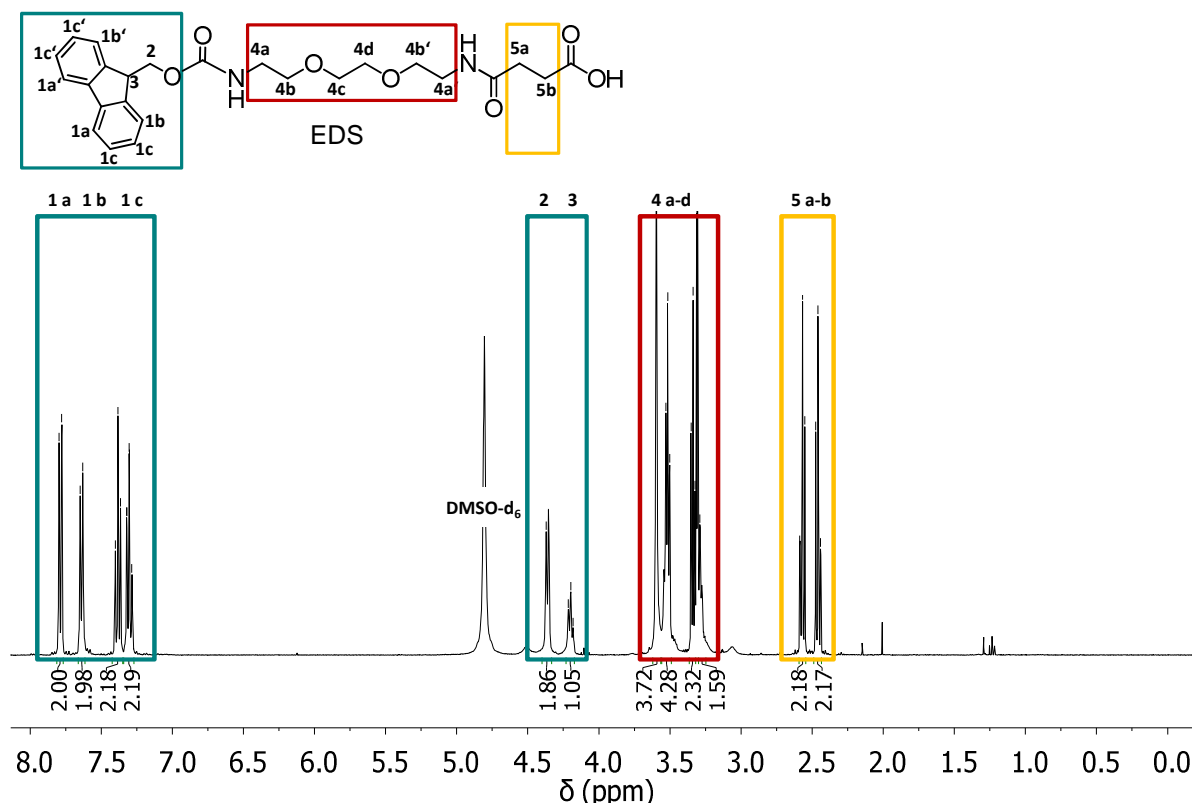
Figure 30: ¹H-NMR spectrum of TDS (recorded in DMSO-*d6*). The individual protons of the molecule are assigned by numbers..

3.1.2. EDS Building Block

Besides building blocks allowing for the introduction of sugar ligands, a second set of building blocks was envisioned allowing for a) variation of the distancing of sugar ligands along the oligomer scaffold and b) control over the properties of the oligomer backbone. Furthermore, these so-called spacer building block should ensure biocompatibility of the oligomers for a potential use in biomedical applications. Therefore, a first spacer building block was designed based on an ethylene glycol unit, a well-known spacer unit applied in polymers for biomedical applications. **E**thylene glycol-**D**iamine was used as precursor, Fmoc-protected and **S**uccinylated to yield the carboxyl group in the building block (**EDS** building block).
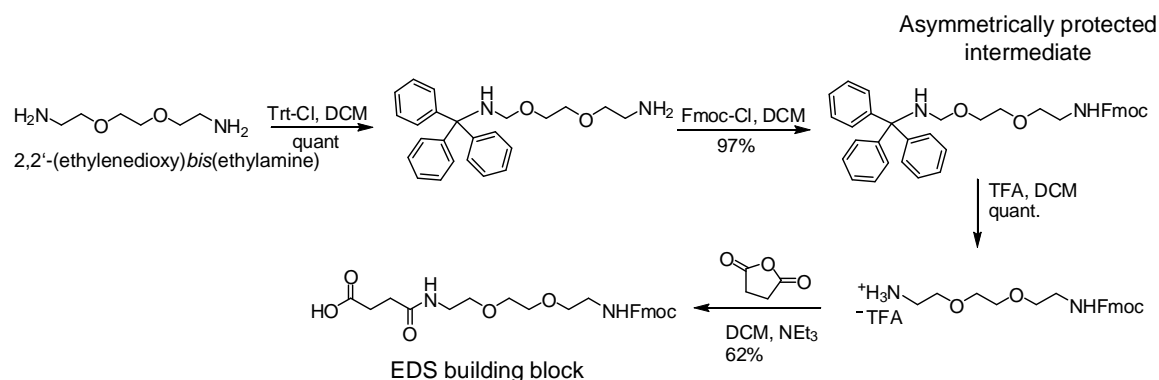
Figure 31: Synthesis of EDS spacer building block.

In detail, 2,2'-(ethylenedioxy)bis(ethylamine) was desymmetrized by mono-protection with tritylchloride in DCM (see Figure 31). By using excess of diamine in high dilution, this reaction proceeded with almost exclusive formation of the mono-trityl-species. Then, the second primary amine was functionalized with the Fmoc group required for solid phase synthesis. Fmoc-chloride in DCM was reacted with the mono-trityl compound to give the asymmetrically protected intermediate. As a next step, the trityl-protecting group was removed using TFA in DCM. The resulting compound was purified by precipitation in Et$_2$O and obtained in 97% yield after the first three steps. The final succinylation was performed in basic DCM followed by recrystallization from hexane/ethyl acetate resulting the final product with a yield of 62%. The complete synthesis was carried out in a scale of up to 12 g with an overall yield of 54% over four steps. Desymmetrization of 2,2'-(ethylenedioxy)bis(ethylamine) can also be accomplished by mono-succinylation followed by Fmoc-protection.[128] This approach would potentially be faster and give higher yields. However, this reaction failed due to significant formation of a di-succinylated species which could not be removed by recrystallization. The identity of the EDS building block was confirmed by NMR and ESI-MS (Figure 32). The purity of the final compound was determined by RP-HPLC as 99%.

Figure 32: ¹H-NMR spectrum of EDS (recorded in DMSO-*d6*). The individual protons of the molecule are assigned by numbers.

3.1.3. Other Spacer Building Blocks

An alphabet of building blocks was established (Table 1) with the above described two synthetic approaches for EDS and TDS building blocks. The other building blocks were synthesized analog to these reactions. This demonstrates the versatility of the novel approach using asymmetric, orthogonally protected diamines to synthesize non-amino acid based building blocks for solid phase. Using them for the oligoamide scaffolds creates a great structural diversity of the scaffold, allowing for both tuning of backbone properties such as hydrophobicity/-philicity, and flexibility and introduction of functionalities. For that, different spacer moieties were synthesized exhibiting different structural properties:

ADS presents an **A**cetyl group on the secondary amine. This building block is intended as spacer building block with a high structural similarity to TDS but without its functional alkyne moiety.

CDS bears as structural feature a disulfide bridge introduced via **C**ystamine as starting material. This moiety can be cleaved reductively and thus allows for a controlled
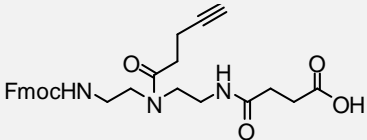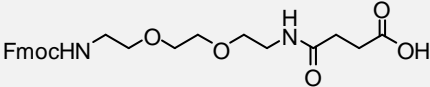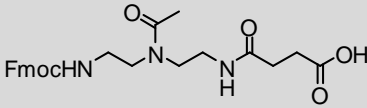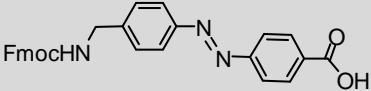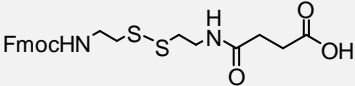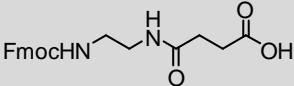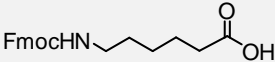
degradation/fragmentation of the oligo/polymers. This can for example be used for drug delivery applications releasing a specific cargo from a targeting moiety.

SDS is a building block with ethylenediamine as precursor being the shortest possible aliphatic diamine. It can be applied as smaller, more hydrophilic alternative to EDS.

HDS is a hydrophobic spacer which was synthesized in one step by Fmoc protection from the corresponding amino-**H**exanoic acid.

AZO can be considered as hydrophobic linker, including an **azo**benzene-moiety. Moreover, due to this azobenzene unit, it can change its configuration from trans to cis upon irradiation at a specific wavelength. It was synthesized according to literature protocols by Dr. David Bléger from Humboldt University.[129,130]

Table 1: Table of the synthesized building blocks and their names.

Name	Structure (Synthesis according to TDS)	Name	Structure (Synthesis according to EDS)
TDS		EDS	
ADS		AZO*	
		CDS	
		SDS	
		HDS	

* synthesized by a different protocol from collaboration partner

All in all, two versatile protocols for the synthesis of building blocks have been developed. The building blocks meet the above described criteria for application in solid phase synthesis. Three of the derived building blocks will be further used for the synthesis of glycooligomers. **TDS** serves as conjugation site for the carbohydrate moieties introduced by CuAAC reaction. **EDS** is

used as flexible, hydrophilic spacer to adjust the distance between the carbohydrate presenting positions. **AZO** serves as hydrophobic, stiff, light switchable moiety in the oligomer scaffold.

3.2. Synthesis of Glycooligomers

The overall goal of this thesis is to synthesize sequence-defined, monodisperse glycooligomers for studies of multivalent ligand-receptor interactions. Solid-phase synthesis according to standard peptide protocols yields the desired monodispersity and sequence-definition of the oligomers. Moreover, the resulting oligoamide scaffold generated by multiple amidation reactions has the advantage of being biocompatible[118,125] and result in a reduced immunogenicity.[56]

To obtain *glyco*oligomers, conjugation sites presented in the side chain of the scaffold have to be coupled to sugar ligands. A reliable reaction without the need of additional protecting groups was envisioned as conjugation method for sugar ligands. Especially so-called click reactions are known to fulfill these criteria. Besides thiol-ene coupling[131], Staudinger ligation[132] or native chemical ligation[133], CuAAC is widely employed for polymer and bioconjugation chemistry.[91,102] Latter was chosen because of its excellent reliability and tolerance regarding different solvents and substrates. Therefore the TDS building block (the synthesis was described in the previous chapter) was applied in solid phase synthesis and serves as conjugation site for the introduction of sugar ligands via CuAAC. Additionally, spacer building blocks are incorporated into the scaffold to create defined distances between the carbohydrate moieties presented on the backbone. Here, EDS building block based on ethylene glycol serves as flexible, hydrophilic moiety whereas AZO building blocks were used as hydrophobic and stiff spacer units. With these building blocks in hand and in combination with a sugar conjugation protocol, synthesis of glycooligomers can be achieved in several ways (see Figure 33):

One possibility is the coupling of building blocks with sugar ligands already attached during building block synthesis. This approach has the disadvantage of needing a library of different building blocks for variation of sugar ligands which can be difficult to obtain by synthesis in solution. In addition to that, differently functionalized sugar building block could couple differently efficient resulting in the need to optimize the coupling reactions. Furthermore, protecting groups of the hydroxyl moieties are needed to prevent side reactions during coupling reactions. A second possibility is the coupling of sugar ligands in solution to a preassembled backbone, after cleavage from resin. This approach would need only a small amount of sugar ligand to conjugate. However, reaction conditions have to be optimized for each scaffold and subsequent purification is most likely needed. The same simultaneous conjugation of sugar ligands can also be carried out directly on solid phase after assembly of the desired scaffold.
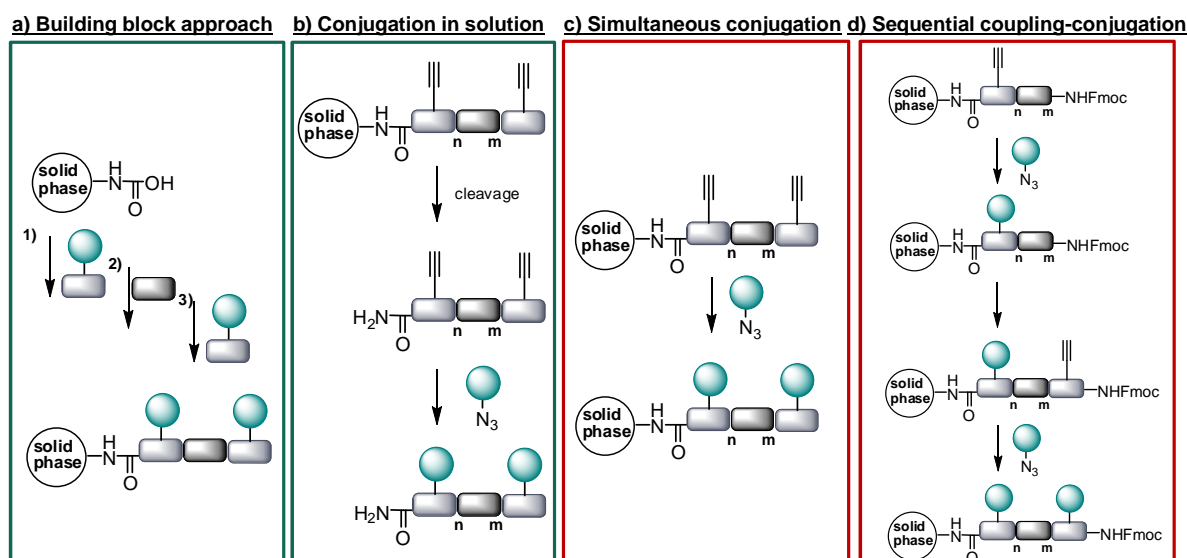
Figure 33: Schematic representation of the different strategies to introduce sugar ligands to a glycooligomer: a) Sugar presenting building blocks can be coupled on solid phase, b) sugar ligands are coupled in solution after assembly and cleavage of the desired oligomer backbone, c) the conjugation of sugar ligands is performed on solid phase after assembly of the desired oligomer backbone, d) conjugation of sugar ligand is carried out directly after the coupling step.

Another possible approach is a sequential coupling-conjugation method which conjugates the sugar ligand directly after coupling of alkyne building block. Latter two approaches were employed in this thesis and will be described in detail in the following.

3.2.1. Homomultivalent Glycooligomers

The initial approach to obtain multivalent glycooligomers was the use of a simultaneous conjugation via CuAAC of multiple sugar ligands to a preassembled oligoamide scaffold. Therefore stepwise addition of alkyne presenting and spacer building blocks is performed leading to an alkyne presenting oligomer attached to the resin. This is followed by coupling of sugar azide ligands to all alkyne side chains of the oligomer and cleavage of the final glycooligomer from the resin. This leads to homomultivalent structures presenting one type of sugar in the side chains. Coupling of carbohydrate moieties via CuAAC directly on solid phase in contrast to coupling in solution was chosen due to the following advantages: Potential cross coupling reactions such as Glaser coupling cannot occur.[63] No protecting groups for the carbohydrate units are necessary and the use of excessive reagent for complete conversion is possible because the resin can be simply washed. Indeed, the first description of copper-catalyzed 1,3 dipolar cycloaddition between azide and alkyne was also carried out on solid support.[63] For a first set of homomultivalent ligands, the EDS spacer building block was used and combined with the TDS building block. Thus the number and position of TDS building

blocks introducing one alkyne side chain per building block determines the number and position of the sugar ligands in the final oligomer.

In detail, the synthesis was carried out as follows: A tentagel resin was chosen as solid support. This hydrophilic resin, swellable both in aqueous and organic solvents[134], was used for glycooligomer synthesis because the final products are polar structures and the conjugation step requires water as solvent. A trityl linker on the resin which can be cleaved under mild acidic conditions was chosen in order to protect the sugar ligands from degradation. Ethylenediamine was attached to the resin in order to release a primary amine at the C-terminal site. It can serve as additional conjugation functionality e.g. for a fluorescent label and further enhances the polarity of the oligomer.

Figure 34 shows the exemplary protocol for the synthesis of a pentameric structure consisting of three TDS building blocks spaced with one EDS building block each and thus carrying three sugar ligands in the final oligomer:

The initial attachment to the resin proceeds by coupling of a TDS building block to the free amine of the ethylenediamine linker. In general, 8 equivalents building block, 8 equivalents activation reagent (Benzotriazol-1-yloxy)tripyrrolidinophosphonium hexafluorophosphate (PyBOP) together with 4 equivalents Hydroxybenzotriazole (HOBT) additive and 16 equivalents diisopropylethylamine (DIPEA) as base were used. HBTU was also used for building block coupling. However it was only successful in the formation of oligomers of up to six building blocks.Beyond that, the formation of byproducts was observed. Therefore all following structure were obtained by using PyBOP/HOBT as activation reagents.
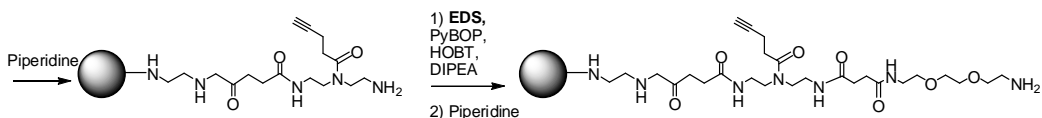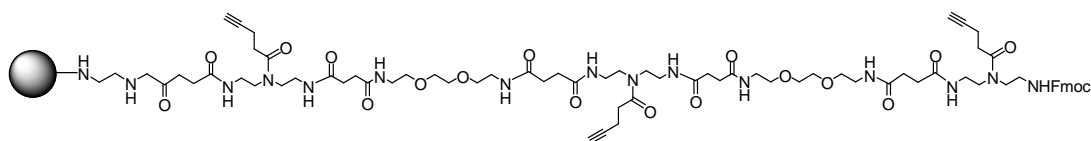
1) Coupling of building block
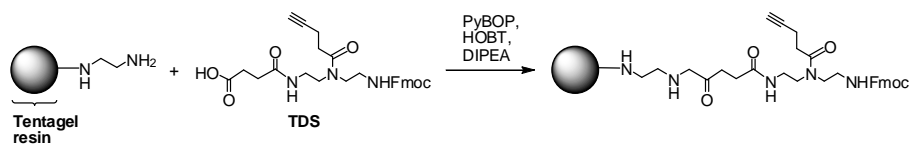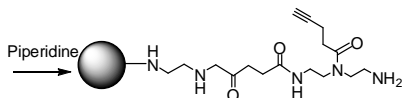
**2) Fmoc-deprotection**   **3) Coupling of second building block**

**4) Further coupling, three times repetition of 2) and 3)**

Figure 34: Solid phase synthesis of oligomers by repetitive coupling of building blocks.

After the first coupling step, the temporary N-terminal Fmoc protecting group was cleaved with piperidine. A primary amine was released serving as coupling site for the next building block. EDS was attached to the growing chain as second building block by the above described coupling conditions. This was again followed by Fmoc removal. Further coupling proceeded by repetitive execution of the coupling and Fmoc deprotection reactions until the desired sequence was assembled.

The next step was the simultaneous conjugation with sugar ligands. Their number and position was determined in the backbone assembly step by introduction of the TDS building blocks. In order to obtain monodisperse, sequence-defined glycooligomers, the conjugation of sugar azide ligands to the alkyne moieties has to proceed with 100% yield. Different carbohydrates (mannose, galactose and glucose) equipped with an azide unit were synthesized according to literature.[80]

1) Capping of primary amine
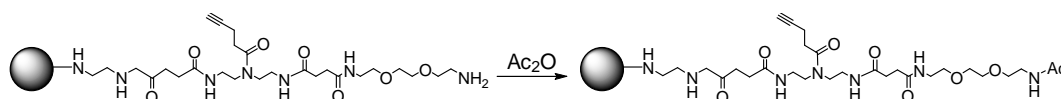
2) CuAAC on resin
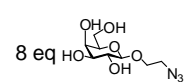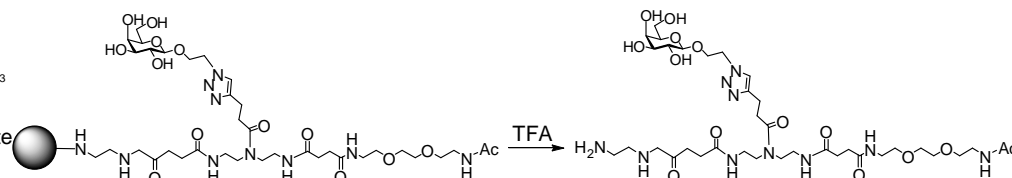
3) Cleavage from resin
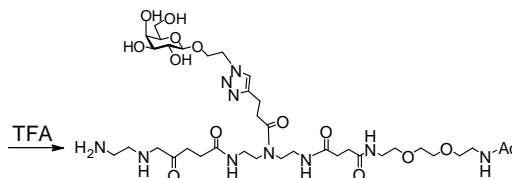
Figure 35: Simultaneous conjugation of carbohydrate moieties on solid phase to the alkyne displaying oligoamide scaffold (the exemplary system shows only two building blocks, the standard case described in this thesis employs at least five building blocks).

Figure 35 shows the employed protocol for conjugation of carbohydrates: At first, the terminal amine unit was capped with acetic anhydride. CuAAC reaction in presence of the free amine group gave incomplete conversion. It is likely the amine moiety complexes the copper catalyst leading to impeded product formation. Following standard conditions, $CuSO_4$ was reduced in situ with ascorbate to give the active catalytic species.[135] CuAAC reaction was carried out directly on resin with 8 eq. azido-ethyl-carbohydrates per alkyne unit in presence of 20 mol% $CuSO_4$ and ascorbate.

One limitation often discussed for CuAAC is residual copper found in the final products. Depending on the further applications of the product, this might lead to undesired side effects such as toxicity during *in vitro* or *in vivo* testing. Therefore, in order to quantitatively remove copper, a washing protocol employing the use of 0.2 mM sodium diethyl-dithiocarbamate in DMF was established. If copper ions are available, a yellow bis(diethyldithiocarbamate)-copper(II) complex is formed.[136] By inductive coupled plasma mass spectrometry (ICP-MS), a technique for the detection of heavier elements, it was determined that no traces of copper (sensitivity in parts per billion range) were present after employing the diethyl-dithiocarbamate wash.

As a final step in glycooligomer synthesis on solid phase, the oligomer was cleaved from the resin by 30% TFA in DCM followed by precipitation in Et_2O. After centrifugation and decanting of the ether, the product was dissolved in water and lyophilized. All oligomers were isolated in comparably high yields (~70%).

RP-HPLC: 5/95 MeCN/H_2O→ 30/70 MeCN/H_2O in 60 min   ESI-MS positive mode
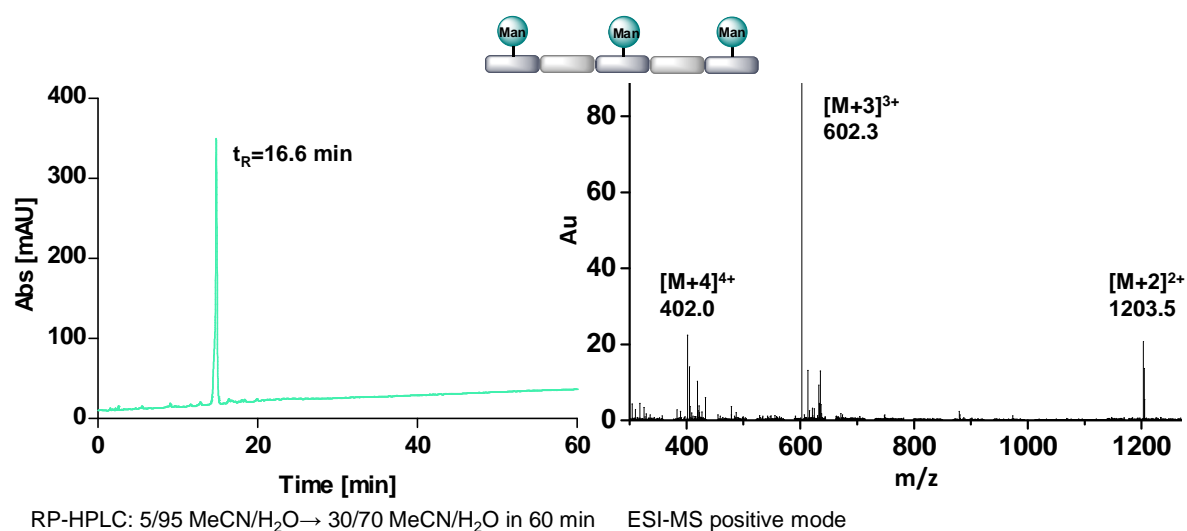
Figure 36: Exemplary RP-HPLC of Man(1,3,5)-5. The signal was determined at 214 nm. Man(1,3,5)-5 was obtained in a purity of above 95%

Analysis of the crude product showed high purities of ~95%. Lower purity was obtained for Man(all)-10 and Gal(all)-10 therefore preparative HPLC was carried out to purify the product from by-products. A representative RP-HPLC and an ESI-MS spectrum for a pentameric oligomer presenting three Mannose ligands can be seen in Figure 36. All glycooligomers were characterized by ^{1}H-NMR and ESI-MS (see Table 2). The expected mass to charge ratios were found for all homomultivalent structures confirming the synthesis of monodisperse, sequence-defined structures.
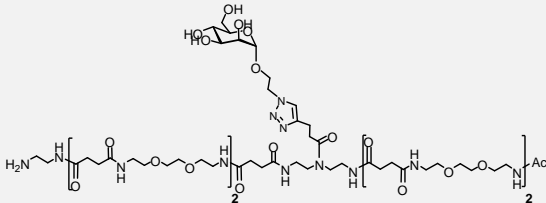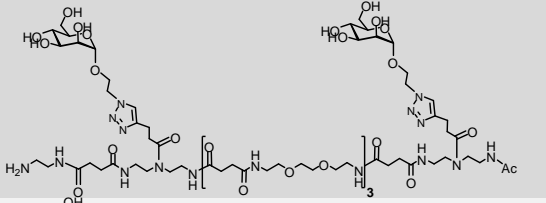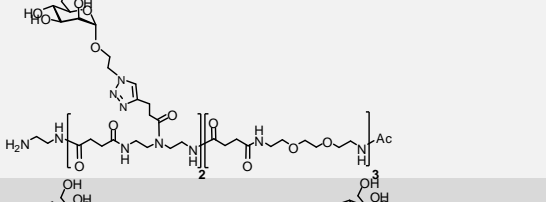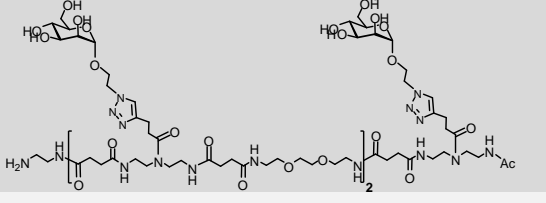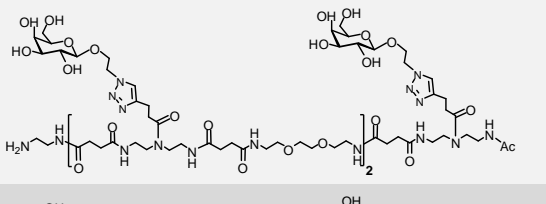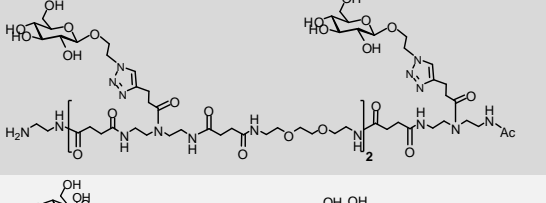
Table 2: Calculated exact mass of the synthesized homomultivalent compounds and the m/z found by ESI-MS (positive mode)

Compound name	M_w calcd.	m/z found
Man(3)-5	1536.8	769.4 [M+2H]$^{2+}$
Man(1,5)-5	1820.9	911.8 [M+2H]$^{2+}$
Man(1,3)-5	1820.9	911.4 [M+2H]$^{2+}$
Man(1,3,5)-5	2105.1	1053.8 [M+2H]$^{2+}$
Gal(1,3,5)-5	2105.1	1053.8 [M+2H]$^{2+}$
Glc(1,3,5)-5	2105.1	1053.6 [M+2H]$^{2+}$
Man(all)-5	2373.3	892.3 [M+3H]$^{3+}$
Gal(all)-5	2373.3	892.3 [M+3H]$^{3+}$
Man(all)-10	5244.5	1050.2 [M+5H]$^{5+}$
Gal(all)-10	5244.5	1050.3 [M+5H]$^{5+}$

Table 3 lists all synthesized homomultivalent glycooligomers. The nomenclature specifies the kind of monosaccharide (mannose=Man, galactose=Gal and glucose=Glc), its position in the backbone in parentheses and the overall length of the backbone (5=pentam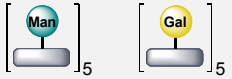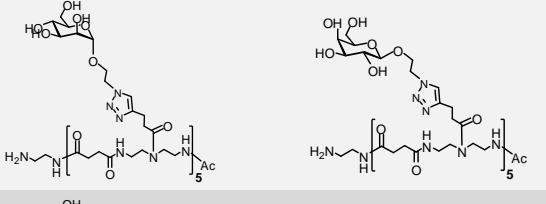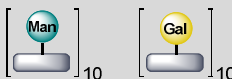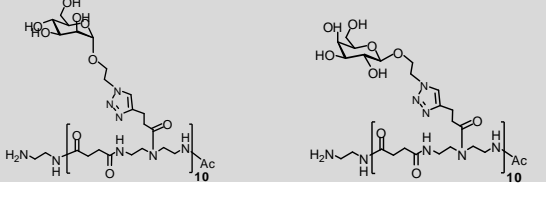eric). Ten different structures were synthesized, eight of them have a constant length of five building blocks with a different number of spacer units: Man(3)-5 is a symmetric structure carrying one mannose unit surrounded by two EDS spacers on each side. Man(1,5)-5 and Man(1,2)-5 are both divalent structures with two mannose sugars but differing in spacing. Man(1,5)-5 is symmetric, with the two mannoses on each end and three EDS in between. Man(1,2)-5 presents both carbohydrate units adjacent to each other followed by three EDS spacers. Man(1,3,5)-5 presents a trivalent structure with each mannose unit separated by one EDS moiety. Equivalent structures with galactose or glucose ligands are Gal(1,3,5)-5 and Glc(1,3,5)-5. Man(all)-5 is a pentavalent structure bearing 5 mannose units directly next to each other, no EDS spacer was employed. Gal(all)-5 is a structural analogue with galactose moieties instead of mannose. The last two structures are Man(all)-10 and Gal(all)-10, which also do not exhibit any EDS spacer, displaying 10 carbohydrates.

Table 3: Overview over the homomultivalent structures, short graphical representations and names.

3.2.2. Heteromultivalent Glycooligomers

By the previously described synthetic approach, glycomimetic structures displaying *one type* of sugar ligand were synthesized. The overall goal of this thesis is to carry out multivalent lectin-receptor binding studies with glycomimetic structures. However biological systems are inherently heterogeneous.[137] Therefore, the synthesis of heteromultivalent glycooligomers was another central aim of this thesis. As described above, four approaches are generally possible to conjugate sugar ligands to the oligoamide scaffolds: conjugation of sugar to a preassembled backbone, either in solution or directly on solid phase, introduction of sugar ligands already on the building block level and a sequential coupling-conjugation strategy. Only the last two approaches can be used for the functionalization with *different* sugar ligands while keeping a sequence-definition.

As the use of sugar-functionalized building blocks would require a large set of different building blocks and potentially requires optimization of coupling conditions, the sequential coupling-conjugation strategy was chosen. This strategy combines the advantage of a repetitive conjugation protocol with conjugation directly on solid support.

The sequential coupling-conjugation approach is based on the stepwise addition of building blocks until the desired position of the first sugar ligand is reached. Then a TDS (alkyne) building block is introduced. After successful coupling of the building block, the alkyne side chain is immediately functionalized with a sugar azide. Only after complete functionalization of the side chain, the terminal Fmoc protecting group is cleaved and the oligomer chain can be further extended by addition of the next building block. Upon reaching the position of the second sugar ligand, again TDS is introduced and can now be conjugated to a different sugar azide. This sequential coupling of building blocks immediately followed by conjugation can be repeated multiple time resulting in heteromultivalent, sequence-defined, monodisperse glycooligomers.

In detail, the synthesis of the exemplary structure of GalManGal(1,3,5)-5 glycooligomer will be described in the following section(see Figure 37): As initial step, a TDS building block, displaying one alkyne moiety in the side chain, was coupled to the ethylenediamine linker attached to the resin.
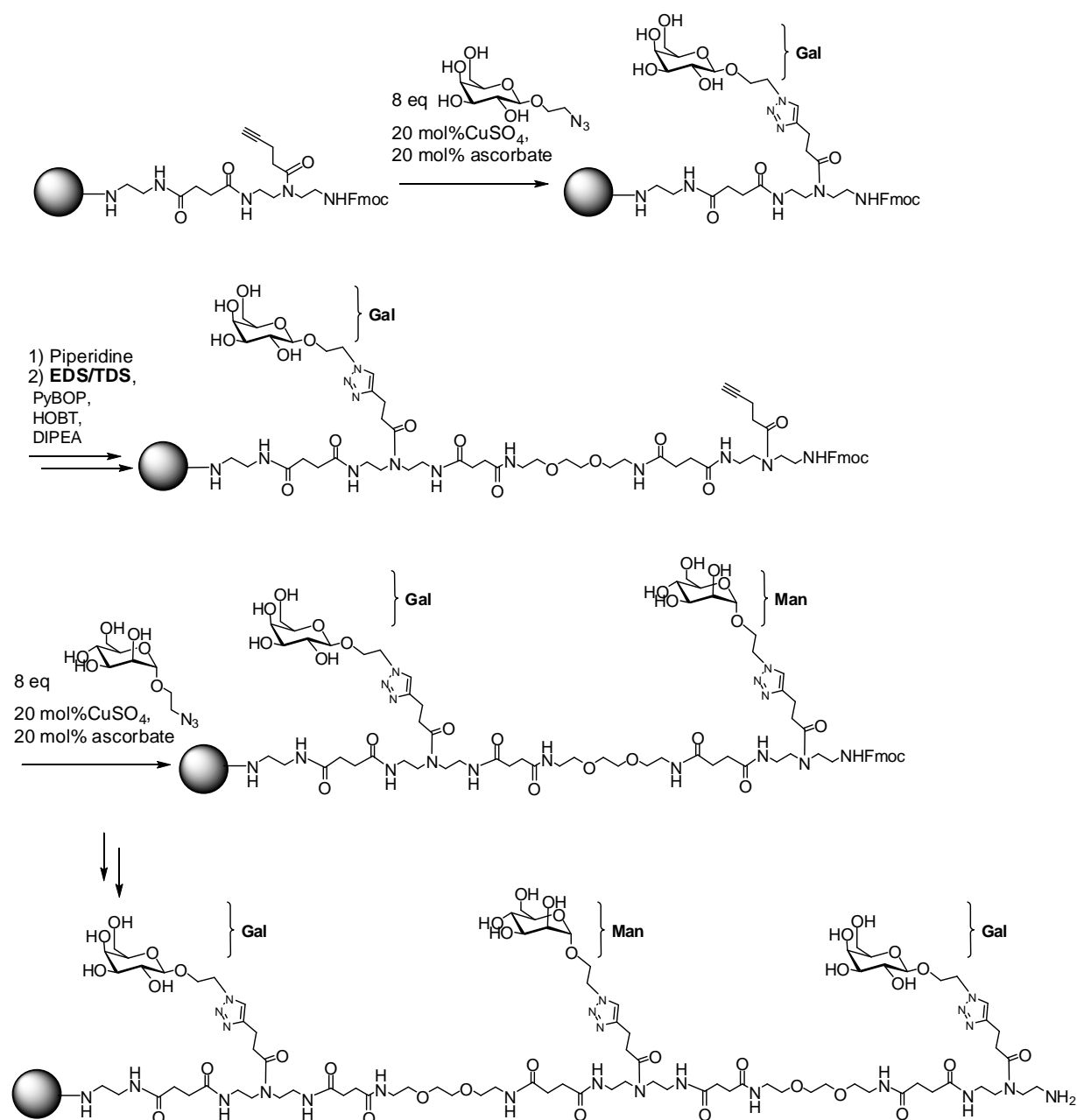
Figure 37: Sequential coupling and conjugation of carbohydrate moieties on solid phase of exemplary heteromultivalent structure GalManGal(1,3,5)-5.

The same reaction conditions (resin, coupling reagents, molar ratios) as previously established for the homomultivalent oligomers were applied for the sequential coupling-conjugation protocol. Directly after coupling of the first TDS building block, CuAAC reaction with 2-azidoethyl galactopyranoside was carried out in presence of the temporary Fmoc protecting group. The previously described click conditions of 8 eq sugar azide, 20 mol% $CuSO_4$ and ascorbate were used here as well. After complete conjugation, the Fmoc protecting group was removed with piperidine. Then, the coupling of the next two building blocks, EDS and TDS,
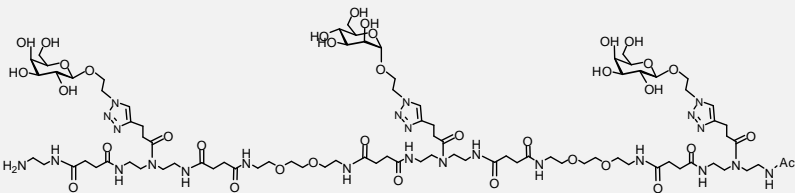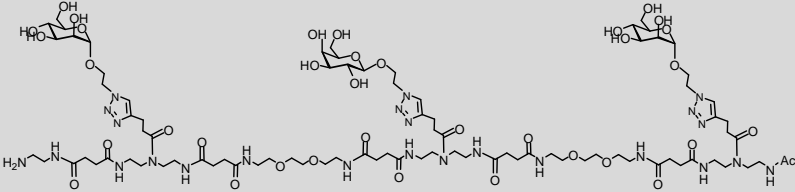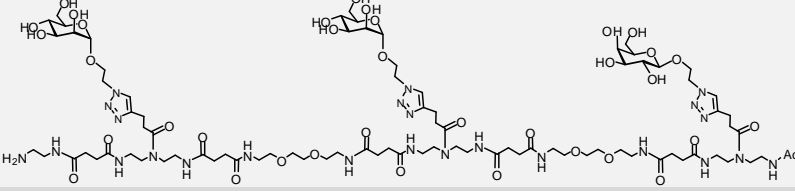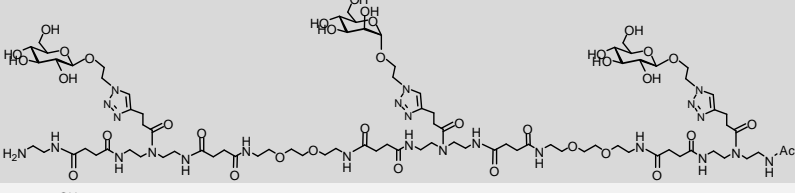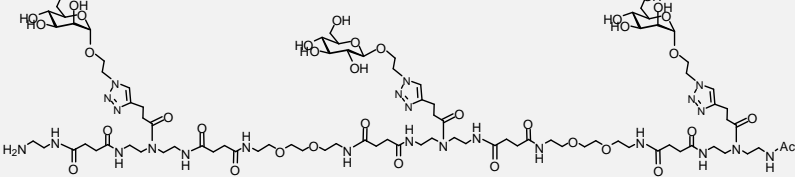
proceeded. The second alkyne presenting TDS was conjugated to 2-azidoethyl mannopyranoside. The sequence of GalManGal(1,3,5)-5 was completed by another coupling of EDS and TDS, followed by conjugation with 2-azidoethyl galactopyranoside. Synthesis of GalManGal(1,3,5)-5 was then finalized by N-terminal Fmoc removal and capping of the released primary amine with Ac$_2$O. Cleavage and isolation was performed as described for homomultivalent structures.

Five different heteromultivalent structures were synthesized (see Table 4) according to the sequential coupling-conjugation protocol. They represent analogues of the trivalent Man(1,3,5)-5 oligomer with successive replacement of the Man ligands towards galactose or glucose ligands. Taking into account only the mannose moieties of the heteromultivalent systems, these oligomers can be considered analogues of the monovalent or divalent ligands Man(3)-5 and Man(1,5)-5 with galactose or glucose ligands now occupying the previously non-functionalized positions of the oligomer chain. Nomenclature is again defined by the series of sugar ligands, their position on the backbone in parentheses and the overall number of building blocks after parentheses. GalManGal(1,3,5)-5 consists of one mannose unit at position three, galactose moieties are presented in position one and five and the overall oligomer consists of five building blocks. In structure ManGalMan(1,3,5)-5 this pattern is reversed. ManManGal(1,3,5)-5 presents also two mannose units but on position one and three, on position five a galactose unit is attached. GlcManGlc(1,3,5)-5 presents two glucose moieties on position one and five and one mannose unit in the middle. ManGlcMan(1,3,5)-5 is again a reverse analog of this structure.

3. Results and Discussion

Table 4: Overview of the heteromultivalent structures, short graphical representations and names.

Compound	Heteromultivalent Structure
GalManGal(1,3,5)-5	
ManGalMan(1,3,5)-5	
ManManGal(1,3,5)-5	
GlcManGlc(1,3,5)-5	
ManGlcMan(1,3,5)-5	

The synthesized structures were characterized by ESI-MS and ^{1}H-NMR (see Figure 38). The purity of the compounds was determined by RP-HPLC. Figure 39 shows the obtained chromatograms of the heteromultivalent structures. The crude products directly from resin were obtained in a high purity of above 95%.

Figure 38: Exemplary ¹H-NMR of ManGalMan(1,3,5)-5 (recorded in D₂O). The protons of selected structural units are marked with colored boxes.

RP-HPLC: 5/95 MeCN/H₂O→ 70/30 MeCN/H₂O in 60 min

Figure 39: RP-HPLC of the synthesized heteromultivalent structures. They all show a similar retention time of 16.6 min. The purity of the crude compounds is above 95%.
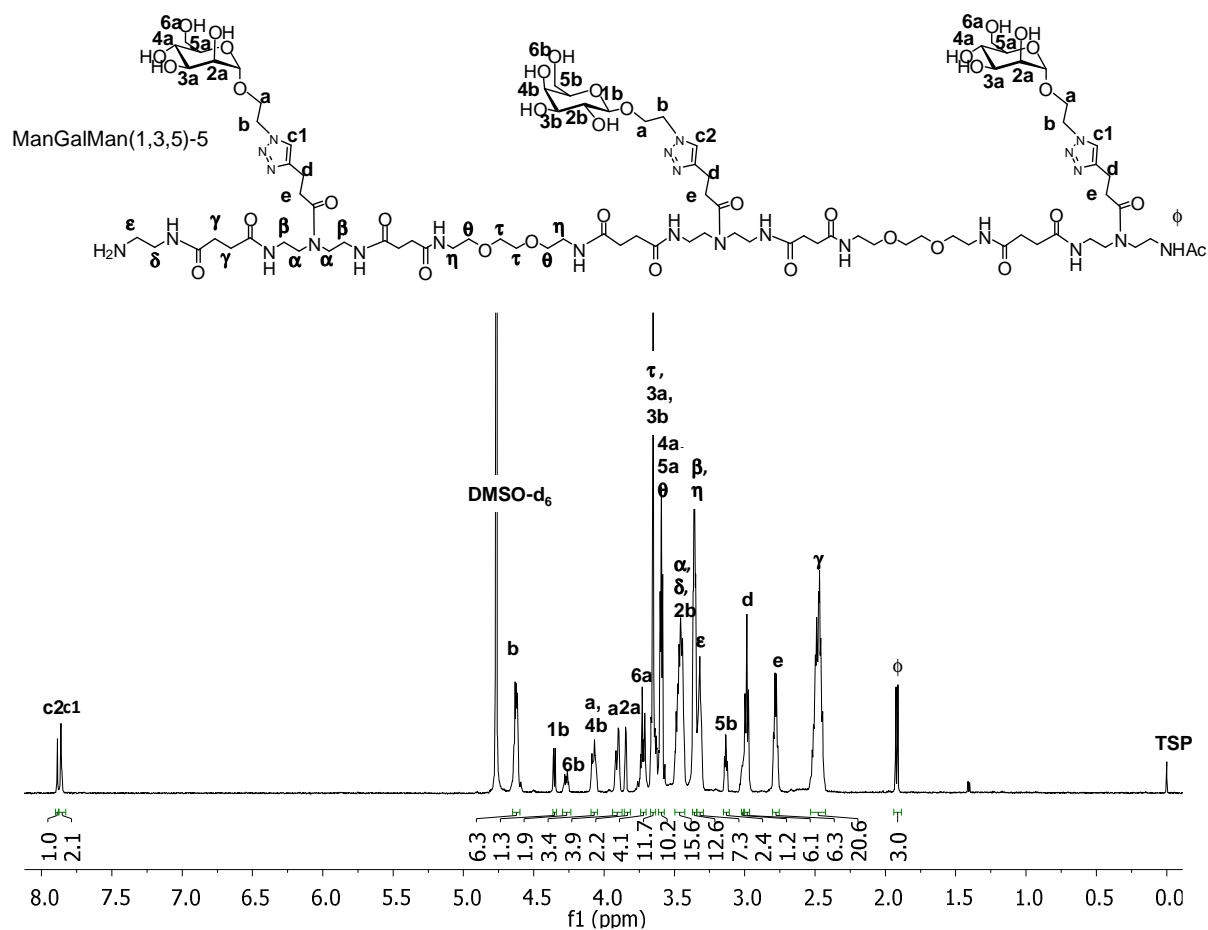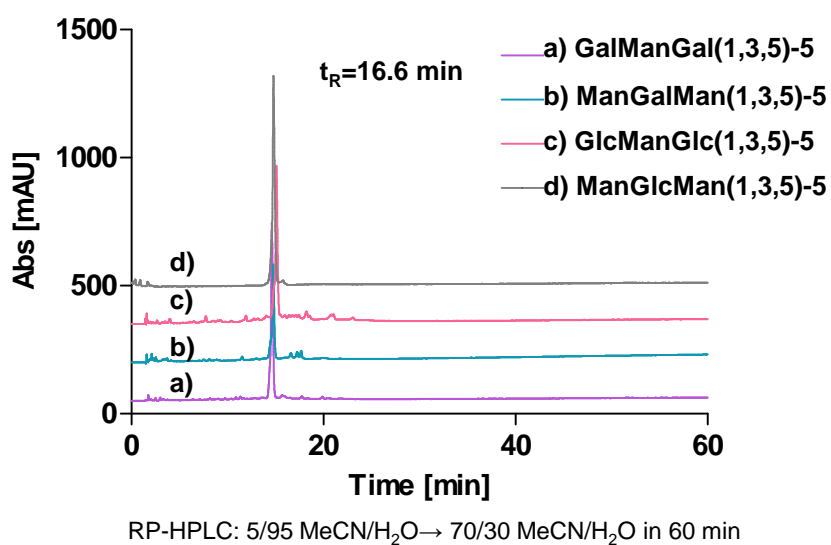
3.2.3. Photoswitchable Glycooligomers

So far, the synthesis of glycooligomer structures varying the position, number and kind of sugar ligands was described. While for the homomultivalent ligands the focus was on variations of the sugar ligand density and position along the scaffold, the heteromultivalent structures combined different sugar ligands. However, so far EDS as hydrophilic and flexible spacer unit has been used exclusively, thus giving no variations in the backbone properties. Not only the number, position and kind of sugar ligand can influence the resulting binding properties of the glycooligomers but also the physicochemical properties of the backbone can influence their interactions with protein receptors. In order to investigate the influence of the scaffold, a third set of glycooligomer now applying an AZO spacer building block was synthesized. On the one hand, AZO is a hydrophobic, stiff spacer building block derived from azobenzene. On the other hand, this moiety has the special attribute to change its configuration (trans→cis) upon irradiation with light. By the introduction of such a building block into the main chain of the glycooligomer, the overall conformation of the scaffold should change upon irradiation. This would result in a different spatial orientation of the carbohydrate moieties presented on the oligomer scaffold.

The synthesis of the AZO spaced structures proceeded according to the synthesis of the homomultivalent structures replacing EDS by AZO building blocks.
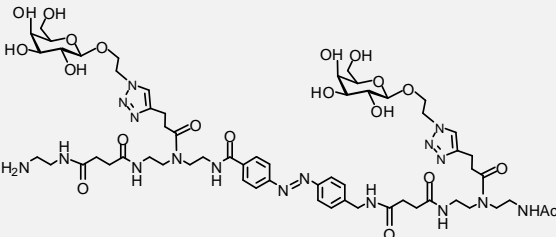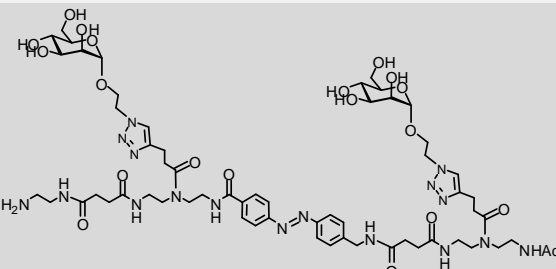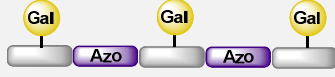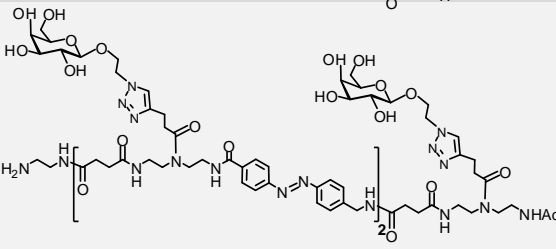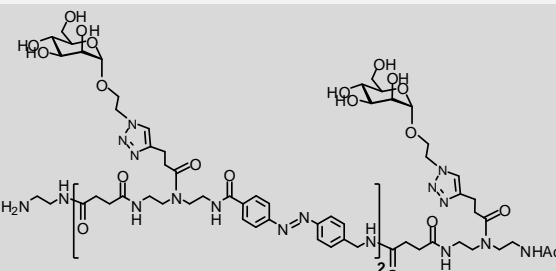
In detail, an exemplary synthesis of AZO-Gal(1,3)-3 is proceeded as following: As initial step, a TDS building block, displaying one alkyne moiety in the side chain, was coupled to the ethylenediamine linker attached to the resin. The same reaction conditions (resin, coupling reagents, molar ratios) as previously established for the homomultivalent oligomers were applied. After addition of TDS followed by Fmoc deprotection, coupling of the AZO spacer proceeded. The sequence was finalized by attachment of a second TDS building block. Then, the N-terminal Fmoc was cleaved and the released primary amine was capped with Ac_2O. The two alkyne moieties-displayed on the oligoamide backbone were then subject to simultaneous CuAAC reaction with 2-azidoethyl galactopyranosides employing conditions as described above.

All in all, four AZO spaced structures were synthesized (see Table 5). The utilitzed nomenclature in this thesis is now modified by definition of the employed spacer moiety preceeding definition of sugar ligand. Two different AZO spaced sequences were synthesized: AZO-Gal(1,3)-3 and AZO-Man(1,3)-3 consist of overall three building blocks with two sugar moieties and one AZO spacer. AZO-Gal(1,3,5)-5 and AZO-Man(1,3,5)-5 are pentameric structures with two AZO units,

and three carbohydrate moieties. These structures are analogues to the pentameric EDS spaced trivalent structure Man(1,3,5)-5 presented previously.

Table 5: Overview over the AZO spaced structures, short graphical representations and names.

Compound	Photoswitchable Structure
AZO-Gal(1,3)-3	
AZO-Man(1,3)-3	
AZO-Gal(1,3,5)-5	
AZO-Man(1,3,5)-5	

The purity of the crude AZO-spaced structures, determined by RP-HPLC, was ~80%. This represents app. 15% more side products compared to the crude homo- or heteromultivalent oligomers using EDS spacer building block. This result might be attributed to a less efficient coupling of the hydrophobic AZO spacer. Consequently, the crude products were purified by preparative RP-HPLC.

The identity of the synthesized structures was confirmed by ESI-MS and ^{1}H-NMR. The obtained mass-to-charge ratios are summarized in Table 6.

Table 6: Calculated exact mass of the AZO spaced compounds and the m/z found by ESI-MS (positive mode).

Compound name	M_w calcd.	m/z found
AZO-Gal(1,3)-3	1367.6	684.8 $[M+2H]^{2+}$
AZO-Man(1,3)-3	1367.6	684.8 $[M+2H]^{2+}$
AZO-Gal(1,3,5)-5	2119.0	707.5 $[M+3H]^{3+}$
AZO-Man(1,3,5)-5	2119.0	707.5 $[M+3H]^{3+}$

All in all, this chapter described the solid phase synthesis of monodisperse, sequence-defined glycooligomers varying the number, position and kind of sugar ligand as well as the properties of the oligomeric scaffold.

The approach was based on the coupling of building blocks on solid phase in combination with the CuAAc conjugation of sugar azide ligands. By straight-forward variations of the general synthetic protocol, homomultivalent, heteromultivalent and differently spaced glycooligomers were obtained. Due to the high flexibility and variability of the solid phase approach, oligomers varying individual structural parameters known to influence multivalent binding could be readily obtained. In total, ten homomultivalent glycooligomers varying number and distance between sugar ligands were obtained. The inherent heterogeneity of natural oligosaccharides was copied by synthesizing heteromultivalent oligomers. Therefore five trivalent structures carrying two different carbohydrate moieties in different combinations were synthesized. Finally, a first set of photoswitchable glycooligomers was obtained by introducing the AZO spacer building block. The successful synthesis of the presented set of highly-defined glycooligomers as well as product isolation in high purity and yield underlines the versatility of the developed solid phase strategy based on coupling novel functional building blocks on solid support.

In the next chapter, the different glycooligomers will be used as multivalent glycomimetic ligands in lectin-receptor binding studies investigating the influence of the chemical structure on the resulting binding affinity.

3.3. Lectin Binding Studies

So far, the synthesis of sequence-defined, monodisperse glycooligomers via solid phase coupling of tailor-made building blocks was presented. These glycomimetic structures will now be used in lectin-receptor binding studies for the study of multivalent effects.

Synthetic sugar ligand presenting scaffolds have been used before as binding ligands for different biological receptors as described in chapter 1.2. Studies with glycodendrimers and – polymers showed binding enhancements caused by increased number of sugar ligands[138], optimal density of carbohydrate moieties[78] and optimal spacing between sugar ligands matching the distance of binding pockets on the receptor[31,36]. In addition, scaffold composition[33] and heterogeneity[137] of sugar ligands play a role in multivalent binding. However, these parameters were mainly observed independently or even in contradiction depending on the scaffolds or synthetic strategies used. Studies investigating the underlying multivalent binding effects in a more generalized fashion are scarce.[37,39,44] This is mainly hampered by the low structural variability of the used scaffolds and the difficulty to vary structural parameters individually.

This limitation can be overcome with the synthetic platform presented in this thesis. Glycooligomers varying the number, position and kind of sugar ligands presented along different scaffolds will be subject to ligand-receptor binding presented in this chapter. It is divided into three subchapters: At first the influence of number and spacing of sugar ligands within homomultivalent glycooligomers will be examined. Then, the effect of heterogeneity in sugar ligand presentation combining binding sugars with non-binding sugar ligands will be investigated. In the third subchapter, the effect of both, stiffness/flexibility and hydrophilicity/hydrophobicity, will be examined by the use of different spacer units incorporated into the backbone. Moreover, the spatial distribution of sugar ligands presented on the glycooligomers will be examined. This change can be induced by a light triggered change in cis/trans isomerization of the applied AZO building block resulting an overall change in conformation of the backbone.

Different binding assays were used to determine the glycooligomer-receptor interactions and gain deeper insight into the molecular mechanism of ligand-receptor interaction. Each binding assay has its specific measurable range and limitation which helps to elucidate certain effects in multivalent binding.

3.3.1. Homomultivalent Glycooligomers

A first series of homomultivalent oligomers was presented in chapter 3.2.1 differing in the number of mannose ligands as well as the overall length of the scaffold. In this chapter, this new platform will be evaluated regarding their receptor binding. Concanavalin A (Con A) was chosen as target receptor, because it presents an ideal model lectin due to its well characterized structural features. Additionally, it has relevance as model lectin for e.g. mannose binding FimH present on bacteria and thus potential biomedical applications of glycooligomers e.g. in antibacterial therapy.

Con A is a plant lectin isolated from jack bean seeds (Canavalia ensiformis). It exists as tetrameric form at pH higher than 7, as dimer at pH lower than 6. Each monomer is equipped with one saccharide binding site as well as a Mn^{2+} site and a Ca^{2+} site. Its binding pockets are 6.5 nm apart, as determined by x-ray crystal structures.[139] Con A binds with high affinity to mannose and a four times lower affinity to glucose.[140] Apart from being a model receptor for biologically relevant lectins, binding of Con A was reported for many different mannose-presenting carbohydrate mimetics.

For the quantification of ligand-receptor binding and a comparative study of the glycooligomer-Con A interactions, a variety of well-established binding assays can be potentially employed.[141] In the following section of this thesis, different assays will be applied to characterize the binding of glycooligomer ligands trying to look at different aspects of the ligand/receptor interactions. Binding affinities of *all* the homomultivalent glycooligomers, mono- to decavalent, were determined by an inhibition/competition assay using soft colloidal probe reflection interference contrast microscopy (SCP-RICM) which will be discussed at first. These studies were complemented with other assays (dual focus fluorescence correlation spectroscopy, inhibition/competition SPR assay, turbidimetry assay) in order to analyze in more detail specific binding effects of single oligomers.

SCP-RICM is based on the adhesion of ligand-functionalized hydrogel beads on a receptor-functionalized glass surfaces resulting in ligand-receptor interactions at the interface and a defined contact area. This contact area can be detected via optical microscopy and is directly related to the adhesion energy via the Johnson-Kendall-Roberts model (JKR).[142] Glycoligands can now be added to this set-up as inhibitors of the particle/surface adhesion. With increasing concentration of the inhibitor, the contact area will decrease until the particle detaches from the surface. Plotting the inhibitor concentration dependent decrease in adhesion energy (contact area) will give a sigmoidal curve that can be fitted with the Hill equation and derives the so-called IC_{50} values for ligand affinity (the inhibitory concentration where 50% of the ligand-

receptor interactions at the interface are released in favor of inhibitor-receptor binding).

Therefore the SCP-RICM technique allows for inhibition/competition studies of the here presented glycooligomers and the determination of their IC_{50} values. [143]
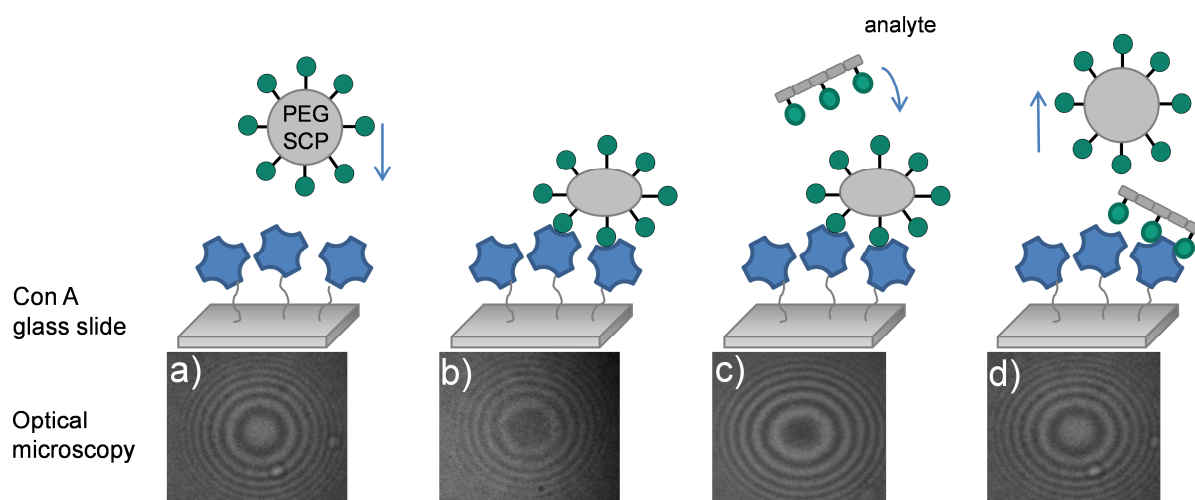
Figure 40: Principle of inhibition/competition assay based on SCP-RICM. a) and b): A mannose functionalized, soft PEG particle (SCP), binds to a Con A functionalized glass slide. The induced deformation of the soft particle is monitored by an optical microscope, showing a distinct interference pattern. c) and d): By addition of inhibitor, *e.g.* glycooligomer, the PEG particle detaches from the glass surface which induces a change in interference pattern. With this effect, adhesion energies are obtained, which are calculated in IC_{50} values.

Specifically, a glass slide was functionalized with Con A and PEG hydrogel beads were functionalized with Mannose. During the experiment, the mannose functionalized PEG particle (SCP) sedimented onto the Con A covered surface (Figure 40 a). Binding between the SCP and Con A glass slide occured resulting in a deformation and adhesion of the particle. This distinct contact area was measured by an optical microscope (Figure 40 b) and used to calculate the surface energy via JKR model. For the inhibition assay, this initial energy was set as 100% binding.

Upon addition of glycooligomer solution, binding between SCP and Con A surface was inhibited as glycooligomer bound to the Con A surface and therefore blocked binding of the SCP. A decrease in contact area of the SCP to the Con A covered glass slide was observed (Figure 40 c). Further addition of glycooligomer led to a complete detachment of the SCP. Serial dilutions of glycooligomers were measured resulting a decreasing surface energy. Plotting the decrease in adhesion energies derived from the contact area of SCPs against the increasing concentration of glycooligomer inhibitor gave sigmoidal curves. They were fitted with Hill equations resulting in IC_{50} values as measure for the inhibitory affinity of the glycooligomers.

This inhibition/competition assay was used to determine the affinities of the homomultivalent glycooligomers Man(3)-5, Man(1,5)-5, Man(1,2)-5, Man(1,3,5)-5, Man(all)-5 and Man(all)-10.

Gal(1,3,5)-5 and EDS-5 were measured as negative controls. Both Gal(1,3,5)-5 and EDS-5 show no affinity to Con A thus confirming no unspecific interactions of either scaffold or non-binding ligands. Methyl α-D-mannose (α-Me-Man) was applied as positive control as well as monovalent reference for comparison of the multivalent glycooligomers. A binding affinity of 620±20 μM was determined which represents a value similar to values previously reported in literature.[40,60,144–147]

Serial dilutions between 0.5 μM and 100 μM of the mannose presenting glycooligomers Man(3)-5, Man(1,5)-5, Man(1,2)-5, Man(1,3,5)-5, Man(all)-5 and Man(all)-10 were measured. Figure 41 shows the obtained data points with their respective fit curves. Monovalent Man(3)-5 showed the lowest binding affinity. Divalent Man(1,2)-5 and Man(1,5)-5 showed enhanced affinity compared to monovalent Man(3)-5. Comparing symmetric divalent Man(1,5)-5 structure and asymmetric Man(1,2)-5, a similar binding was observed. The trivalent Man(1,3,5)-5 glycooligomer presented a significantly enhanced affinity compared to the mono- and divalent species. For Man(all)-5 and Man(all)-10, penta- and decavalent structures, further increases in binding affinity were observed.
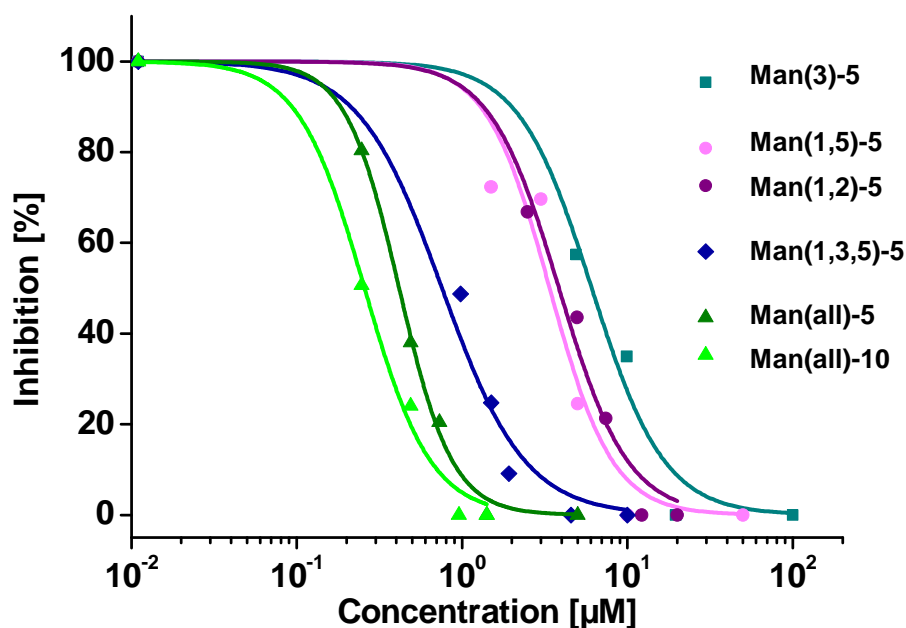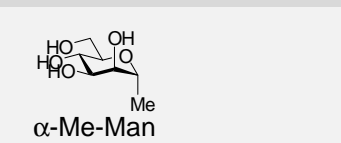
Figure 41: Binding curves of glycooligomers Man(3)-5, Man(1,5)-5, Man(1,2)-5, Man(1,3,5)-5, Man(all)-5 and Man(all)-10 determined by SCP-RICM. The error values are smaller than the symbols.

All glycooligomers show the expected sigmoidal dependence of the adhesion energy with increasing ligand concentration. Therefore all curves were fitted with Hill equations and inhibition concentration values (IC$_{50}$) were determined at 50%, the half point, of the curves (see Table 7). Relative activity (RA) was calculated by division of the IC$_{50}$ value of α-Me-Man by a

valence corrected IC_{50} value of the structure (*e.g.* trivalent →620 μM/(IC_{50} [μM]·3)). Relative activities allow for the comparison of the binding affinities obtained in this thesis to values reported in literature. Furthermore it is a measure for multivalency as a structure bearing x binding ligands should result in an increase of binding affinity more than x times and thus a relative affinity higher than one.

Table 7: IC_{50} values and relative affinities (RA) determined by SCP-RICM.

Compond	IC_{50} [μM] (SCP-RICM)	Relative activity
Man(3)-5	6.1±0.7	102
Man(1,5)-5	3.4±0.5	91
Man(1,2)-5	3.9±0.3	79
Man(1,3,5)-5	0.8±0.1	258
Man(all)-5	0.4±0.1	310
Man(all)-10	0.3±0.1	206
α-Me-Man	620±20	1

All structures showed an inhibitory potential in the low micromolar range. The binding of the different glycooligomers in order of their number of sugar ligands will be discussed in the following:

The monovalent Man(3)-5 structure yields a binding affinity of 6.1±0.7 μM. A relative activity of 102 was obtained. This means that the binding of Man(3)-5 is app. 100 times increased

compared to monovalent reference α-Me-Man, although displaying only one mannose unit. This is a very surprising result which has not been observed in literature so far. The only examples which report small increases in binding affinity with modified mannose ligands were shown by Roy et al. who reported a *p*-nitrophenyl mannose derivate with a 8.7 times better relative activity than α-Me-Man determined by enzyme linked lectin assay (ELLA).[40] Lindhorst et al. reported mannose with aromatic aglycon having a relative potency of 39 as inhibitor for E.coli.[148] However, no example for the measurement of a potential multivalent scaffold presenting only one sugar ligand has been reported in literature. Man(3)-5 is composed mainly of hydrophilic ethylene glycol based spacer units. Ethylene glycol structures, *e.g.* PEG, are known to be highly hydrated when dissolved in water. It is also known that contacts between the ligand and the protein are often mediated by water molecules, with water acting as a molecular "mortar". [8,50,52] Therefore, potentially the hydration shell around Man(3)-5 could enhance its binding affinity due to release of water upon binding and a resulting gain in entropy.

Man(1,5)-5, presenting two mannose units, showed an IC_{50} of 3.4±0.5 µM which is app. half of the IC_{50} of the monovalent Man(3)-5 structure. This relates to a relative activity (RA) of 91. As described above, RA is calculated by division of the IC_{50} value of α-Me-Man by a valence corrected IC_{50} value of the structure which allows for a comparison of the binding affinities obtained in this thesis to values reported in literature.

The observed relative activity of the divalent glycooligomer is high compared to literature values for other, comparable divalent systems. Toone et al. reported a relative activity of 2 (380 µM) for a divalent structure with aromatic core (hemagglutination assay).[46] Roy et al. observed IC_{50} values between 12-69 (6 and 37 µM) for divalent aliphatic structures measured by ELLA.[40]

One possible multivalent effect contributing to the binding of multivalent ligands is chelate binding where at least two ligands attached to a scaffold bind simultaneously to two binding sites of the receptor (see Figure 42).
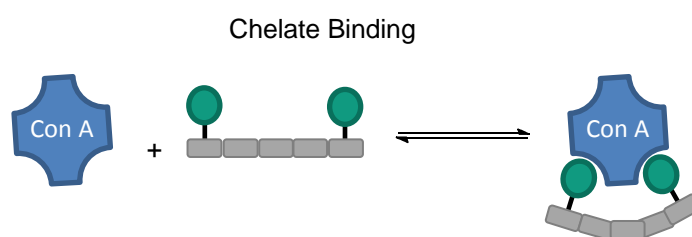
Figure 42: Schematic representation of chelate binding between Con A receptor and divalent glycooligomer.

Binding affinity is increased about three to five orders of magnitude[31,36,37] because translational and rotational entropic penalties were already brought up by the first binding event and need to be paid only once.[34,35] The distance between sugar ligands has to be optimal for chelate binding.[36,37] The two mannose moieties of Man(1,5)-5 considering an all-trans linear conformation (determined by addition of bond lengths) span from anomeric center to anomeric center app. 7 nm. This distance is very similar to the distance of the two binding sites of Con A which are ~6.5 nm apart. An all-*trans* linear conformation however is questionable since the structure is highly flexible and therefore likely to engage in a coiled conformation.

In order to examine the hypothesis of chelate binding, a divalent structure was chosen which structurally precludes chelating binding due to a very small distance between sugar ligands. Therefore, an asymmetric structure with two mannose units adjacent on positions 1 and 2 (spanning app. 2.7 nm, determined as above) was synthesized. With the here described approach of solid phase synthesis of glycooligomers such a structure can be synthesized straight-forward by a simple change in the synthesized sequence. This again highlights the versatility of this approach. Man(1,2)-5 yields a binding affinity of 3.9±0.3 µM and a relative activity of 79. Interestingly, these values are identical within the error to the relative activity observed for Man(1,5)-5. As there is no change in affinity, it is assumed that a chelate binding is unlikely for the divalent structures. It can also be concluded that Man(1,5)-5 with mannose ligands on both ends probably does not engage in a linear conformation (see Figure 43).
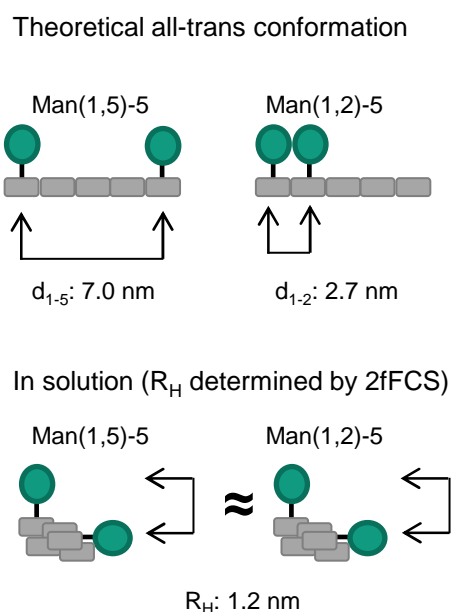
Figure 43: Schematic representation of change in conformation of EDS spacers.

From measurements of trivalent Man(1,3,5) (results will be shown in the next chapter), it is known that the pentameric trivalent all Mannose glycooligomer has a hydrodynamic radius of

app. 1.2 nm in solution. This most likely stems from the highly flexible EDS spacers incorporated in the main chain. This linker unit is based on ethylenedioxy units (PEG-like) connected by amide bonds. It has been proposed in literature that PEG-based spacers tend to decrease in end-to-end distance by three times in comparison to a theoretical all extended conformation due to coil formation.[36,149] Similar effects and thus similarly small hydrodynamic radii can be expected also for the pentameric divalent glycooligomers and thus a chelate binding is highly unlikely.

Nevertheless, the high relative activity of 80 indicates additional binding effects leading to an increase in binding affinity. Another important effect observed in multivalent binding is the so-called statistical rebinding. This effect describes the equilibrium of binding and dissociation of multiple sugar ligands in close proximity to a single receptor binding site (see Figure 44). As one binding ligand dissociates from the protein, another ligand is readily available to take its place[39].
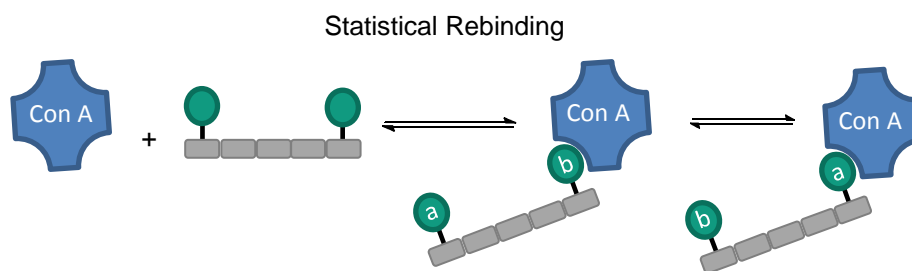
Figure 44: Schematic representations of multivalent effect of statistical rebinding between Con A receptor and glycooligomer.

This also called bind-and-slide-effect[8,44] was shown to result in one order of magnitude gain in affinity [39] which is indeed consistent with the observed binding affinities of the divalent glycooligomers.

Furthermore, it is known that this effect is favored by a high local concentration of binding sugars.[45] Therefore rebinding occurs favorably when the ligands are in close proximity. The conformation of the oligomeric backbone resulting in a small distance of 1.2 nm between the mannose ligands therefore should lead to the identical binding affinities of Man(1,5)-5 compared to Man(1,2)-5 (see Figure 43).

Trivalent Man(1,3,5)-5 structure exhibited an IC_{50} of 0.8±0.1 µM, corresponding to a relative activity of 258. Hence, Man(1,3,5)-5 binds app. three times better than the two divalent ligands, Man(1,5)-5 and Man(1,2)-5, regarding relative activity. A comparison to literature known

affinities of trivalent glycostructures proves that this affinity is exceptionally high. Literature known trivalent structures showed IC_{50} values e.g. of 17 µM (RA=31) determined by hemagglutination assay[46], 21.2 µM (RA=2.6) determined by SPR assay[150] and 22 µM (RA=12) [151] determined by ELLA. The observed high binding enhancement could be again discussed regarding a combination of chelate effect and statistical rebinding. Again, a chelate effect is highly unlikely due to the compact coil conformation of the pentameric oligomer backbone as was previously discussed Man(1,3,5)-5 displays only one additional mannose ligand compared to the divalent ligands while yielding a three times enhanced binding affinity. Partially, this can be rationalized by an enhanced effect of statistical rebinding but probably not to such a large extent. Therefore the exceptional high binding affinity of the trivalent structure has to be examined more detailed.

As stated above, SCP-RICM inhibition/competition assay was measured for all homomultivalent structures, mono- to decavalent. So far the results of the mono- to trivalent glycooligomers have been discussed. However, in order to further evaluate potential binding mechanisms for these three structures, additional binding experiments were performed and will be discussed in the following section. The discussion of SCP-RICM binding results for penta- and decavalent structures will be continued at the end of this chapter.

An additional inhibition/competition binding assay based on surface plasmon resonance (SPR) was performed with the mono-, di- and trivalent glycooligomers Man(3)-5, Man(1,5)-5 and Man(1,3,5)-5. In contrast to the SCP-RICM assay, here glycooligomer and Con A will form a binding complex in solution and a potential influence of the ligand- and receptor-presenting surfaces should be excluded. In this assay, binding of Con A in solution to a mannose functionalized SPR sensor chip is measured. The obtained binding signal determined for Con A alone relates to 100% binding. Upon addition of inhibitor, less Con A is available to bind to the surface, thus the response signal decreases. By measuring serial dilutions of glycooligomers preincubated with Con A, decreasing binding is observed. Plotting the obtained inhibition in percent over concentration, results in sigmoidal curves similar to those determined by SCP-RICM assay. By fitting the obtained data points with Hill equations, IC_{50} values are obtained.

In detail, a 0.1 µM solution of Con A was injected in a continuous flow over a α-D-mannose poly(acrylamide) (M_w app. 10 kDa) modified SPR sensor chip (see Figure 45). The obtained binding signal with only Con A in the flow solution was set as 100% binding.
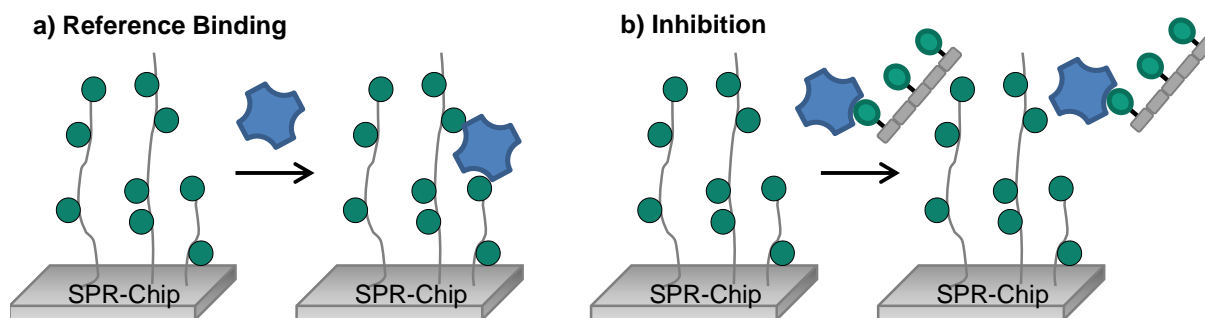
Figure 45: Schematic representation of the SPR inhibition/competition assay. The gold sensor surface is functionalized with a mannose polymer. a) A binding signal is detected by flowing the lectin over the surface. The obtained response is set as 100% binding. b) By addition of glycooligomer as inhibitor, less Con A is available to bind to the sensor surface thus the binding signal is decreased.

Concentrations from 0.3 up to 100 μM of the glycooligomers were measured showing a decrease in binding. Figure 46 shows the binding curves obtained by plotting the inhibition in percent over the individually measured concentrations of glycooligomer. Each data point presents the mean of at least three measurements; the error is the standard deviation. An unfunctionalized TDS-(1,3,5)-5 backbone without sugar ligands served as negative control to rule out unspecific binding of the backbone. As expected, no binding was measured for this control. Binding of α-Me-Man was measured as positive control yielding an IC_{50} of 750 μM which is comparable to literature known values[40,60,144–146] and the IC_{50} value obtained by SCP-RICM.
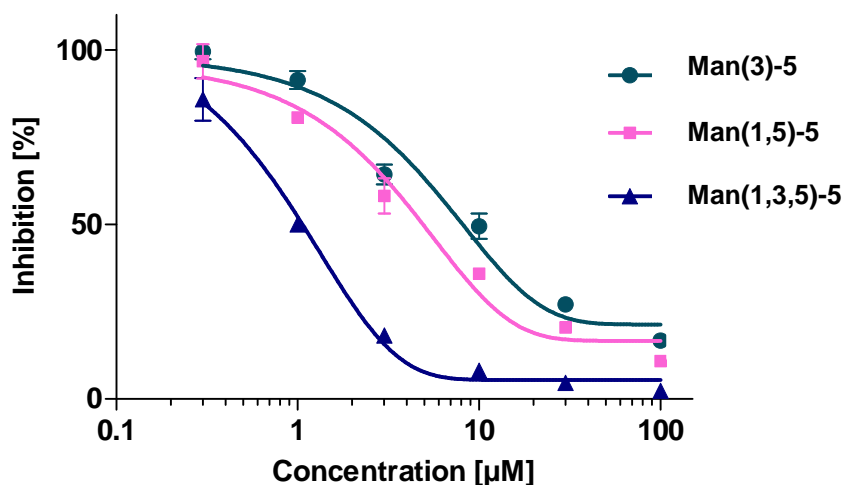
Figure 46: Binding curves of mono-, di- and trivalent glycooligomers determined by SPR inhibition assay. Some error values are smaller than the symbols.

The binding curves of Man(3)-5, Man(1,5)-5 and Man(1,3,5)-5 show the same trend as previously measured by SCP-RICM. The mono- and divalent structure yield a similar binding, whereas the trivalent structure has a high gain in affinity. Also regarding IC_{50} values and relative activities, very similar values compared to SCP-RICM were obtained (see Table 8).

Table 8: IC$_{50}$ values and relative affinities determined by inhibition SPR.

Compound name	IC$_{50}$ [µM]	RA
Man(3)-5	8	96
Man(1,5)-5	5	77
Man(1,3,5)-5	1	257
α-Me-Man	750	1
TDS-(1,3,5)-5	not binding	-

This result is on the hand encouraging since it confirms the obtained measured values by SCP-RICM. On the other hand no different effect in binding could be detected. This leads to the assumption that SPR technique is able to detect the same binding phenomena as SCP-RICM.

Another standard assay often used for characterizing the ligand-receptor complex formation is the turbidimetry assay. This assay is based on a rise of turbidity by the formation of insoluble complexes between glycomacromolecules and Con A (see Figure 47). This can be measured by absorbance changes at 450 nm over time of app. equimolar solutions (~50 µM) of Con A and glycooligomer in buffer.
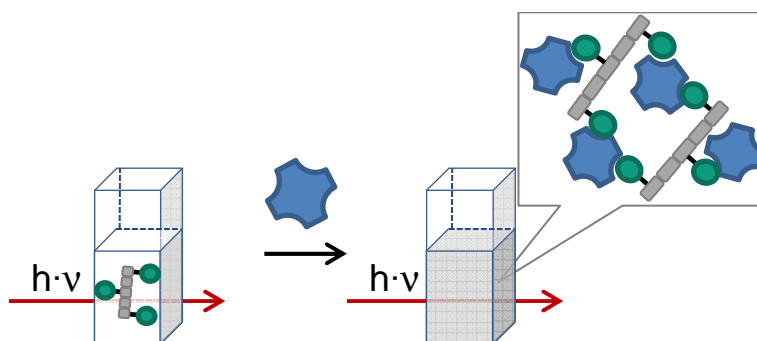
Figure 47: Schematic representation of the turbidimetry assay. A solution of glycooligomer in buffer is placed in a quartz cuvette. Upon addition of an equimolar solution of Con A in buffer, turbidity of the previously clear solution arises resulting in a decrease in detected light. It indicates a crosslinking between the glycooligomer and Con A molecules which results in the formation of insoluble complexes.

Man(3)-5, Man(1,5)-5 and Man(1,3,5)-5 were examined by turbidimetry assay. Figure 48 shows the obtained data points. Mono- and divalent Man(3)-5, Man(1,5)-5 show no increase in absorption, thus no formation of insoluble clusters proceeds. In contrast, trivalent Man(1,3,5)-5 yields full absorption within 189 s showing cluster formation. This indicates the necessity of at least three mannose ligands to induce crosslinking between several Con A molecules. It is important to note that crosslinking would be an unwanted effect in all other binding

experiments (e.g. inhibition competition experiments). Therefore cluster formation was excluded by using Con A in much lower concentration compared to the ligand.
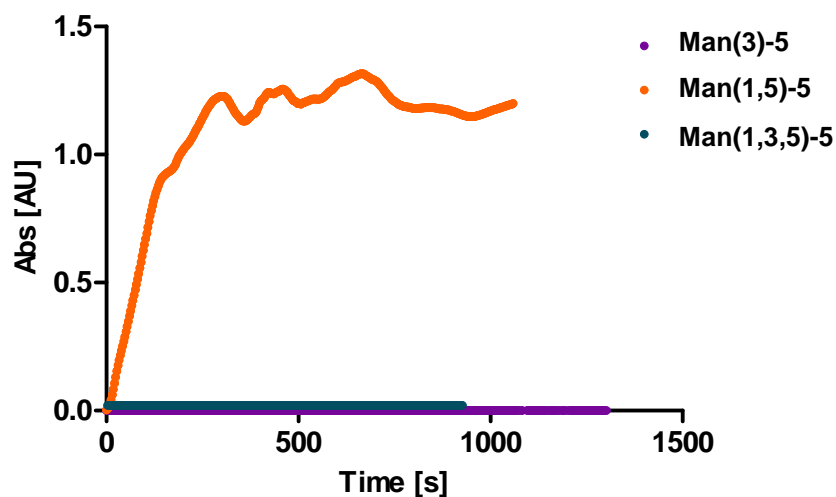
Figure 48: Turbidimetry assay detected by UV-VIS spectroscopy of Man(3)-5, Man(1,5)-5 and Man(1,3,5)-5.

Although turbidimetry measurements gave a first indication for the formation of clusters, this method is limited to a qualitative observation of this effect. Affinities cannot be determined as in the above described SCP-RICM and SPR inhibition/competition measurements. In order to investigate the effect of cluster formation also in terms of affinity, a different assay has to be used.

In order to investigate the binding of Man(1,3,5)-5 further, dual focus fluorescence correlation spectroscopy (2fFCS) was performed in cooperation with by Pauline Maffre and Prof. Dr. Ulrich Nienhaus, KIT. This assay derives three parameters: By measuring the hydrodynamic radius the initial size of the glycooligomer, the size of the glycooligomer-Con A complex and the binding affinity in solution can be determined.

2fFCS[152] is a single-molecule based technique using fluorescence emission time correlations to determine hydrodynamic radii.[153,154] It involves the detection of fluorescently labeled molecules diffusing in and out of the detection volume of a confocal microscope setup. Their size can be precisely determined from the transit times through the volume. Man(1,3,5)-5 was labeled with a fluorescence marker (Atto 647N) which was coupled as an NHS ester to the primary amine at the C-terminus of the backbone. The glycooligomer was then incubated with Con A solutions of increasing concentrations ranging from 0.5 to 50 µM. Hydrodynamic radii were calculated from experimentally obtained diffusion coefficients via the Stokes-Einstein relation. Hydrodynamic

radii (R_H) are plotted in Figure 49 as a function of the Con A concentration.
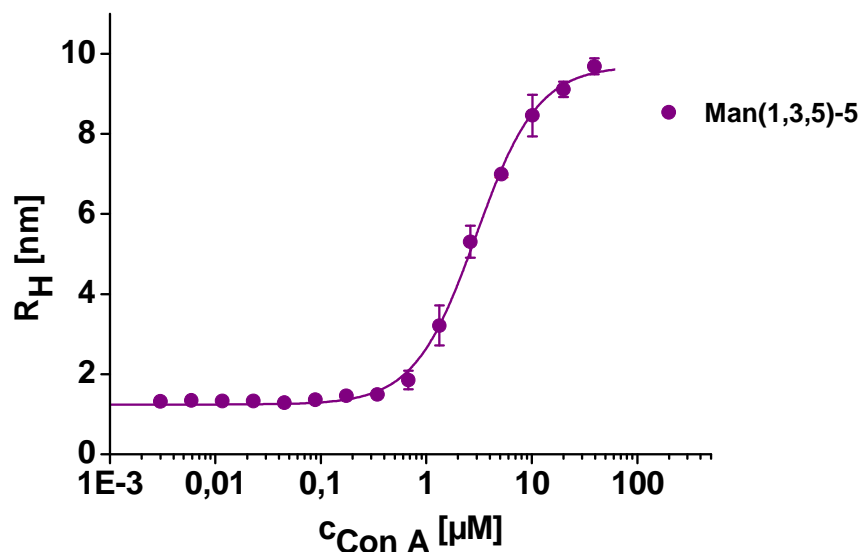
Figure 49: 2fFCS measurement of Man(1,3,5)-5. It can be seen that the hydrodynamic radius of the lectin/glycooligomer complex rises quickly with increasing concentration of Con A.

In absence of the protein, Man(1,3,5)-5 resulted a hydrodynamic radius of 1.2 nm. Upon addition of Con A, a size increase of up to 8.5±0.1 nm was observed. The hydrodynamic radius of Con A is known to be 4.3 nm.[155] Therefore it is indicated that there is no 1:1 complex between Con A and Man(1,3,5)-5 present, since this would have an approximate size of 5.5 nm. It was then examined if multiple Man(1,3,5)-5 are involved in the complex by measuring the brightness of the molecules diffusing through the detection volume. If multiple glycooligomers were to bind to one Con A molecule, an increase in brightness would be expected due to their fluorescence label. No increase in brightness of the diffusing structures at different Con A concentrations was observed (see Figure 50).
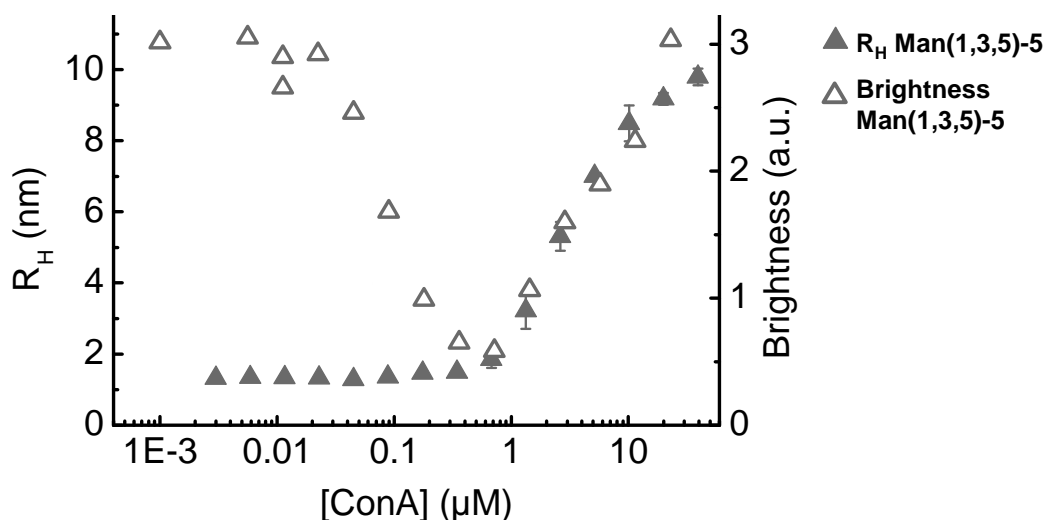
Figure 50: Brightness study of Man(1,3,5)-5 together with R_H for comparison. With increasing concentration of Con A the brightness of the fluorescent labeled glycooligomer does not exceed its hydrodynamic radius. Therefore complexation of several glycooligomer units to the Con A receptor can be excluded.

Therefore, it is concluded that a single Man(1,3,5)-5 molecule interacts with several Con A molecules, at least two, to generate the additional size increase of 3.1 nm with respect to the 1:1 complex.

By fitting the obtained data points with Hill equations, K_D' values which present the concentration of free Con A at the transition midpoint were calculated. K_D' is comparable to the IC_{50} values obtained by the inhibition/competition SCP-RICM and SPR experiments, since both describe the ligand receptor interaction at 50% binding. A K_D' of 3.0.±0.1 µM for Man(1,3,5)-5 was obtained. Hence, the affinity obtained by this solution based assay is three times higher than the affinity of app. 1 µM determined by surface based SCP-RICM and SPR assays; however it is in the same order of magnitude.

It can be concluded from the hydrodynamic radii studies of Man(1,3,5)-5 that glycooligomers presenting at least three mannose can lead to intermolecular crosslinking between several Con A molecules. This formation of soluble clusters is one of the described multivalent binding mechanism which result in increased binding affinity (see Figure 51). Such multivalent binding contributions can only be detected by turbidimetry or 2fFCS assays and cannot be differentiated by other assays such as SPR or SCP-RICM.
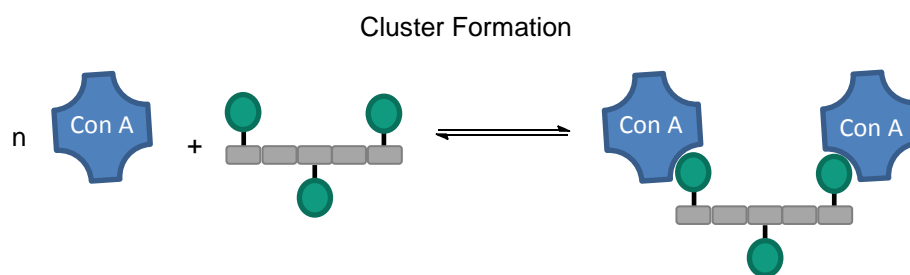
Figure 51: Schematic representation of the multivalent effect of soluble cluster formation.

From a structural point-of-view, it is not clear why the trivalent mannose oligomer is able to crosslink two Con A receptor molecules and a divalent glycooligomer is not. It is known from literature that a trimannosyl-moiety 3,6-di-O-(α-D- mannopyranosyl)-α-D-mannopyrose which is located on the outer arm of natural oligomannose-type carbohydrates presents a major epitope recognized by Con A.[140] A significant enhancement in affinity for glycomimetics scaffolds displaying three mannose ligands compared to di- or even tetravalent systems was also reported by Toone et al[46], Lehn et al[146] and Nishida et al[156]. It was suggested that the trimannosyl motif yields enhanced binding due to the recognition by an extended binding site present on Con A.[53,157,158] This effect was termed subsite multivalency.[55] At this point this effect can neither be excluded nor attributed to the binding of trivalent glycooligomers.

So far, binding of mono- to trivalent structures presenting one to three mannose ligands on the oligomer scaffold was examined in this thesis. Affinities were at first determined by inhibition/competition assay measured by SCP-RICM. These results were confirmed with SPR assay showing very similar inhibition values. Additional turbidimetry and 2fFCS measurements indicated that starting from the trivalent system, the multivalent effect of intermolecular cluster formation takes place. Now, the discussion of the SCP-RICM studies and the influence of valency of glycooligomers will be continued.

Pentavalent Man(all)-5 was studied in order to examine the effect of a further increased number of carbohydrate units. Therefore the overall number of building blocks, hence the approximate length, was kept constant. An IC_{50} value of 0.4±0.1 µM was obtained by SCP-RICM. This relates to a relative activity of 310 and thus the highest relative activity measured for all samples presented in this thesis. Compared to trivalent Man(1,3,5)-5 the relative activity is increased by about 52 which relates to a gain of 17%. It is surprising that presentation of two additional sugar ligands in Man(all)-5 compared to Man(1,3,5)-5 did not lead to a much higher increase in affinity since a higher relative increase in affinity was observed from the di- to trivalent system. Apart from two additional mannose ligands, Man(all)-5 compared to Man(1,3,5)-5, does not contain

EDS spacer moieties in its backbone. The absence of the highly hydrated ethylene glycol spacers might result in a relative loss of affinity. Since the length was kept constant it is likely that only the effect of statistical rebinding can be considered as affinity enhancing multivalent effect. Thus statistical rebinding seems to contribute less to the overall binding affinity in comparison to the release of water. This is indeed one of the first design rules derived from the glycooligomer binding studies: for Con A binding, an optimal number of Man ligands is between 3-5 and the polymeric backbone should include one or several hydrophilic spacer.

All structures discussed so far consist of 5 building blocks. This number was initially chosen as the overall length of a pentameric oligomer is 7 nm in all-trans linear conformation and thus close to the distance between two Con A binding pockets of 6.5 nm. However, 2fFCS showed that a much smaller size of app. 1.2 nm is adopted by pentameric oligomers.

In order to examine whether longer oligomer chains adopt a larger hydrodynamic size and therefore could potentially span two binding sites inducing chelate binding, a glycooligomer consisting of 10 building blocks, Man(all)-10, was synthesized. Moreover, five additional mannose ligands are presented in this structure compared to Man(all)-5.

The obtained IC_{50} value (measured by SCP-RICM) is 0.3 µM±0.1 (RA 206). In literature a value of 70 µM (RA=11) for a decavalent polyglycerol dendrimer[60] determined by inhibition SPR and 0.5 µM (RA=200) for a decavalent succinimidyl polymer determined by solid phase binding assay[45] was described. Thus the affinity of the precision glycooligomer is comparable to previously described decavalent polymeric systems. Overall, Man(all)-10 has the lowest IC_{50}, of all here examined structures and therefore the highest affinity. However relative activity *drops* about 100-fold compared to Man(1,5)-5. The IC_{50} value is identical within the error compared to the value obtained for Man(all)-5 presenting only half the number of binding ligands. Thus we cannot assume a chelate binding contribution for the decavalent system as this should lead to a pronounced increase in binding affinity. It has been shown that an exact match between distance of sugar ligands and receptor pockets is crucial for chelate binding. Small structural differences such as one C-O bond can cause a significant loss of affinity.[36,37] It is possible that the Man(all)-10 structure is too long for an efficient chelation. Nevertheless, the display of five additional mannose ligands compared to Man(all)-5 should lead to enhanced binding caused by the statistical rebinding effect. This effect might be hampered in the Man(all)-10 structure, since its scaffold consists only of less flexible TDS building blocks. Furthermore, the decavalent system presents a high number of triazole motifs in close proximity. It has been hypothesized that the formation of a secondary structure caused by the triazole moieties might occur. Such a secondary structure would influence the conformational dynamic of Man(all)-10 and hinder a statistical rebinding.

To summarize the findings for the binding of homomultivalent glycooligomers: The Con A lectin binding of six homomultivalent structures was measured by different binding assays. All structures show an at least 100-fold increase in binding in comparison to monovalent α-Me-Man. All obtained affinities of the here presented mono- to decavalent structures exceed literature known relative binding activities. This indicates that the here presented oligomeric structures are efficient binder.

A comparison between the presented glycooligomers yields a non-linear relation between IC_{50} value and number of presented mannose ligands (see Figure 52).
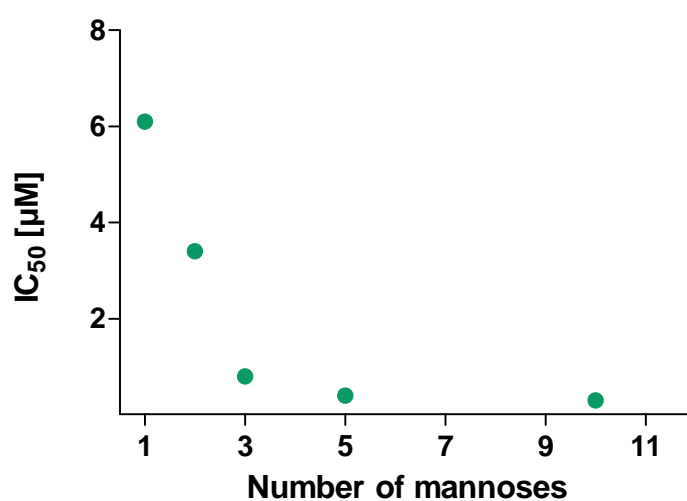
Figure 52: Binding activity in dependence of number of presented mannoses on the backbone.

IC_{50} decreases rapidly from mono- to trivalent glyco-structure reaching a plateau for Man(1,3,5)-5. The penta- and decavalent structures show the lowest IC_{50} value, however the relative decrease is much smaller. It seems that the display of three mannose units presents a kind of cut-off for efficient binding. It mimics the naturally occurring trimannosyl-moiety located on the outer arm of natural oligomannose-type carbohydrates which was demonstrated to be the major epitope recognized by Con A[140] due to its recognition by an extended binding site[53,157].

Different multivalent effects were taken into account as reason for the high binding affinities of the glycooligomers. The chelate effect was discussed in detail for the di-, and decavalent structures. The theoretical distance between sugar ligands on these scaffolds is long enough to span over two binding pockets of Con A. However, the results of the structures with adjacent mannose units (Man(1,3)-5) yielding approximately the same binding affinity compared to the

one presenting mannose ligands on each end (Man(1,5)-5) disfavor a potential chelate binding. On the one hand, statistical rebinding seems to play a key role as multivalent effect that enhances binding affinity of the here presented structures. On the other hand, formation of soluble clusters was proven for the trivalent structure by measurement of hydrodynamic radius. It can be assumed that this effect plays a role in binding also for the penta- and decavalent structures. A third factor contributing to the binding affinity of the glycooligomers is the introduction of EDS, ethylene glycol, spacer units. The hydration shell around these units could enhance binding affinity due to release of water during the binding event which results in entropic gain. This interesting finding will be further investigated in chapter 3.3.3.

3.3.2.<u>Heteromultivalent Glycooligomers</u>

The previous subchapter presented Con A lectin binding of mannose presenting structures displaying one type of sugar. Such exclusive homomultivalent structures do not occur in nature. For example, high mannose oligosaccharide, being one of the most repetitive structures, displays several (5 to 8) mannose units always in combination with N-acetyl glucosamine.[56] In order to mimic the natural principle of heterogeneity, glycooligomers presenting different sugars along a polymeric backbone have to be realized. This was achieved by a straight-forward modification of the synthetic solid phase-protocol from simultaneous conjugation of ligands to a sequential coupling-conjugation protocol as described in 3.2.2.

The following chapter will now present the results on the binding studies for the heteromultivalent glycooligomers comparing them to the homomultivalent structures. In order to further elucidate potential binding mechanisms, additional experimental data will be discussed: Saturation transfer difference NMR studies (STD-NMR) were applied to examine the proximity of the sugar ligands to Con A and therefore determine the binding sugar ligands. Dual focus fluorescence assay was applied to measure the hydrodynamic radius of the Con A-glycooligomer complex giving insight into the complex size and affinity of hetero-glycooligomers in solution.

The examined heteromultivalent structures all consist of three sugar units presented on a pentameric oligomer backbone. Heteromultivalent glycooligomers represent analogues of the trivalent Man oligomer Man(1,3,5)-5 with successive replacement of the Man ligands towards Gal or Glc ligands. Considering only the Man ligands of the heteromultivalent structures, they can also be seen as analogues of the monovalent or divalent glycooligomers Man(3)-5 and Man(1,5)-5, with Gal or Glc ligands now occupying the previously non-functionalized positions 1, 3 and 5 of the oligomer chain (see Table 9).
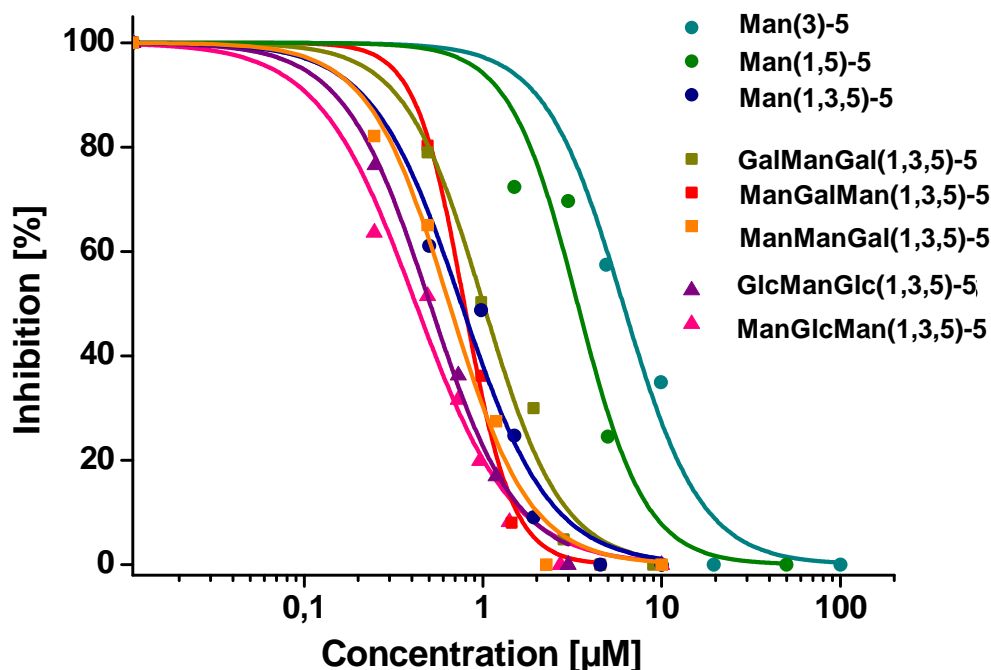
Figure 53: Inhibition curves determined by SCP-RICM of heteromultivalent structures and homomultivalent structures for comparison.
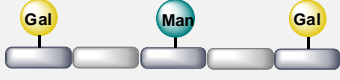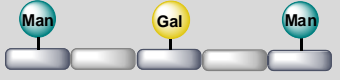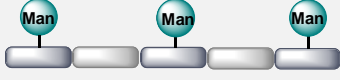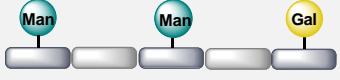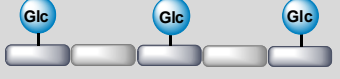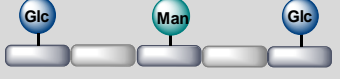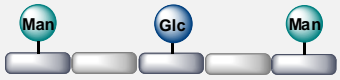
Binding affinities were first determined by SCP-RICM inhibition/competition assay (for details of this measurement technique see 3.3.1). These measurements were carried out by Daniel Pussak, MPI KGF. Figure 53 displays the obtained inhibition curves of heteromultivalent glycooligomers GalManGal(1,3,5)-5, ManGalMan(1,3,5)-5, ManManGal(1,3,5)-5, GlcManGlc(1,3,5)-5 and ManGlcMan(1,3,5)-5. Homomultivalent structures Man(3)-5, Man(1,5)-5 and Man(1,3,5)-5 are shown as comparison.

It can be seen that GalManGal(1,3,5)-5 binds with much higher affinity than its homomultivalent analogue Man(3)-5. A similar result is obtained for ManGalMan(1,3,5)-5 and Man(1,3)-5. These two structures show affinity in the range of trivalent Man(1,3,5)-5. For the glucose modified structures the binding is enhanced compared to the homomultivalent Man(1,3,5)-5 structure.

Table 9 shows IC_{50} values obtained by fitting the measured data points with Hill equations.

Table 9: IC$_{50}$ values of heteromultivalent structures determined by SCP-RICM in comparison with similar homomultivalent structures.

Compound	IC$_{50}$ [µM] (SCP-RICM)	Compound	IC$_{50}$ [µM] (SCP-RICM)
Man(3)-5	6.1 ± 0.7	GalManGal(1,3,5)-5	1.0 ± 0.1
Man(1,5)-5	3.4 ± 0.5	ManGalMan(1,3,5)-5	0.8 ± 0.1
Man(1,3,5)-5	0.8 ± 0.1	ManManGal(1,3,5)-5	0.7 ± 0.1
Glc(1,3,5)-5	2.1 ± 0.1	GlcManGlc(1,3,5)-5	0.4 ± 0.1
		ManGlcMan(1,3,5)-5	0.5 ± 0.1

At first, the IC$_{50}$ values obtained for four trivalent structures with the same geometry but different ligand composition, GalManGal(1,3,5)-5, ManManGal(1,3,5)-5, ManGalMan(1,3,5)-5, and Man(1,3,5)-5, are compared: A decrease in inhibition would be expected by exchanging binding mannose ligands towards non-binding galactose ligands due to a decrease in statistical probability of one or more Man ligands binding to the Con A receptor. However, all four trivalent structures present similar IC$_{50}$ values of about 1 µM. This could indicate that all trivalent systems undergo monovalent binding via one Man ligand while the other, binding or non-binding, ligands promote steric stabilization of the ligand-protein complex. Steric shielding has been discussed in literature only for homomultivalent glycopolymers where the non-binding parts of the glycopolymer, both scaffold and ligands, shield the glycopolymer-protein complex against competition by other ligands or inhibitors (see 1.2.2).[87,159]

If a solemnly steric contribution for the non-mannose sugar ligands is assumed, similar results would also be expected for the mannose and glucose modified oligomers. Surprisingly, the IC$_{50}$

values for the trivalent GlcManGlc(1,3,5)-5, ManGlcMan(1,3,5)-5 are around 0.5 µM and thus even lower than the IC_{50} of Man(1,3,5)-5 oligomers with 0.8 µM. As control, the all Glc trivalent oligomer Glc(1,3,5)-5 showed an increase in IC_{50} up to 2.1 µM. This can be readily explained due to the lower affinity of Glc towards Con A when compared to Man. The IC_{50} of Glc(1,3,5)-5 (2.1 µM) is roughly 2.6 times higher for the trivalent Glc oligomer compared to the trivalent Man oligomer (0.8 µM). It has been reported before that monovalent Glc structures bind app. four times lower than mannose functionalized analogues (affinity(Man)=4*affinity(Glc))[140]. Assuming a monovalent binding mode of the presented trivalent ligands via a Man ligand and only considering steric shielding contributions from the additional ligands, the Glc presenting oligomers should have the same IC_{50} values as the Gal or all Man presenting structures. Indeed, this has been observed in literature for tri- and tetravalent dendron structures where the exchange of Man units to Glc units resulted in similar IC_{50} values as for the all Man structures in binding to Con A.[160] However, a clear difference between the Glc and Gal modified oligomers can be seen here. Alternatively, statistical effects can be taken into account, where the overall chance of a Man or Glc ligand binding to a Con A receptor molecule is increased with the overall number of binding ligands. Then again, the trivalent Glc and Man heteromultivalent oligomers should have at maximum the same inhibitory potency as the all-Man system; however 'mixtures' of Glc and Man on the oligomer exhibit a lower IC_{50} value and thus increased inhibitory potency. A similar finding was shown by García Fernandez et al., who presented a ß-cyclodextrin scaffold displaying different combinations of Glc and Man ligands that showed an amplified Con A binding determined by enzyme-linked lectin assay (ELLA) in comparison to the all-Man system of the same valence. For these systems, an increase in affinity due to a more dynamic binding and unbinding or so-called sliding of the heteromultivalent systems and thus a gain in entropy leading to enhanced binding was suggested and experimentally shown via ITC measurements.[161] The dynamic structure of Man-Glc combining glycooligomers is also supported by a recently published study by Haddleton et al. who showed that polymers with mixtures of Man and Glc side chains have about the same IC_{50} value as the all-Man polymer but are more easily inhibited with monovalent Me-Man.[162]

This kind of inhibition/competition measurements and resulting IC_{50} values are limited to present relative affinities of the glycooligomers in competition to another binding ligand (here Methyl-mannose). It cannot be determined which sugar ligands attached to the backbone actually take part in the binding process. One possibility to determine this is the use of STD-NMR. This assay gives information about the proximity of certain parts of the glycooligomer to the lectin. Therefore it can be used to identify which parts of the glycooligomers interact with the Con A receptor during complex formation. STD-NMR studies were carried out by Jonas Aretz

and Dr. Christoph Rademacher, MPI KGF.

In STD-NMR, spin diffusion transfers saturation is selectively introduced into the protein hydrogen network to a low molecular weight interaction partner. From this so-called on-resonance spectrum, a reference spectrum is subtracted in which the saturation does not perturb any resonances of the interaction partners. The resulting difference spectrum comprises only signals from the ligand that are in close proximity to the receptor interface. The build-up of the intensity of these resonances in the difference spectrum as a function of saturation time is related to the distance of the respective proton to the receptor (see Figure 54).[163,164]
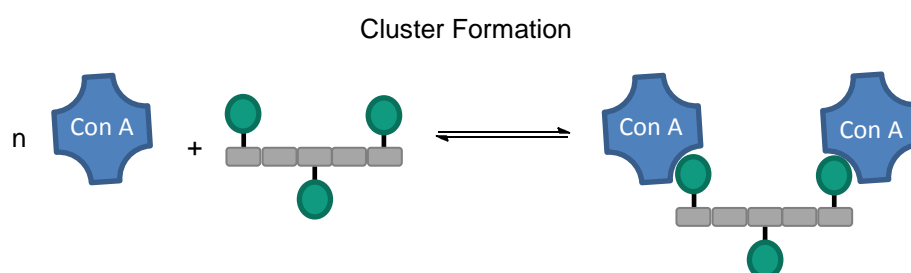
Figure 54: Schematical representation of STD-NMR. a) An initial reference spectrum determines all proton signals caused by a receptor-ligand complex. b) Upon irradiation the signals of ligand in close proximity to the receptor (=binding ligands) disappear from the spectrum. c) By subtraction of both spectra only the binding ligands are left.

STD-NMR measurements were carried out for heteromultivalent glycooligomers ManGalMan(1,3,5)-5 and GalManGal(1,3,5)-5 and mono- to trivalent Man ligands for comparison. It was focused on the Man-Gal combining glycooligomers as this should allow for differentiating between binding and non-binding parts of the molecule. Binding interactions of the Gal residues can be excluded (in contrast to glucose ligands presented on GlcManGlc(1,3,5)-5 and ManGlcMan(1,3,5)-5). Consequently, secondary binding effects through the combination of Man and Gal ligands can potentially be identified.

Glycooligomers in absence of Con A as well as the alkyne precursor backbone lacking mannose moieties served as negative controls. No signals were observed in the respective STD-NMR experiments. Binding epitopes of the examined homo- and heteromultivalent structures in presence of 20 µM Con A were determined using STD build-up curves with saturation times ranging between 0.5 and 8 s.[163] With this, a relative degree of saturation was determined and categorized in low, medium, strong or no saturation (see Table 10). A graphical representation with the exemplary structure ManGalMan(1,3,5)-5 is shown in Figure 55.
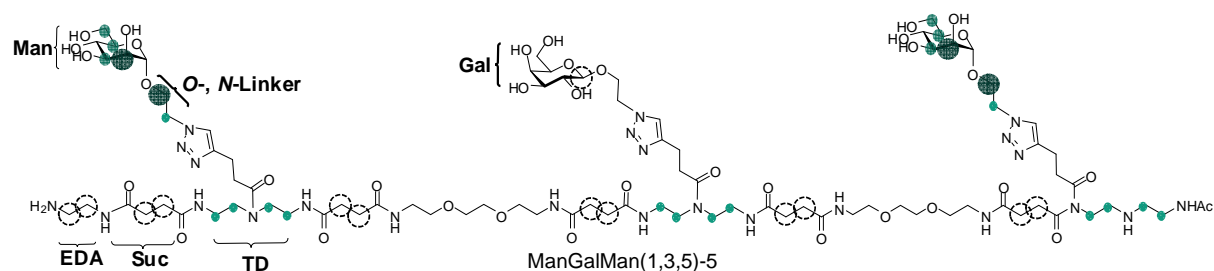
Figure 55: Binding epitope of ManGalMan(1,3,5)-5. The relative degrees of saturation of the individual protons are depicted by differently sized circles proportional to the degree of saturation.

The mannose ligands on all glycooligomer structures experience significant saturation transfer at H2(Man). The anomeric proton of Man could not be examined due to interference with the solvent suppression scheme applied during the STD-NMR experiment. All other Man protons H3(Man)-H6(Man) show high to moderate saturations. Interestingly, the linker protons next to the anomeric center also receive a high degree of saturation of above 70% in all structures. Hence, a possible direct contribution of this particular stretch of the linker cannot be excluded. Most importantly, the carried out STD-NMR measurements show a lack of saturation of the anomeric proton at of galactose (H1(Gal)).

Table 10: The relative degrees of saturation of the individual protons of all examined structures are shown and categorized into strong, medium, low and no saturation.

Compound	strong	medium	weak	No
GalManGal (1,3,5)-5	H2(Man)			H1(Gal) EDA NHAc
ManGalMan(1,3,5)-5	H2(Man) O-Linker	H3(Man), H5(Man) H6(Man)	N-Linker NHAc	H1(Gal) EDA
Man(3)-5	H2(Man) O-Linker	H4(Man), H5(Man) H6(Man), N-Linker	TD NHAc	Suc EDA
Man(1,5)-5	H2(Man) H5(Man) O-Linker	H3(Man), O-Linker	H4(Man) H6(Man) N-Linker TD NHAc	Suc EDA
Man(1,3,5)-5	H2(Man)	H3(Man), H4(Man) H5(Man), H6(Man) O-Linker N-Linker	TD NHAc	Suc EDA

Other protons from the Gal moiety are not resolved directly, due to overlap of chemical shifts, but chemical shift pattern of the resulting STD-NMR spectra indicate absence of saturation of this sugar. Hence, this subunit is not in close proximity to the receptor. Moreover, the backbone of the TDS building block (TD) receives low saturation transfer and the succinyl protons of both building blocks (Suc) experience no saturation at all. Protons from individual EDS building blocks are not distinguishable as their chemical shifts overlap with H3 and H4 of the unresolved sugar protons.

STD-NMR revealed that only mannose ligands interact with the receptor upon complex formation, a contribution of scaffold or non-binding sugars was ruled out. However, it is still questionable why scaffolds presenting only one or two mannose ligands together with non-binding galactose yield app. the same binding affinity as a structure carrying three mannose units as determined by surface-based SCP-RICM inhibition/competition assay. A solution based binding assay measuring Con A lectin binding without competitor is desired.

For this purpose 2fFCS (for details of this technique see 3.3.1) was performed. Shortly, 2fFCS measures the hydrodynamic radius of the glycooligomer-lectin complex by means of fluorescence diffusion. This technique also allows for a calculation of binding affinities similar to SCP-RICM. Studies were performed by Pauline Maffre and Prof. Dr. Ulrich Nienhaus, KIT. Again, only the Man-Gal combining glycooligomers were examined as additional binding of glucose ligands on Man-Glc oligomers would interfere with the differentiation of binding and non-binding parts.
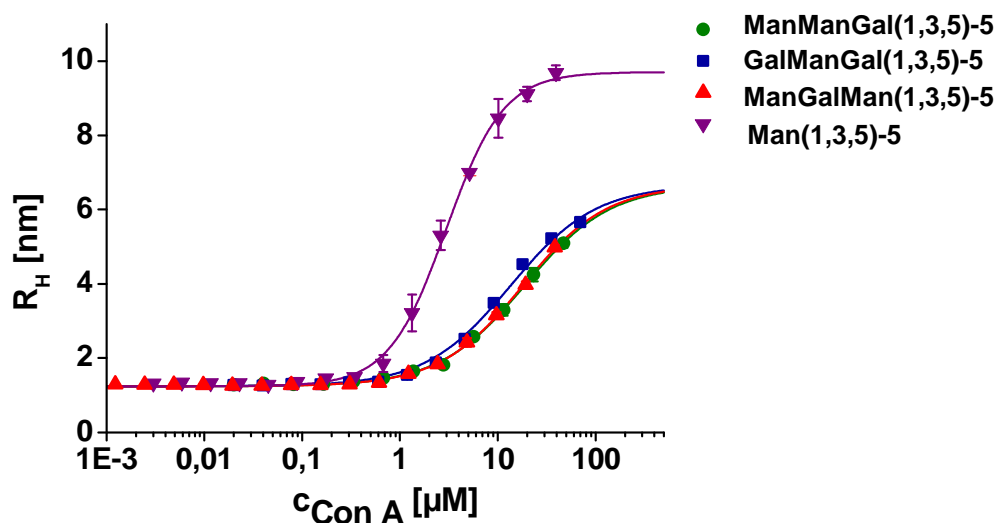
Figure 56: Hydrodynamic radius of hetero glycooligomers ManGalMan(1,3,5)-5, GalManGal(1,3,5)-5, ManManGal(1,3,5)-5. The dotted lines are Hill fits of the measurements.

Figure 56 shows the obtained data plotting the R_H of the heteromultivalent structures GalManGal(1,3,5)-5, ManGalMan(1,3,5)-5 and ManManGal(1,3,5)-5 against increasing concentration of Con A. Homomultivalent, trivalent Man(1,3,5)-5 is also shown for comparison. Table 11 summarizes the obtained values.

Table 11: The obtained hydrodynamic radii of the heteromultivalent structures.

Compound	$R_{H\text{-initial}}$ [nm]	$R_{H\text{-max}}$ [nm]	ΔR_H [nm]
GalManGal(1,3,5)-5	1.2 ± 0.1	6.6 ± 0.1	5.4 ± 0.2
ManGalMan(1,3,5)-5	1.2 ± 0.1	6.6 ± 0.1	5.4 ± 0.2
ManManGal(1,3, 5)-5	1.2 ± 0.1	6.6 ± 0.1	5.4 ± 0.2
Man(1,3,5)-5	1.2 ± 0.1	9.7 ± 0.1	8.5 ± 0.2

All glycooligomers have the same initial R_H of 1.2 nm in absence of Con A. This indicates that all glycooligomer structures adopt a coiled structure in aqueous solution. This is most likely caused by the overall flexibility of the backbone consisting of TDS and EDS building blocks.

With increasing concentration of Con A, R_H increases as a result of complex formation. In the transition region, R_H is an average over non-bound glycooligomers and protein-bound glycooligomers. Hereall three heteromultivalent structures show a similar increase in hydrodynamic radius by ~5 nm to a maximum value of 6.6 nm. Given that a Con A molecule has an approximate R_H of 4.3 nm[155], it can be concluded that one Con A molecule binds to one heteromultivalent ligand, resulting in the observed increase in R_H. This result was expected for GalManGal(1,3,5)-5, which has only one binding site. For divalent ManGalMan(1,3,5)-5 and ManManGal(1,3,5)-5 cluster formation would theoretically be possible since two mannose units are present. However for homomultivalent structures it was already shown by turbidimetry assay (described in 3.3.1) that mono- and divalent glycooligomers are not able to crosslink between Con A molecules.

Turbidimetry assay was also performed with heteromultivalent structures. No cluster formation was measured for GalManGal(1,3,5)-5, ManGalMan(1,3,5)-5, ManGlcMan(1,3,5)-5 and GlcManGlc(1,3,5)-5. This result is consistent with the result from hydrodynamic radius studies. It can be concluded that no cluster formation, neither soluble nor insoluble, is induced by heteromultivalent structures. In comparison to that, the hydrodynamic radius of trivalent, homogeneously functionalized Man(1,3,5)-5 increases of 8.5 nm indicating cluster formation as

described in chapter 3.3.1.

It is a very interesting observation that the size increase by 5.4±0.1 nm determined for all three heteromultivalent structures is about 0.9 nm larger than what is expected for one Con A molecule (R_H of 4.3 nm) together with one glycooligomer (R_H of 1.2 nm). This could indicate that the oligomer engages in a different conformation in the complex with the protein than alone.

2fFCS binding assay is not limited to determine hydrodynamic radii, but can also be used to determine binding affinities as described above. In this thesis, affinities have so far been determined by either SCP-RICM or SPR measurements. Using 2fFCS to determine affinities is especially interesting as this assay measures direct complex formation in solution in contrast to previously applied inhibition/competition assays. By plotting the obtained data points for hydrodynamic radii in dependence of Con A concentration sigmoidal curves are obtained (Fig. 31). These can be fit with Hill equations. K_D' values are obtained giving the value of free Con A at the transition midpoint. K_D' is comparable to IC_{50} values obtained by SCP-RICM as both values report the binding of ligand to receptor at 50%. The fit curves are shown in

Figure 56 as lines; the fit parameters are summarized in Table 12.

In addition to K_D' values, Hill coefficients (n) were derived. Hill coefficients serve as indicators for cooperativity determining how many glycooligomers are bound to Con A. For GalManGal(1,3,5)-5 which has only one Con A binding site, the Hill coefficient (n) was fixed to 1. The Hill coefficients obtained from the fits for ManGalMan(1,3,5)-5 and ManManGal(1,3,5)-5 are very close to 1, which is consistent to the conclusion drawn by analysis of hydrodynamic radius that only one Con A molecule is bound. For Man(1,3,5)-5 an n-value of 1.48±0.04 was obtained which indicates cooperativity, meaning more than one glycooligomers is bound to the Con A receptor. This result is again consistent with the results obtained from hydrodynamic radius analysis and turbidimetry assay.

Table 12: Comparison of K_D' values obtained by 2fFCS and IC_{50} values obtained by SCP-RICM.

Compound	Hill coefficient (n)	K_D' [μM]	IC_{50} [μM][a]
GalManGal(1,3,5)-5	1[a]	14±1	1.0±0.1
ManGalMan(1,3,5)-5	0.99±0.04	19±1	0.8±0.1
ManManGal(1,3, 5)-5	1.02±0.04	18±1	0.7±0.1
Man(1,3,5)-5	1.48±0.04	3.0±0.1	0.8±0.1

[a] fixed parameter in Hill fit

Evaluating now K_D', all heteromultivalent glycooligomers yield values in the same range of app. 17 μM. For GalManGal(1,3,5)-5 a K_D', of 14 ±1 μM was obtained. For ManGalMan(1,3,5)-5 and ManManGal(1,3,5)-5 K_D' of ~18 μM are even identical within the error. A similar result was also obtained in SCP-RICM affinity studies. The almost identical behavior of the three heteromultivalent structures is surprising and supports the hypothesis drawn from the results above: Both structures bind with only one mannose unit and the increase in binding affinity of the heteromultivalent structures is driven mostly by steric shielding of the other non-binding sugar ligands.

Interestingly, the K_D' value obtained by 2fFCS of the homomultivalent structure gives a clear difference to the K_D' value of the heteromultivalent structures. Trivalent Man(1,3,5)-5 gives 3.0 ± 0.1 μM which corresponds to a six times increased affinity compared to divalent (regarding only binding sugar ligands) ManManGal(1,3,5)-5 and ManGalMan(1,3,5)-5 by displaying only one additional mannose. This result is in contrast to SCP-RICM measurements in which the affinity obtained for Man(1,3,5)-5 was app. the same as for the Man-Gal glycooligomers.

It is known that different affinity assays can lead to different results depending on the set-up.[145] For the results obtained in this work, it can be differentiated between the assay performed at the interface (SCP-RICM) and the assay performed in solution (2fFCS). In contrast to complex formation in solution, during SCP-RICM measurements, first a protein receptor-functionalized surface is incubated with the glycooligomer and then tested against a sugar-functionalized SCP. Due to the packing of receptors and ligands on the surfaces, no differences in the competition of the ligand-receptor surface for the homo- or heteromultivalent glycooligomer with the ligand-SCP can be observed. No difference can be detected between blocking of SCP either caused by binding to two binding pockets of Con A or caused by a steric shielding of the non-binding ligands (Figure 57). Both binding mechanisms cannot be distinguished leading to similar IC_{50} values for both systems in SCP-RICM. While this clearly shows how dependent possible conclusions on binding mechanisms are on the assay applied, this can also be highly relevant in the context of potential applications of multivalent glycooligomers. Both assays, in solution or at the interface, have biological relevance, *e.g.* glycooligomers inhibiting pathogen/cell interactions or binding to soluble toxins.

a) At the interface (SCP-RICM)　　　**b) In solution** (2fFCS)

$IC_{50} \approx 1\ \mu M$　　　$IC_{50} = 3.0\pm0.1\ \mu M$　　$IC_{50} = 14\pm1\ \mu M$
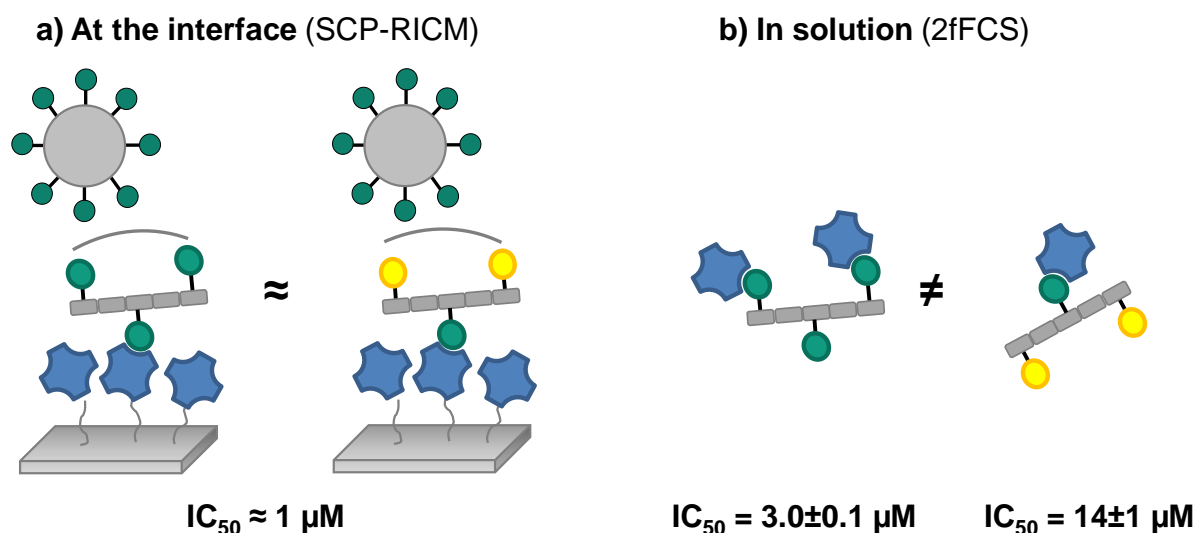
Figure 57: Schematic drawing of ligand-receptor binding in 2fFCS and SCP-RICM measurements determining K_D' and IC_{50} values respectively.

In summary, a series of heteromultivalent glycooligomers presenting a combination of mannose/galactose and mannose/glucose units were examined in Con A lectin binding studies. Heteromultivalent structures were comparable to the homomultivalent structures in terms of length and number in order to evaluate differences that arise from heterogeneity. Different binding assays were used to elucidate diverse effects in binding: STD-NMR showed that only mannose ligands presented on the oligomer scaffold take part in the binding process. 2fFCS studies yielded the same hydrodynamic radius of 1.2 nm for all ethylene glycol spaced scaffolds presenting three sugar ligands which indicates a coiled conformation for these structures when not bound to a receptor. Cluster formation in Con A binding was confirmed to be only possible with a minimum number of three mannose units although only two Mannose ligands take part in the complex formation. Moreover it was revealed that steric shielding plays a key role for the increased affinity of multivalent glycooligomers. This effect seems to be particularly prominent if one or both components, receptors and ligands, are bound to a surface modelling *e.g.* natural cell-cell or cell-pathogen interactions.

3.3.3. Photoswitchable Glycooligomers

In the two previous chapters the change of number, spacing and type of sugar ligands on multivalent binding were examined. It was shown that binding affinity is not only dependent on the sugar ligands but also on the scaffold. On the one hand the scaffold determines the actual distance between the sugar ligands which is important for both statistical rebinding and chelate formation. Latter relies on an optimal match between the distance of binding pockets and sugar ligands on the scaffold whereas a short distance in sugar ligands raises local sugar ligand concentration and therefore is beneficial for rebinding. On the other hand, the backbone is responsible for the overall structural hydrophobicity/-philicity. Already indicated by the monovalent structure in studies of homomultivalent glycooligomers, a positive contribution of EDS spacers was observed due to their hydrophilicity. Upon binding, water molecules can be released into bulk resulting in a gain in entropy upon ligand-receptor binding.

In order to investigate the positive contributions of the scaffold in more detail, such as flexibility and hydrophilicity, this chapter now focuses on variations of the sugar ligand presenting *scaffold*. Therefore the sugar ligands as well as the coupling chemistry applied for attaching the sugar ligands to the scaffolds are kept constant. However, the previously introduced spacing building block EDS is now exchanged towards the so-called AZO building block. EDS accounts for a high flexibility and hydrophilicity whereas AZO spacers are stiff and more hydrophobic. In addition to that, the AZO building block can change its configuration from trans to cis upon irradiation leading to an overall change in structural conformation of the glycooligomers. This affects the spatial distribution and distance of sugar ligands while keeping the other parameters of the glycooligomer fixed. Overall this again nicely shows the versatility of the solid phase approach using functional building blocks allowing for the straightforward variation of individual parameters of the glycoligand *e.g.* by exchanging building blocks.

The following chapter is divided into two parts: At first, the switching behavior of AZO containing glycooligomers will be characterized. In the second part, the AZO containing glycooligomers are evaluated for their binding properties towards PA-IL lectin receptor by means of SPR assays and in dependence of their cis or trans configuration. All AZO structures are also compared to their EDS analogues.

Previously, the widely investigated lectin receptor Con A was used as model receptor for the studies described in this thesis. In this subchapter the binding of switchable glycooligomers to PA-IL (also called LecA), a lectin present on Pseudomonas Aeruginosa, will be examined. This bacterium is known as major opportunistic human pathogen, often occurring in hospital acquired diseases.[110] It is resistant against many antibiotics and disinfectants, therefore the

development of alternative therapies such as multivalent anti-adhesive drugs is desired.[124,165] Pa-IL, a tetrameric, calcium dependent lectin specific for galactose structures, plays an important role in the infection process of Pseudmonas Aeruginosa.[166] PA-IL is composed of 121 amino acids (51 kDa) associated as homotetramers.[167] The crystal structure reveals a tetrameric arrangement with a general rectangular shape with the smaller distance of binding sites being 2.6 nm and the longer one being 7.9 nm apart.[168] PA-IL binds to α-Gal-disaccharides, α-galactosides and β-galactosides with decreasing affinity. Multivalent β-galactose displaying scaffolds have been proposed as high affinity ligands[169–173]. Although targeting of PA-Il could lead to the development of an effective treatment of Pseudomonas Aeruginosa infections, rational design of ligands based on multivalent interactions are scarce.[36,174,175]. PA-IL is not only an interesting target due to its biomedical relevance, it is also an ideal lectin to examine a potential spatial effect as the smaller binding site distance is only 2.6 nm apart. Because of that, even small changes in length/conformation of the glycooligomer can be expected to show an effect on the binding affinity. Another reason for the use of a different receptor for this subset of glycooligomer structures is the possibility to compare whether the previously derived rules for multivalent binding can also be transferred to other lectins and thus can be considered general design principles.

The AZO building block contains an azobenzene structural unit which is known to exist in a trans (E) and cis (Z) form (see Figure 59 a).[176,177] Both forms can reversibly isomerize upon light irradiation. UV-light at 350 nm induces the *trans → cis* isomerization. The cis isomer adopts a bent conformation with its phenyl rings twisted ~ 55° out of the C-N=N-C plane.[178] This wavelength corresponds to the energy of the π-π* molecular orbital transition, while the n-π* transition is attributed to the band centered at 420 nm (see Figure 59). By switching from trans to cis, the band at 420 nm slightly increases, while the band at 350 nm decreases until the molecule reaches a photostationary state (PSS) in which the cis isomer of the azo moiety predominates. By irradiation with light at 420 nm the azo unit can be switched back to its trans configuration. As the trans form is thermodynamically more stable, the relaxation cannot only be induced by light at 420 nm, but also thermally.[179]

It was shown in the literature that azobenzene moiety containing amino acid derivates incorporated in peptides can be used to induce conformation changes in the structure of peptides.[180,181] Here the same azobenzene amino acid building block was synthesized by Dr. David Bléger from Humboldt University following literature protocols[129,181], and was incorporated in the glycooligomer scaffold (see Figure 58) (for synthesis see chapter 3.2.3). Two azobenzene containing galactose modified glycooligomers were synthesized: a trimeric oligomer carrying two Galactose residues spaced by one AZO building block and a pentameric oligomer

presenting three Galactose residues equally spaced by one AZO building block resulting in a total of two azobenzene moieties per molecule (see Table 13).
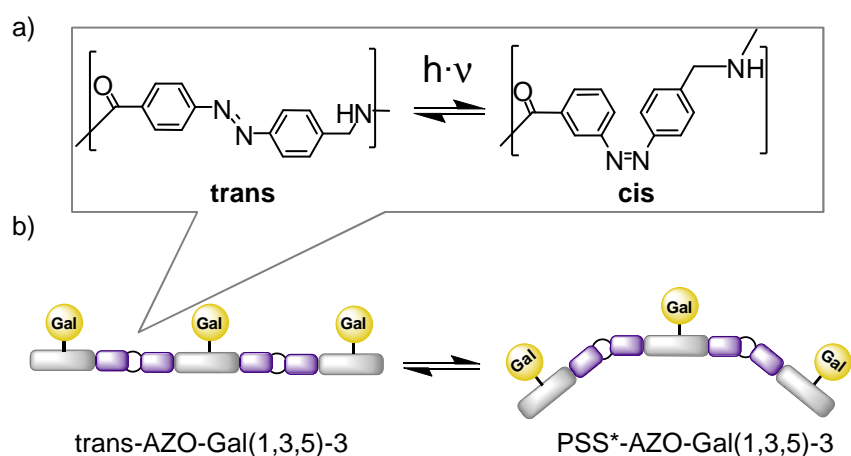
Figure 58: a) The cis and trans isomers of the azobenzene moiety incorporated in the AZO building block which can be switched upon irradiation. b) Schematic representation of the glycooligomer before and after irradiation (PSS=photo stationary state).

First, the photoswitchable properties of the glycooligomers were evaluated. Therefore irradiation of AZO-Gal(1,3)-3 and AZO-Gal(1,3,5)-5 glycooligomers was carried out by placing a 2 mM solution in a quartz cuvette and into a beam of light with a wavelength of 350 nm (1000W Xe lamp equipped with the adequate optical filters). The switching was monitored by UV-VIS spectroscopy, (see Figure 59) showing a decrease in the maximum at ca. 350 nm corresponding to the π-π* transition of the azobenzene moiety whereas the second maximum at ca. 450 nm (n-π* transition) increased.

AZO-Gal(1,3)-3 upon 350 nm irradiaton in DMSO at 25°C
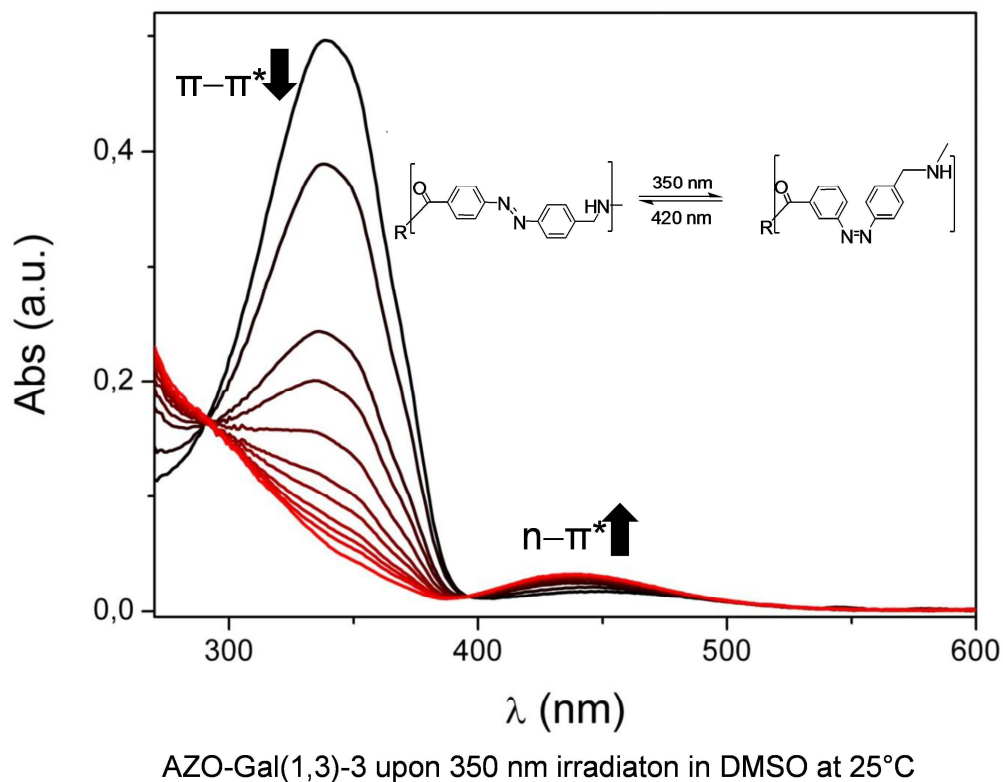
Figure 59: UV-VIS spectrum of AZO-Gal(1,3)-3 before and after irradiation.

As the AZO oligomer is switched from trans to cis, the polarity of the oligomer changes (cis azobenzenes are generally more polar than the trans forms), therefore the switching process could also be monitored by RP-UPLC (see Figure 60).

RP-UPLC: 5/95 MeCN/H$_2$O→ 95/5 MeCN/H$_2$O in 10 min
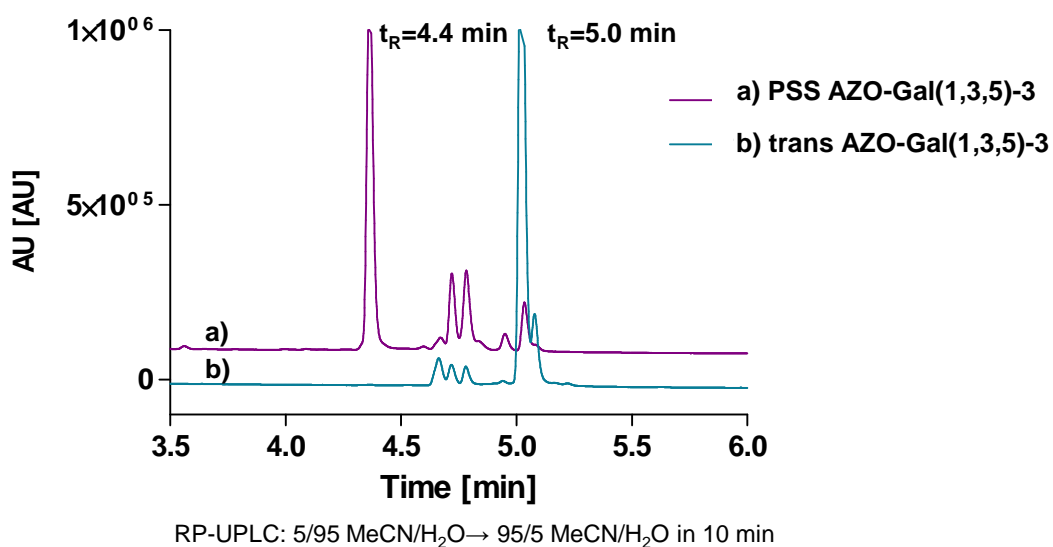
Figure 60: RP-UPLC of Gal-AZO(1,3,5)-5 before and after irradiation.

Figure 60 shows the obtained RP-UPLC of AZO-Gal(1,3,5)-5. Before irradiation, a peak at t_R=5.0 min indicated the configuration of both azobenzene units within the main chain in trans, a small portion of 10% mixed conformation (cis/trans and trans/cis) was visible at t_R=4.7-4.8 min. After app 30 min irradiation at 350 nm, the PSS was reached. The 5.0 min peak decreased, the mixed conformation-peak increased and a new peak at t_R=4.4 min became visible. This peak is identified as the all-cis of AZO-Gal(1,3,5)-5. The same measurement was carried out for AZO-Gal(1,3)-3, with a PSS containing 72% of cis isomers. The reversibility of the isomerization process was also checked by chromatography. The molecule relaxes back to its initial conformation by either irradiation with light at 420 nm or thermal relaxation. The latter was done by heating the AZO-glycooligomers for 60 min in the dark. HPLC of AZO-Gal(1,3,5)-5 after thermal treatment showed similar retention times as were recorded for the initial trans-structures. For the glycooligomers to be used in binding studies, the life time of the PSS state has to be in the range of several hours. HPLC measurement of glycooligomers left at room temperature for 48 hours showed no change in conformation which is in accordance to stabilities of similar azobenzene structures presented in literature.[181,182]

After the successful switching of the AZO spaced structures, binding measurements were carried out. Table 13 shows the two individually measured conformations of AZO spaced divalent and trivalent structures as well as the EDS spaced structures which were subject to PA-IL lectin binding.

Table 13: Table of galactose presenting scaffolds with AZO building blocks as spacers and comparable structures with EDS spacers.

Compound Name	Structure
trans-AZO-Gal(1,3)-3	
PSS-AZO-Gal(1,3)-3	
trans-AZO-Gal(1,3,5)-5	
PSS-AZO-Gal(1,3,5)-5	
EDS-Gal(1,3)-3	
EDS-Gal(1,3,5)-5	

At first, an inhibition/competition assay as described in subchapter 3.3.1 was carried out. In order to test the specificity of the assay, two control structures were measured: methyl β-D-galactose, as known monovalent binder of PA-IL, and a mannose functionalized AZO-scaffold. For latter, no binding was detected which confirms the Gal-specificity of the assay. For methyl β-D-galactose an IC_{50} of $55 \pm 6\,\mu M$ was obtained which is in accordance with literature values of $63\,\mu M$ determined by similar inhibition SPR assays.[168]

Serial dilutions (0.1 to $400\,\mu M$) of the AZO-scaffolds in trans-/PSS-configuration and the EDS-scaffolds were measured as inhibitors for $1\,\mu M$ PA-IL. Figure 61 shows the obtained data curves. Each data point was derived by two individual measurements; the error is the standard deviation. Some error values are smaller than the symbols. Overall, the trivalent structures (EDS and AZO spaced) bind better than the corresponding divalent structures. Furthermore, the EDS spaced structures bind better than their AZO spaced analogues, the trivalent EDS spaced oligomer therefore being the best binder in this assay.
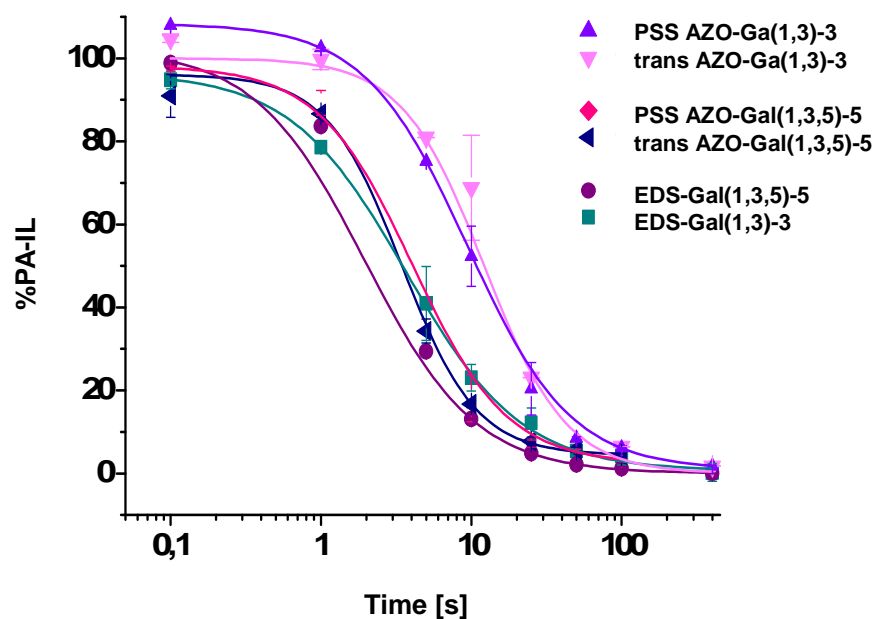
Figure 61: Inhibition curves of AZO-Gal-scaffolds in trans/PSS-state and the EDS-Gal scaffolds as comparison determined by inhibition SPR measurements.

Table 14 summarizes the obtained IC_{50} values after fitting the obtained data points with Hill equations. For the divalent AZO-Gal(1,3)-3 in trans conformation an IC_{50} value of 5.3 ± 0.3 µM was obtained, for its PSS conformer 9.4 µM was measured. AZO-Gal(1,3,5)-5 displaying three galactose moieties on the AZO spaced scaffold in trans conformation yielded an IC_{50} value of 3.4 ± 0.4 µM. An IC_{50} of 4.1 µM of the photostationary state of AZO-Gal(1,3,5)-5 was obtained. In order to examine contributions of the scaffold the number of galactose ligands was kept the same but AZO was exchanged by EDS building block. EDS-Gal(1,3)-3 yielded an IC_{50} value of 3.2 ± 0.2 µM, the trivalent EDS-Gal(1,3,5)-5 exhibited 2.0 ± 0.6 µM. A comparison to literature shows similar IC_{50} values in the low µM range (determined by inhibition SPR assay) for tetravalent cyclic and linear glycooligomers presenting four galactose residues binding to PA-IL.[168,174]

Table 14: IC$_{50}$ values obtained by SPR inhibition assay of the AZO-Gal and EDS-Gal structures.

Compound name	IC$_{50}$ [μM]
AZO-Gal(1,3)-3	
Trans	5.7±1.7
PSS	9.4±0.1
AZO-Gal(1,3,5)-5	
Trans	3.4±0.4
PSS	4.1±1.3
EDS-Gal(1,3)-3	3.2±0.2
EDS-Gal(1,3,5)-5	2.0±0.6
β-Me-Gal	55±6
AZO-Man(1,3,5)-5	n.b.

PSS = Photo stationary state

The comparison between the AZO scaffolds shows an increasing affinity for trivalent structures compared to divalent structures. The trivalent AZO-Gal(1,3,5)-5 binds app. two times better than divalent AZO-Gal(1,3)-3 while displaying only one additional galactose ligand. Similarly, EDS-Gal(1,3,5)-5 binds 60% better than divalent EDS-Gal(1,3)-3. Thus this result is in general consistent with the findings previously reported for homomultivalent structures binding to Con A (subchapter 3.3.1) but the amount of increase is not as high as observed for the mannose structures. An increase from a divalent to a trivalent structure yielded affinity enhancement of app. 4 times, a two-fold increase was observed for the display of five mannose ligands compared to three mannose ligands for binding to Con A. This leads to the assumption that in general a higher number of sugar ligands is beneficial for binding, however the amount of affinity increase is highly dependent on the specific ligand-receptor pair.

Regarding the scaffold contributions, it can be seen that both structures, di- and trivalent, incorporating EDS spacers have an enhanced binding compared to the AZO-scaffolds. EDS-Gal(1,3)-3 and EDS-Gal(1,3,5)-5 show app. two times higher affinity than the corresponding AZO-Gal(1,3)-3 and AZO-Gal(1,3,5)-5. Thus the EDS spacer seems to be beneficial for the ligand-receptor binding. For homomultivalent structures interacting with Con A (see chapter 3.3.1) it was discussed how a high local concentration of binding sugars favors statistical rebinding.[45]

Assuming that the EDS spacers engage in a folded conformation in water, as described above, ligand rebinding might be facilitated. Another positively contributing effect might be the higher hydrophilicity of the EDS structures compared to the AZO structures. As discussed in 3.3.1, the structures containing the ethylene glycol spacers are highly hydrated in water. Contacts between ligand and protein are often mediated by water molecules [8,50,52] therefore the hydration shell around EDS spaced glycooligomers could enhance its binding affinity due to release of water upon binding and a resulting gain in entropy. This finding is also supported by thermodynamic data obtained by Sinaida Lel measuring isothermal calorimetry using the EDS spaced mannose glycooligomers as controls where she found a positive entropic contribution to the overall Gibbs binding energy (data not shown).

A comparison between the trans and PSS AZO structures gives the following results: The affinity of the trivalent structure in trans conformation AZO-Gal(1,3,5)-5 (IC$_{50}$: 3.4 ± 0.4 µM) shows a slight difference of 0.7 µM to the IC$_{50}$ value of the irradiated PSS-AZO-Gal(1,3,5) (IC$_{50}$: 4.1 ± 1.3 µM) structure. This change ranges within error. Therefore it can be concluded that no change in affinity can be determined for the different conformers. Regarding the divalent PSS (IC$_{50}$: 9.4 ± 0.1 µM) and trans (IC$_{50}$: 5.7 ± 1.7 µM) conformers, a change of 3.7 µM referring to 60% can be observed. Thus for the divalent structure, a change in conformation seems to lead to a more pronounced effect also on the binding properties. This might result from the overall shorter length of the scaffold in which the conformational change becomes more distinct than for the longer trivalent structure. In addition, an effect in conformational change could be evened out for the trivalent structure AZO-Gal(1,3,5)-5 by the presentation of the additional sugar moiety. Comparing the obtained results with data from literature, it is found that investigations of switchable multivalent structures are scarce. Azobenzene mannobiosides have been tested as ligand for type 1 fimbriae of E. coli.[183] Another example is the interaction of divalent to octavalent lactose presenting glycoclusters with one azobenzene core being examined as ligand for peanut agglutinin and Con A.[184,185] Both studies showed no change in affinity between different conformers. The major difference between these structures and the presented AZO structures is the incorporation of multiple azobenzene moieties in the main chain. This should potentially result in a more significant change in conformation and thus binding properties as was probably observed for the divalent AZO glycooligomer.

Indeed there are several possible multivalent binding modes that can be influenced by the change in conformation of the AZO units. As the distance between the binding pockets at the small end of PA-IL is only 2.9 nm apart it could be possible that switching influences a chelate binding effect. However this binding mechanism usually results in an increase of binding affinity of several magnitudes. Therefore the here observed 60% difference is unlikely to be caused by

chelate binding. Another possible explanation might be the accessibility of the galactose moieties. The oligomer in cis conformation could be distorted in a way that the galactose moiety cannot reach the binding pockets as efficiently as before in the trans state which could hamper a statistical binding and sliding effect.

The SPR inhibition/competition assay is based on binding between the ligand and receptor in solution. This might give the molecules the opportunity to turn in a manner that compromised binding of the cis state might be partially compensated. In order to overcome this limitation, a direct binding SPR measurement was carried out. For this, AZO-Gal(1,3)-3 and AZO-Gal(1,3,5)-5 were bound covalently to the SPR sensor surface. PA-IL is then incubated with the sensor in a flow cell giving a binding signal as interaction with the galactose oligomer occurs (see Figure 62).
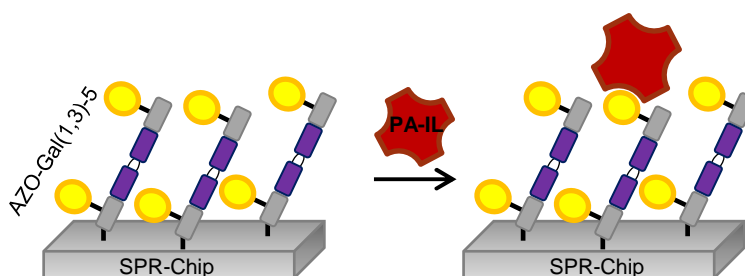
Figure 62: Schematic representation of direct SPR measurements. The glycooligomer is attached to the gold sensor surface. PA-IL lectin is flown in running buffer over the SPR chip. An increase in response is detected upon binding of PA-IL to the glycooligomer.

Functionalization of the sensor surface with both the trans isomer and the PSS isomer was carried out by two ways: The glycooligomer in trans and its corresponding PSS, irradiated in solution, were separately attached on different sensor surfaces (ex-situ irradiation).

Another approach to measure both is to carry out the irradiation/switching directly on the chip. For that, the initial trans oligomer was attached to the surface and its binding to PA-IL was measured. Then, this surface was irradiated with light at 350 nm for one hour and again measured with PA-IL.

Attachment of glycooligomers on sensor chips was achieved by activation of the carboxy-groups presented on the dextrane layer of the sensor surface by EDC and NHS. The generated active esters bind to the free amine groups at the C-terminal site of the glycooligomer. Five different concentrations of PA-IL between 0 and 25 µM were measured. The equilibrium constant K_D was

obtained by fitting the obtained values at the turning point between binding- and dissociation-curve with a steady-state affinity model.
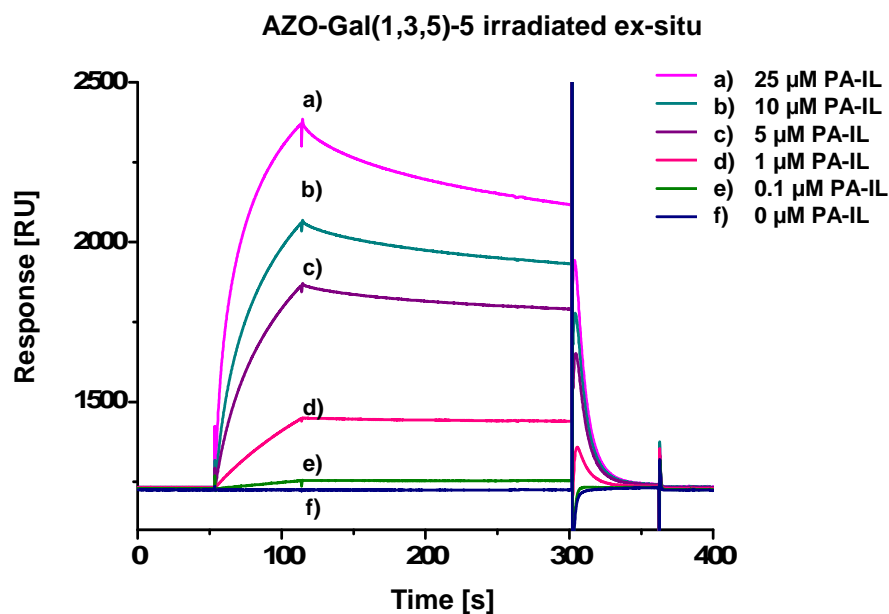
Figure 63: Obtained sensorgram by flowing serial dilutions of PA-IL over the sensor surface functionalized with AZO-Gal(1,3,5)-5.

The results of PA-IL binding directly to the glycooligomer surface with both types of switching can be seen in Table 15.

Table 15: K_D values obtained by SPR direct binding assay of the AZO-Gal structures.

AZO-Gal(1,3)-3	K_D [µM]	AZO-Gal(1,3,5)-5	K_D [µM]
Trans	1.7±0.1	Trans	3.3±0.3
Ex-situ irradiation	2.4±0.1	Ex-situ irradiation	7.4±0.9
Irradiation on chip	1.8±0.1	Irradiation on chip	3.2±0.9

AZO-Gal(1,3)-3 in its initial trans conformation gives an equilibrium binding constant of 1.7 ± 0.1 µM. Attachment to the chip after irradiation yields a K_D of 2.4 ± 0.1 µM. When binding was carried out after irradiation directly on the chip, a binding value of 1.8 ± 0.1 µM was obtained. For the trivalent trans AZO-Gal(1,3,5)-5 a K_D of 3.3 ± 0.3 was observed. Its corresponding PSS, irradiated in solution, gave an equilibrium binding constant of 7.4 ± 0.9.

Irradiation on the chip yielded a K_D of 3.2 μM.

It can be seen that irradiation on the chip did not give a significant change in binding of PA-IL. It can be concluded that a change in of the azobenzene-moiety does probably not occur. The sensor surface consists of a thin gold film. It is possible that the light cannot be efficiently absorbed by the azo-moiety as it is reflected by the metal, or more probably, that the azobenzenes lack sufficient free space for the isomerization to take place

Comparing the obtained values for binding of ex-situ switched glycooligomers, a slightly decreased affinity of both divalent and trivalent structures in PSS compared to trans was observed. This result is in accordance with the inhibition measurements in which also the trans state showed better binding than the PSS. The affinity of divalent AZO-Gal(1,3)-3 in its PSS state decreased app. 70% compared to the trans conformer. Trivalent AZO-Gal(1,3,5)-5 shows a more distinct effect of app. a twofold increase in affinity of trans compared to PSS state. Overall, the observed changes in affinity are more pronounced for the binding assay carried out directly on the chip surface compared to the solution based inhibition/competition assay. This can be explained by the fixation of one end of the glycooligomer to the surface and thus a hindrance in rotation of the glycooligomer. This can be considered a preorganization of the glycooligomer leading to a more effective change in sugar ligand presentation of the glycooligomer to the receptor in dependence of the conformation.

In summary, two glycooligomers incorporating AZO moieties in the main chain and presenting galactose ligands in the side chain were subject to switching induced by UV-light. The four different and two analogue structures with EDS spacers were then subject to PA-IL lectin binding investigated by one surface based and one solution based assay. From the results it can be concluded that a higher number of sugar ligands leads to enhanced binding affinity independent of the kind of sugar ligand-receptor pair, while the overall affinity as well as relative increases in affinity are dependent on the choice of sugar ligand and binding receptor. Furthermore, the results show that a more hydrophilic and flexible backbone consisting of EDS spacers is beneficial for binding activity in comparison to the more stiff and hydrophobic AZO spacing building blocks. As for the changes in, trans conformation of glycooligomers revealing a longer, more stretched backbone, is beneficial for binding. This binding enhancement was more pronounced in the surface based binding assay in which the glycooligomer is preassembled on the surface.

4. Conclusion and Perspectives

The aim of this thesis was to develop a synthetic approach based on solid phase synthesis towards a novel platform of sequence-defined glycomacromolecules which can be used as tools to study multivalent ligand-receptor interactions.

As a first step, functional building blocks suitable for solid phase coupling were synthesized. Two different types of building blocks were developed: a functional building block which could serve as carbohydrate conjugation site and spacer building blocks controlling the spacing of sugar ligands along the backbone as well as the chemical properties of the scaffold. The building blocks were functionalized with both an Fmoc-protected amine function and a carboxylic acid unit for application in solid phase peptide synthesis. An alkyne moiety, usable for CuAAC reaction, was established as carbohydrate conjugation site. The synthesis of this building block started from diethylenetriamine first giving an asymmetric protected intermediate. This precursor allowed for the selective functionalization of the secondary amine yielding a structure with a pendant alkyne moiety in the side chain. Then, both orthogonal protecting groups were successively removed releasing amine functions and the Fmoc- and carboxy unit were installed. This synthetic protocol allows for the large scale synthesis of highly pure products without the need of chromatographic purification thus meeting all requirements for the synthesis of building blocks for solid phase coupling.

For the second class of building blocks, the spacer unit, special focus was devoted to the synthesis of a flexible, hydrophilic unit based on ethylene glycol. The synthetic route established for the conjugation building block could be adapted with small changes. Starting from diethylenedioxy diamine, both amine functions were desymmetrized with orthogonal protective groups. This was followed by successive removal and installation of Fmoc- and carboxyl function giving high yields of the final spacer. In addition, the developed synthetic approach was not limited to the ethylene glycol building block. It was used to generate an alphabet of in total seven spacer building blocks with different lengths and polarity. In general, high purities of above 99% while excluding laborious chromatographic purification were achieved.

In the second part of this thesis, the previously developed building blocks were then applied for the synthesis of glycooligomers on solid phase (chapter 3.2). Alkyne presenting TDS building block, ethylene glycol based EDS spacer and azobenzene-moiety containing AZO spacers were coupled on solid phase employing standard peptide coupling protocols. For the coupling of carbohydrate moieties in the side chain, a highly reliable conjugation method was desired. Therefore, a CuAAC reaction protocol conjugating the alkyne presenting scaffolds with

carbohydrate azides directly on-resin was developed. Additionally, a specific purification protocol was employed yielding products free from traces of copper, a prerequisite for the further analysis of glycooligomers in biological assays.

This thesis specifically aimed for providing access to: a) homomultivalent glycooligomers, b) heteromultivalent glycooligomers c) photoswitchable glycooligomers. Therefore, at first a simultaneous CuAAC reaction protocol was employed for the synthesis of homomultivalent glycooligomers: After the assembly of scaffolds containing multiple EDS and TDS units, all alkyne conjugation sites were functionalized with the same sugar ligand. Using this synthetic route, ten homomultivalent structures were synthesized differing in their overall length from five to ten building blocks with controlled number and spacing of mannose ligands from one to ten.

Secondly, heteromultivalent structures were synthesized by a sequential coupling-click approach conjugating different carbohydrates. This protocol involved conjugation of one type of sugar ligand directly after coupling of a TDS building block keeping the Fmoc-protecting group at the chain end. After Fmoc-removal, further coupling of building blocks was followed by conjugation of another sugar ligand. By repeating these steps, five heteromultivalent glycooligomers consisting of five building blocks were synthesized. Each pentameric oligomer presents three sugar ligands with combinations of mannose together with galactose or glucose.

Lastly, photoswitchable glycooligomers were synthesized. The EDS building block employed in the structures before was exchanged towards an azobenzene-building block. This spacer allowed for both, a more hydrophobic and stiffer backbone structure compared to scaffolds incorporating flexible, ethylene glycol based EDS spacers as well as for a light-induced change in configuration from trans to cis. This results in a change of scaffold conformation and therefore a change in the spatial presentation of the sugar ligands. Four AZO spaced structures consisting of three to five building blocks presenting two to three galactose or mannose ligands were synthesized.

All in all these three sets of glycooligomers present rational variations of parameters known to influence multivalent binding effects of polymeric glycomimetics. This refers to number and spacing of sugar ligands; ligand heterogeneity and backbone properties. With this glycooligomer set in hands, multivalent ligand-receptor interactions were studied (presented in Chapter 3.3): a) The interaction of homomultivalent structures with Con A lectin, b) binding of heteromultivalent structures to Con A and c) interaction of photoswitchable structures with PA-IL lectin.

In the first part, Con A binding of glycooligomers consisting of five to ten building blocks with

one to ten mannose ligands was examined by employing different binding assays. Inhibition/competition assays measured by both SCP-RICM and SPR were used to determine IC_{50} values of the glycooligomers. In general, all structures showed very high affinities towards Con A compared to similar structures known from literature. Inhibition/competition studies also revealed that an increasing number of mannose ligands leads to increased binding affinity. This was rationalized by an increase in statistical rebinding rather than a chelate effect. Surprisingly, no linear correlation between the number of sugar ligands and resulting affinity was observed, but an optimal number of binding ligands of three to five mannoses. This was examined further by studying the trivalent structure with 2fFCS yielding the hydrodynamic radius of the lectin-glycooligomer complex. It was found that by presenting three mannose units, more than one Con A molecule was bound to the glycooligomer forming so-called soluble clusters via intermolecular crosslinking. Therefore, a combination of the cluster formation effect, a statistical rebinding along with an entropic gain from water release through the hydrophilic oligomer scaffold can be identified as the main contributing multivalent effects for homomultivalent glycomimetic ligands.

In the second part of lectin binding studies, binding of heteromultivalent structures to Con A was examined. Five structures consisting of five building blocks presenting each three ligands composed of combinations of mannose together with galactose or glucose were studied. These structures represent analogues of mono- and divalent homomultivalent structures now occupying previously unfunctionalized positions one and three with non-binding or less binding galactose or glucose moieties. IC_{50} values were determined by inhibition competition assay using SCP-RICM. Interestingly, it was found that the obtained binding affinities of the trivalent heterofunctionalized structures were app. the same as for the trivalent all mannose structures although presenting less mannose units. This was rationalized by the multivalent effect of steric shielding of the non-binding sugar ligands which prevent binding of competitor in the binding assay. In order to rule out other effects, two additional binding assays were performed: By STD-NMR it was confirmed that only the mannose units of the glycooligomers are in close proximity to the lectin and thus take part in the binding process. By 2fFCS, the hydrodynamic radius of the lectin/glycooligomer complex was studied revealing that heteromultivalent structures are not capable to form soluble clusters.

The third part of lectin binding studies was dedicated to studying the effect of changing the oligomeric backbone properties. Therefore the EDS spacers were exchanged towards AZO spacers. AZO, in contrast to EDS, is stiffer and more hydrophobic. Additionally it is possible to switch its configuration from trans to cis by UV-light. Latter was used to induce a conformational change of the oligomer backbone resulting in a changed spatial orientation of sugar ligands. Two structures consisting of three building blocks, either AZO or EDS spaced, carrying two galactose

ligands and two structures consisting of five building blocks, either AZO or EDS spaced, carrying three galactose ligands were subject to binding to PA-IL lectin. IC_{50} values were determined by inhibition/competition assay using SPR. The direct comparison of EDS vs. AZO spaced structures showed that binding is enhanced by the flexible, hydrophilic EDS spacers. Inhibition/competition assays were also performed on the cis- and trans- conformers of AZO glycooligomers. An increased binding of trans conformation of glycooligomers was observed and can potentially be attributed to a longer, more stretched backbone conformation. This finding was even more pronounced in a surface based binding assay presenting the AZO-glycooligomers bound to a SPR chip.

Based on these results, the presented platform of monodisperse, sequence-defined glycooligomers proved to be a valuable tool in studying ligand-receptor interactions and helped to gain a deeper insight into the multivalent interaction modes of polymeric sugar mimetics. Such investigations and derived design rules are of fundamental importance for drugs and for receptor screening applications.

5. Experimental Part

5.1. General Methods and Instrumentation

All chemicals were purchased from Aldrich, except: HOBT purchased from Iris Biotech; TFA, triethylamine, ethylenediamine and copper(II)sulfate from Acros; 4-pentynoic acid, ethyl triflouracetate from Alfa Aesar; Fmoc-Cl was purchased from Novabiochem; DIPEA, piperidine and PyBOP from Merck. Atto 647N NHS-ester was purchased from Atto Tec. HPLC grade solvents were used throughout all reactions without further purification. Reactions were carried out water free and under argon where needed.

TLC was performed on Merck silica gel 60 F254 plates (0.25 mm), aluminum sheets. Compounds were visualized by UV irradiation or staining with Ninhydrin or 3-Methoxyphenol solutions followed by heating. Ninhydrin staining solution (amine staining) was obtained by mixing 240 ml Ethanol, 10 ml water, 2.5 ml glacial acetic acid and 750 mg Ninhydrin. 3-Methoxyphenol (carbohydrate staining) was obtained by mixing 6 ml concentrated sulfuric acid, 200 ml Ethanol and 250 μl 3-Methoxyphenol. Flash column chromatography was carried out using force flow of the indicated solvent on Davisil silica gel from Davison (40-65 micron).

FT-IR spectra were recorded on a Perkin-Elmer Spectrum 100 with ATR sampling.

NMR spectra were either measured with a Varian 400-MR (400MHz) or a Varian Premium Compact (600 MHz). The proton signal of residual, non-deuterated solvent was used as internal reference for ^{1}H NMR spectra (δ = 7.26 ppm for CDCl$_3$, 4.79 ppm for H$_2$O, 3.31 ppm for MeOD, 2.50 ppm for DMSO) . For ^{13}C NMR spectra, the chemical shifts are reported relative to the carbon signal of the solvent (δ = 77.16 ppm for CDCl$_3$, 39.52 ppm for DMSO, 49.00 ppm for MeOD). Coupling constants are reported in Hertz (Hz). The following abbreviations are used to indicate the multiplicities: s, singlet; br. s., broad singlet; d, doublet; t, triplet; m, multiplet. MestReNova 6.2.0 was used for data analysis.

STD-NMR spectra were measured with a Varian Premium Compact (600 MHz).Trimethylsilyl propanoic acid (*d4*-TSP) (δ = 0 ppm) was used as internal reference. NMR data with individually assigned protons were subject to STD-NMR studies. Protons were identified after analyzing TOCSY (TOtal Correlation SpectroscopY), COSY (1H-1H, COrrelation SpectroscopY), HSQC (1H-13C Heteronuclear Single Quantum Coherence), PROTON, HMBC (Heteronuclear Multiple Bond Correlation) and H2BC (Heteronuclear 2-Bond Correlation) spectra.

RP-HPLC: Analytical RP-HPLC was performed on Agilent 1200 using an Agilent Zorbax EclipseXDB-C18 (4.6 x 100 mm) column at a flow rate of 1 ml/minute at 60°C. MeCN and water modified with 0.1% triflouroacetic acid were used as eluent. Compounds were dissolved in

water or MeCN. Preparative HPLC was carried out with a Varian Pursuit 10 μ C18 column (250 x 10 mm), at room temperature with a flow rate of 3 ml/minute. UV signal was detected at 214 nm, fluorescence (Fmoc) was detected at 259 nm (extinction) and 311 nm (emission). ChemStation was used for data analysis.

ESI-MS was measured on an Agilent 1100 Series at room temperature with MSD detector. ChemStation was used for data analysis.

UV-Absorbance Spectra were recorded on a PG Instruments T70+ spectrometer using UV-Win version 5.1 for data analysis.

Solid Phase Synthesis: Tentagel-Trt-OH resin was purchased from Rapp Polymers and modified with ethylenediamine as linker. For that, the terminal hydroxyl groups were converted to chloride groups by addition of freshly distilled acetylchloride and heating the mixture at 60°C in toluene for 3 h. After cooling down, ethylenediamine (EDA) was added and shaken for 48 h to obtain tentagel-Trt-EDA resin. Loading of tentagel-Trt-EDA resin was determined by standard loading test: Fmoc-Phenylanlanin was coupled to the resin followed by cleavage with 1,8-Diazabicyclo[5.4.0]undec-7-en (DBU). The UV absorption of the DBU-Fmoc was measured at 304 nm. Fmoc-loading: mmol/g = Abs_{sample}-Abs_{ref} x 6.4. A loading of 0.22 mmol/g was determined.

SPR measurements were performed at 25 °C on a BIACORE X instrument or Biacore T100. Biacore sensor chip SA (Matrix: carboxymethylated dextran pre-immobilized with streptavidin for immobilization of biotinylated interaction partners), sensor chip CM5 (Matrix: carboxymethylated dextran for covalent immobilization of amines via amidation) were purchased from GE Healthcare. Biotinylated α-D-mannose-PAA, biotinylated N-acetyllactosamine-PAA and biotinylated β-D-galactose PAA (PAA = poly[*N*-(2-hydroxyethyl)acrylamide] M_r approx. 30 kDa) were purchased from Lectinity Holdings Inc., Moscow, Russia.

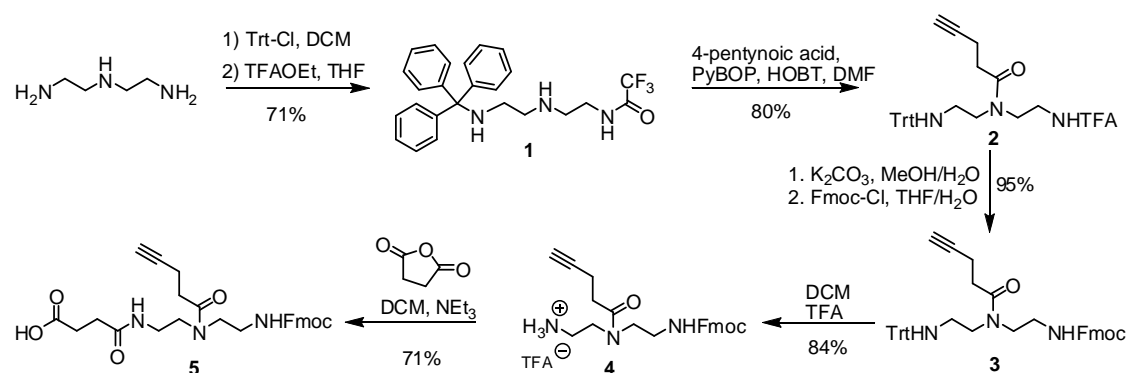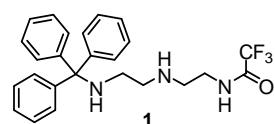## 5.2. Building Blocks

Synthesis of TDS building block:

Figure 64: Synthesis of TDS building block.

<u>2,2,2-Trifluoro-*N*-(2-((2-(tritylamino)ethyl)amino)ethyl)acetamide **1**</u>

To a solution of 33.9 ml (315 mmol) diethylenetriamine in 1000 ml DCM a solution of 19.5 g (70 mmol) TrtCl in 170 ml dichloromethane were added drop wise at 0° C to room temperature. The white slurry solution was stirred 18 h at room temperature. Then it was extracted with sat. $NaHCO_3$ solution. The combined organic phases were dried with $MgSO_4$, filtered and concentrated under reduced pressure to give a colorless oil. The crude product was dissolved in 175 ml THF and 9.2 ml (77.00 mmol) triflourethylacetate were added. After stirring 18 h at room temperature the colorless solution was concentrated under reduced pressure. It was recrystallized from toluene to give 21.9 g (49.6 mmol, 71%) of colorless crystals.

^{1}H NMR (400 MHz, $CDCl_3$): δ = 7.49 – 7.47 (m, 6H), 7.30 – 7.28 (m, 6H), 7.19 – 7.17 (m, 3H), 7.11 (s, 1H), 3.37 (br. s, 2H), 2.75 (t, *J* = 6 Hz, 2H), 2.70 (t, *J* = 6 Hz, 2H), 2.29 (t, *J* = 5.8 Hz, 2H), 1.62 (br. s, 2H) ppm.
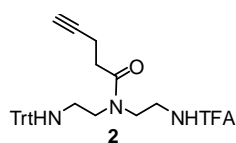
^{13}C NMR (100 MHz, $CDCl_3$): δ = 157.7, 157.3, 156.9, 156.6, 145.9, 128.5, 127.8, 126.3, 120.2, 117.3, 114.5, 111.6, 70.7, 49.4, 47.1, 43.2, 38.9 ppm.

ESI-MS calcd. for $C_{25}H_{26}F_3N_3O$ [M+H][+] 442.2; found 442.2.

<u>*N*-(2-(2,2,2-Trifluoroacetamido)ethyl)-*N'*-(2-(tritylamino)ethyl)pent-4-ynamide **2**</u>


To a solution of 14.5 g (32.8 mmol) **1** in 164 ml DMF, 3.4 g 4-pentynoic acid (34.5 mmol), 18.0 g PyBOP (34.5 mmol) and 5.0 g HOBt (32.8 mmol) and 17.2 ml DIPEA (99 mmol, were added. The mixture was stirred 5 h with at room temperature. Then it was poured in 2 l water and left over night. The cloudy residue was filtered and washed with water. It was redissolved in 250 ml DCM and extracted three times with water, dried over Na_2SO_4 filtered and concentrated under reduced pressure to give 22.8 g (43.7 mmol, 80%) of white foam.

^{1}H NMR (400 MHz, $CDCl_3$): δ = 7.95 (s, 1H), 7.44 – 7.42 (m, 6H), 7.32 – 7.20 (m, 9H), 3.53 – 3.51 (m, 2H), 3.42 – 3.39 (m, 4H), 2.70 (t, *J* = 7.2 Hz, 2H), 2.55 – 2.49 (m, 2H), 2.37 (t, *J* = 6.6 Hz, 2H), 1.65 (t, *J* = 2.5 Hz, 1H), 1.27 (s, 1H) ppm.

^{13}C NMR (100 MHz, $CDCl_3$): δ = 173.9, 145.3, 128.3, 128.0, 126.6, 121.5, 120.0, 117.1, 114.3, 112.2, 82.8, 71.0, 69.0, 49.0, 44.7, 42.4, 40.0, 32.0, 14.6 ppm.

ESI-MS calcd. for $C_{30}H_{30}F_3N_3O_2$ [M+Na]$^+$ 544.2; found 544.2.

<u>(9H-Fluoren-9-yl)methyl (2-(*N*-(2-(tritylamino)ethyl)pent-4-ynamido)ethyl)carbamate **3**</u>
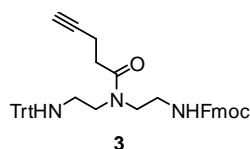
To a solution of 25.9 g potassium carbonate K_2CO_3 in 27 ml water, 22.8 g (28.8 mmol) of **2** dissolved in 240 ml MeOH were added and stirred. After 18 h, MeOH was removed under reduced pressure. The resulting slurry was redissolved with 150 ml tetrahydrofurane and 133 ml water. 6.9 g (26.7 mmol) Fmoc-Cl was added and stirred for 18 h. THF was removed under reduced pressure and the oily residue on the aqueous layer was redissolved with EtOAc. The organic layer was washed three times with water. The collected organic layers were dried over Na_2SO_4, filtered and concentrated under reduced pressure. The product was obtained as white foam (16.4 g, 25.4 mmol, 95 %) and was used without further purification.

^{1}H NMR (400 MHz, $CDCl_3$): δ = 7.68 (d, *J* = 7.5 Hz, 2H), 7.66 (t, *J* = 8.8 Hz, 2H), 7.51 – 7.10 (m, 20H, 4.29 (d, *J* = 6.9 Hz, 2H), 4.27 (t, *J* = 6.8 Hz, 1H), 3.37-3.28 (m, 4H), 3.22 (dd, *J* = 11.3, 5.6 Hz, 2H), 2.62 (t, *J* = 7.3 Hz, 2H), 2.49 – 2.45 (m, 2H), 2.24 (t, *J* = 6.2 Hz, 2H), 1.84 (t, *J* = 2.3 Hz, 1H), 1.63 (s, 2H).
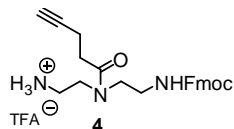
^{13}C NMR (100 MHz, $CDCl_3$): δ = 172.4, 156.5, 145.4, 143.9, 141.2, 128.3, 128.0, 127.6, 127.0,

126.5, 125.0, 119.9, 83.3, 71.0, 68.9, 66.5, 60.3, 48.8, 47.2, 45.4, 42.4, 39.6, 32.1, 21.0, 14.7, 14.1 ppm.

ESI-MS calcd. for $C_{43}H_{41}N_3O_3$ [M+H]+ 647.3; found 647.3.

(9H-Fluoren-9-yl)methyl (2-(*N*-(2-aminoethyl)pent-4-ynamido)ethyl)carbamate **4**


To a solution of 16.4 g (25.3 mmol) **3** in 250 ml DCM, 8.1 ml (50.6 mmol) Triethylsilane (TES) and 25 ml triflouroacetic acid (TFA) were added. The colorless solution was stirred 30 min at room temperature and then coevaporated with toluene. The crude product was redissolved in DCM and precipitated with Et$_2$O resulting in 8.7 g (21.3 mmol, 84%) of a white foam.

^{1}H NMR (400 MHz, CDCl$_3$): δ = 8.15 (s, 2H) 7.71 (d, *J* = 7.5 Hz, 2H), 7.53 (d, *J* = 7.2 Hz, 2H), 7.35 (t, 2H, *J*=7.4 Hz), 7.26 (t, 2H, *J*=7.4 Hz), 5.98 (s, 1H), 4.33 (d, *J*=6.6 Hz, 2H), 4.27 (t, *J* = 6.8 Hz, 1H), 3.60 (br. s, 2H), 3.41 (br. s, 2H), 3.27 (br. s, 2H), 3.15 (br. s, 2H), 2.54 (br. s, 2H), 2.38 (br. s, 2H), 1.91 (s, 1H) ppm.

^{13}C NMR (100 MHz, CDCl$_3$): δ=174.0, 162.2, 162.0, 161.7, 161.3, 156.8, 143.7, 141.2, 129.4, 128.2, 127.70, 127.0, 124.9, 119.9, 118.0, 115.1, 83.0, 69.2, 66.8, 48.3, 47.0, 44.8, 39.3, 38.8, 31.6, 15.24, 14.2 ppm.

ESI-MS calcd. for $C_{24}H_{27}N_3O_3$ [M+H]+ 406.1; found 406.1.

1-(fluorenyl)-3,11-dioxo-7-(pent-4-ynoyl)-2-oxa-4,7,10-triazatetradecan-14-oic acid **5 (TDS)**
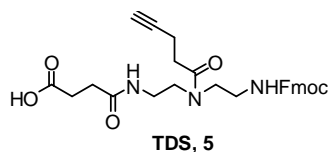
To a solution of 8.7 g (21.3 mmol) **4** in 213 ml dichloromethane, 2.1 g (21.3 mmol) succinic anhydride and 8.9 ml (64.0 mmol) NEt$_3$ were added and stirred for 1 h. The reaction mixture was washed 5 times with 5% aqueous citric acid. The combined organic fractions were dried over Na$_2$SO$_4$ and solvent was removed under reduced pressure. After recrystallization from acetone, the product was obtained as a white solid (7.6 g, 15.1 mmol, 71 %).

^{1}H NMR (400 MHz, DMSO-*d$_6$*): δ = 7.73 (d, *J* = 7.5 Hz, 2H), 7.58 (d, *J* = 7.4 Hz, 2H), 7.34-7.27 (m, 4H), 4.32 (d, *J* = 6.6 Hz, 2H), 4.13 (t, *J* = 6.6 Hz, 1H), 3.43 – 3.18 (m, 8H), 2.60 – 2.50 (m, 4H), 2.46 – 2.36 (m, 4H), 2.24 – 2.15 (m, 1H).

^{13}C NMR (100 MHz, DMSO-*d$_6$*): δ = 174.7, 173.4, 172.8, 157.4, 143.8, 141.1, 127.3, 126.7, 124.6,

119.5, 82.5, 68.7, 66.7, 66.1, 45.6, 45.1, 37.4, 36.9, 31.5, 30.1, 30.0, 28.6, 13.9 ppm.

ESI-MS calcd. for $C_{28}H_{31}N_3O_6$ [M+H]$^+$ 506.3; found 506.2.
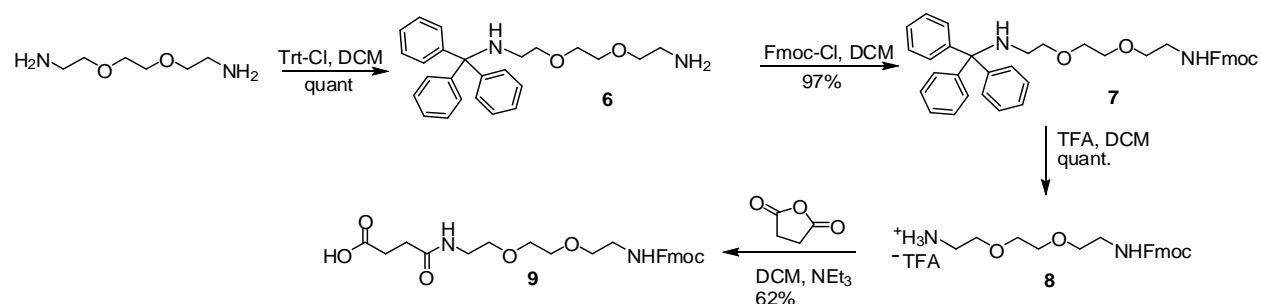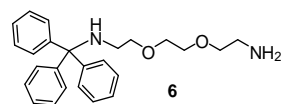
Synthesis of EDS building block:

Figure 65: Synthesis of EDS building block.

2-(2-(2-aminoethoxy)ethoxy)-*N*-tritylethanamine **6**

To a solution of a solution of 25.5 g (172 mmol) ethylenedioxybisethylamine in 430 ml DCM a solution of 12.0 g trityl chloride (43 mmol) in 340 ml DCM, was added dropwise. The slurry white mixture was stirred overnight. The organic phase was washed with saturated NaHCO$_3$ solution. The collected organic phases were dried over MgSO$_4$ and the solvent was removed under reduced pressure to give 16.8 g (43 mmol) of slightly yellow oil. The product was used directly in the next step without further purification.

## (9*H*-fluoren-9-yl)methyl (2-(2-(2-(tritylamino)ethoxy)ethoxy)ethyl)carbamate **7**
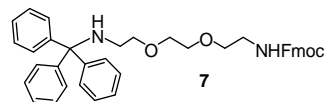
To a solution of 16.8 g (43 mmol) of **6** in 214 ml THF, 11.1 g (42.8 mmol) Fmoc chloride and 29.6 g (214 mmol) potassium carbonate in 214 ml water were added and stirred overnight. THF was removed under reduced pressure and the remaining oil on the water phase was redissolved in 300 ml ethyl acetate. The organic phase was extracted with water, dried over Na$_2$SO$_4$ and the solvent was removed under reduced pressure to give 25.4 g of a white solid (41.5 mmol, 97 %). The product was used directly in the next step without further purification.

(9*H*-Fluoren-9-yl)methyl (2-(2-(2-aminoethoxy)ethoxy)ethyl)carbamate **8**

^+H_3N ～～O～～O～～NHFmoc
^-TFA
8
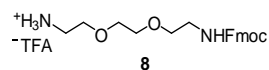
To a solution of 25.4 g (41.5 mmol) of **7** in 410 ml DCM, 13.2 ml TES (83 mmol) and 41 ml TFA were added and stirred for 45 minutes at room temperature. 300 ml toluene was added and TFA was coevaporated under reduced pressure. The remaining crude was redissolved in DCM and precipitated in Et$_2$O. This procedure was repeated until the oil formed a white solid. It was filtered and washed with Et$_2$O to give 15.6 g (42.1 mmol, quant.) product.

^{1}H NMR (400 MHz, MeOD): δ = 8.03 (s, 1H), 7.63 (d, *J* = 7.4 Hz, 2H), 7.53 (d, *J* = 7.1 Hz, 2H,), 7.24 (dt, *J* = 27.4, 7.3 Hz, 4H), 4.23 (d, *J* = 6.6 Hz, 2H), 4.06 (t, *J* = 6.6 Hz, 1H), 3.65-3.38 (m, 8H), 3.24 (br.s, 2 H), 3.02 (br.s, 2 H) ppm.

^{13}C NMR (100 MHz, MeOD): δ = 161.5, 157.4, 143.8, 141.1, 127.4, 126.8, 124.8, 119.6, 69.8, 69.7, 66.1, 46.9, 40.2, 39.1 ppm.

ESI-MS calcd. for $C_{21}H_{27}N_2O_4$+[M+H]$^+$ 371.2; found 371.1.

1-(9*H*-Fluoren-9-yl)-3,14-dioxo-2,7,10-trioxa-4,13-diazaheptadecan-17-oic acid **9** (**EDS**)

HO～～$\overset{O}{\parallel}$～～$\overset{H}{N}$～～O～～O～～NHFmoc
EDS, 9
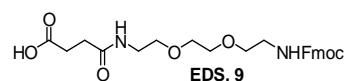
To a solution of 15.5 g (41.7 mmol) of **8** in 410 ml DCM, 17.5 ml NEt$_3$ (125 mmol) and 4.2 g succinic anhydride (41.7 mmol) were added. The mixture was stirred at room temperature for 30 minutes and then extracted with a 5% aqueous solution of citric acid. The organic phase was dried over Na$_2$SO$_4$ and the solvent was removed under reduced pressure. The remaining yellow oil was dissolved in ethyl acetate and some drops of *n*-hexane. A white solid precipitated which was collected by filtration to give 12.1 g of **9** (25.8 mmol, 62%).
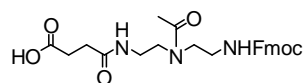
^{1}H-NMR (400 MHz, MeOD) δ = 7.79 (d, *J* = 7.5 Hz, 2H), 7.64 (d, *J* = 7.4 Hz, 2H), 7.38 (t, *J* = 7.4 Hz, 2H), 7.31 (t, *J* = 7.4, 3.8 Hz, 2′H), 4.36 (d, *J* = 6.7 Hz, 2H), 4.20 (t, *J* = 6.7 Hz, 1H), 3.60 (s, 4H), 3.55 – 3.49 (m, 4H), 3.37 – 3.26 (m, 4H), 2.57 (t, *J* = 6.8 Hz, 2H), 2.46 (t, *J* = 6.8 Hz, 2H) ppm.

^{13}C NMR (100 MHz, MeOD): 176.8, 175.2, 172.8, 157.7, 143.7, 141.1, 126.9, 124.9, 119.8, 70.0, 69.4, 66.5, 47.1, 40.6, 39.2, 30.8, 29.9 ppm.

ESI-MS calcd. for $C_{25}H_{30}N_2O_6$ [M+H]$^+$ 471.2; found 471.2.

Synthesis of other building blocks:

Synthesis of ADS:

ADS was synthesized according to the above described synthesis of TDS, the only difference was the use of Ac$_2$O instead of 4-pentynoic acid for the reaction at the secondary amine. To a solution of 10 g (22.7 mmol) asymmetric protected **1** in 227 ml DCM, 3.37 ml (34.0 mmol) Ac$_2$O and 6.55 ml (45.3 mmol) NEt$_3$was added. The reaction was stirred 18 h overnight followed by extraction with water. The combined organic layers were dried over Na$_2$SO$_4$ and solvent was removed under reduced pressure. After recrystallization from acetone, the product was obtained as a white solid (5.2 g, 10.8 mmol, 48 %) of a white solid. It was used in the following steps according to TDS synthetic protocol to give 2.7 g (5.7 mmol, 25% overall yield) ADS.

7-acetyl-1-(9H-fluoren-9-yl)-3,11-dioxo-2-oxa-4,7,10-triazatetradecan-14-oic acid (**ADS**)

^{1}H NMR (400 MHz, DMSO-d_6) δ = 12.06 (s, 1H), 7.89 (d, J = 7.2 Hz, 2H), 7.66 (t, J = 8.2 Hz, 2H), 7.42 (t, J = 7.2 Hz, 2H), 7.34 (d, J = 6.3 Hz, 2H), 4.34-4.29 (m, 2H), 4.21. (t, J = 6.2 Hz, 1H), 3.28 – 3.05 (m, 8H), 2.41 (br. s, 2H), 2.31 – 2.25 (m, 2H), 1.99-1.76 (m, 3H).

^{13}C NMR (100 MHz, DMSO-d_6): δ = 173.9, 173.8, 171.4, 171.1, 171.0, 170.5, 156.3, 155.4, 143.9, 140.7, 127.7, 127.6, 127.2, 127.1, 125.2, 125.1, 120.1, 66.9, 65.3, 48.0, 46.7, 30.0, 29.1, 22.6, 21.3 ppm.

ESI-MS calcd. for C$_{25}$H$_{29}$N$_3$O$_6$ [M+H]$^+$ 468.2; found 468.2 , [M+Na]$^+$ 490.2; found 490.2.

Synthesis of CDS:
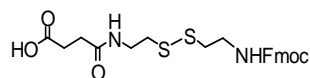
CDS building block was synthesized according to the above described synthesis of EDS. The difference to EDS synthesis was the use of cystamine dihydrochloride as starting material. This salt was converted into a diamine by extraction prior to the first reaction step.

50 g (328 mmol) cystamine dihydrochloride were dissolved in 150 ml water. 20 g (500 mmol) NaOH in 125 ml water were added. This mixture was extracted five times with chloroform. The combined organic phases were dried over Na$_2$SO$_4$ and the solvent was removed under reduced pressure to give 30 g (197 mmol, 60 %) of yellow oil. The product was used directly in the synthetic protocol analog to EDS.

1-(9H-fluoren-9-yl)-3,12-dioxo-2-oxa-7,8-dithia-4,11-diazapentadecan-15-oic acid (**CDS**)

^{1}H NMR (400 MHz, DMSO-d_6) δ= 12.06 (s, 1H), 8.04 (t, J = 5.4 Hz, 1H), 7.89 (d, J = 7.5 Hz, 2H), 7.69 (d, J = 6.4 Hz, 2H), 7.48 (t, J = 5.5 Hz, 2H), 7.41 (t, J = 7.3 Hz, 2H), 7.33 (t, J = 7.4 Hz, 2H), 4.32 (d, J = 6.8 Hz, 2H), 4.21. (t, J = 6.7 Hz, 1H), 3.34 – 3.25 (m, 4H), 2.77 – 2.75 (m, 4H), 2.42 (t, 2H, J = 6.7 Hz,), 2.31 (t, 2H, J = 6.8 Hz).

13C NMR (100 MHz, DMSO-d6): δ = 173.8, 171.1, 156.1, 143.9, 140.7, 127.6, 127.1, 125.1, 120.1, 65.3, 46.7, 38.0, 37.3, 37.1, 30.0, 29.1 ppm.

ESI-MS calcd. for $C_{23}H_{26}N_2O_5S_2$ [M+H]+ 475.1; found 475.0, [M+Na]+ 497.1; found 497.0.

Synthesis of SDS
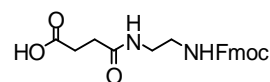
SDS building block was synthesized according to the above described synthesis of EDS. The difference was the use of ethylenediamine as starting material.

4-((2-(((((9*H*-fluoren-9-yl)methoxy)carbonyl)amino)ethyl)amino)-4-oxobutanoic acid (**SDS**)

^{1}H-NMR (400 MHz, DMSO-d_6): δ = 7.89 (d, J = 7.5 Hz, 2H), 7.68 (d, J = 7.4 Hz, 2H), 7.41 (t, J = 7.1 Hz, 2H), 7.33 (t, J = 7.4 Hz, 2H), 4.30 (d, J = 6.9 Hz, 2H), 4.21 (t, J = 6.8 Hz, 1H), 3.08 (t, J = 5.8 Hz, 2H), 3.03 (t, J = 5.6 Hz, 2H), 2.42 (t, J = 7.2 Hz, 2H), 2.30 (t, J = 6.9 Hz, 2H) ppm.

^{13}C-NMR (101 MHz, DMSO-d_6): δ = 173.9, 171.1, 156.1, 143.9, 140.6, 127.7, 127.4, 127.2, 126.96, 125.3, 125.0, 120.2, 120.0, 65.3, 46.8, 46.6, 38.5, 30.0, 29.2 ppm.

ESI-MS calcd. for $C_{21}H_{22}N_2O_5$ [M+H]+ 383.2; found 383.2.

Synthesis of HDS:
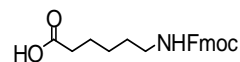
The synthesis of HDS is a one-step procedure from 6-aminohexanoic acid.

To a solution of 2 g 6-aminohexanoic acid (15.25 mmol) and 3.9 g Fmoc-chloride (15.25 mmol) in 76 ml THF a solution of 14.75 g K_2CO_3 (107 mmol) in 76 ml water were added. The biphasic mixture was stirred 18 h overnight. THF was evaporated; the oily residue on the water phase was redissolved in EtOAc. After extracting the mixture with water the combined organic phases were dried with Na_2SO_4 and solvent was removed under reduced pressure. The crude product was recrystallized from acetone to give 3.8 g (15.25 mmol, 70%) of white solid.

6-((((9H-fluoren-9-yl)methoxy)carbonyl)amino)hexanoic acid (**HDS**)

^{1}H NMR (400 MHz, DMSO-d_6): δ = 11.96 (br. s, 1H), 7.89 (d, J = 7.4 Hz, 2H), 7.68 (d, J = 7.4 Hz, 2H), 7.41 (t, J=7.4 Hz, 2H), 7.32 (t, J = 7.4 Hz, 2H), 7.26 (t, J=5.6 Hz, 1H), 4.29 (d, J = 6.9 Hz, 2H), 4.20. (t, J = 6.8 Hz, 1H), 2.96 (dd, J = 12.8, 6.6 Hz, 2H), 2.18 (t, J = 7.3 Hz, 2H), 1.48 (dq, J = 14.9, 7.4 Hz, 2H), 1.39 (dt, J = 14.3, 7.1 Hz, 2H), 1.24 (td, J = 14.8, 7.2 Hz, 2H).

^{13}C NMR (100 MHz, CD_3SO): δ = 174.46, 156.04, 143.91, 140.71, 127.56, 127.01, 125.12, 120.09, 65.09, 46.74, 33.59, 29.11, 25.77, 24.20 ppm.

ESI-MS calcd. for $C_{21}H_{23}NO_4$ [M+H]$^+$ 354.2; found 354.2, [M+Na]$^+$ 376.2; found 376.0 .

5.3. Homomultivalent Structures

Homomultivalent structures were synthesized by repeatedly use of the general coupling protocol and Fmoc cleavage protocol until the scaffold contained the desired number of alkyne groups (by TDS building block) and spacer moieties (EDS building blocks). Then, the *N*-terminal Fmoc moiety was cleaved and the released primary amine site was capped with Ac_2O. This was followed by simultaneous conjugation of the desired sugar azides by general CuAAC protocol. As final step the product was cleaved from solid phase.

General coupling protocol:

Commercially available tentagel-Trt-OH resin modified with EDA was used as resin for solid phase synthesis. After swelling 0.05 mmol (0.23 g) of resin in DCM, the initial coupling to the EDA linker was performed by dissolving 0.4 mmol (8 eq.) of building block in DMF (1.5 ml), followed by the addition of a solution 0.4 mmol PyBOP (8 eq.), 0.2 mmol HOBT (4 eq.) in 1.5 ml DMF. 0.8 mmol (16 eq.) DIPEA was added and the mixture was shaken for 30 sec. This mixture was added to the resin and shaken for one hour. After that, the resin was washed from unreacted reagent app. 5 times with DMF. The Fmoc protecting group was cleaved by addition of a solution of 25% piperidine in DMF three times for 5, 10 and 15 minutes, respectively. After that, the resin was washed carefully with DMF.

Capping of *N*-terminal site:

After successful assembly of the desired number of building blocks on solid phase, the *N*-terminal site was capped with an acetyl group. For that, 3 ml Ac_2O were shaken with the resin for 15 min.

General CuAAC protocol:

To 0.05 mmol of resin loaded with EDS and TDS building blocks, 0.4 mmol (8 eq.) of 2-azidoethyl pyranoside per alkyne group, dissolved in 1.5 ml DMF was added. 20 mol% sodium ascorbate per alkyne group and 20 mol% $CuSO_4$ per alkyne group were dissolved in 0.5 ml water and also

added to the resin. This mixture was shaken for at least four hours and subsequently washed extensively with a 23 mM solution of sodium diethyldithiocarbamate in DMF, water, DMF and DCM.

Cleavage from solid phase:

30% TFA in DCM was added to the desired amount of resin and shaken for one hour. The filtrate was added to cold Et_2O (40 ml). The resulting precipitate was centrifuged and the ether decanted. The crude product was dried in N_2 stream, dissolved in water (1 ml) and lyophilized.
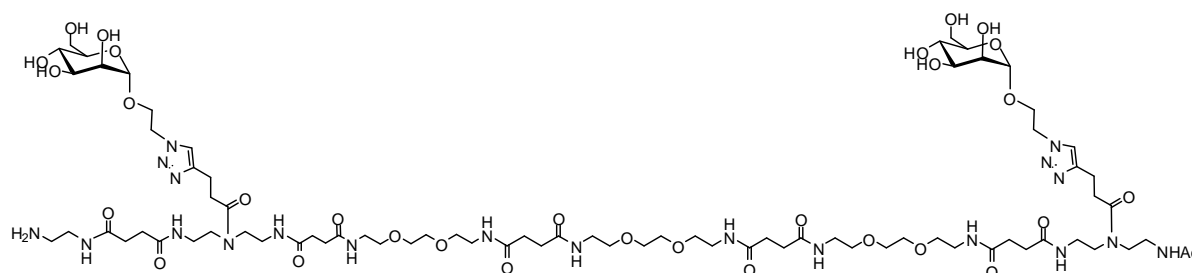
Man(3)-5
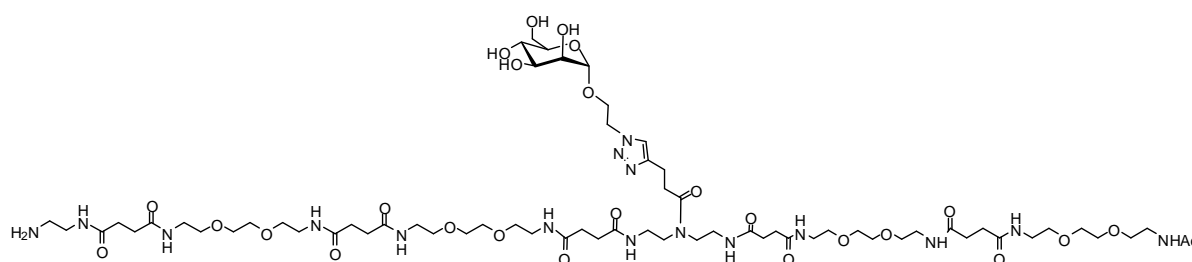
This structure was synthesized by applying the general coupling protocol five times with building blocks in the sequence EDS, EDS, TDS, EDS, EDS. After capping the primary amine, one mannose unit was conjugated to the scaffold according to general CuAAC protocol. The product was cleaved from the resin as final step.

^{1}H NMR (400 MHz, D_2O): δ = 8.37 (s. 1H), 4.70 (br. s, 1H), 4.11 (br. s, 1H), 3.98 (br. s, 1H), 3.87 (br. s, 1H), 3.77-3.72 (m, 5H), 3.69 (br. s, 20H), 3.65-3.62 (m, 21H), 3.54–3.50 (m, 9H), 3.41-3.39 (m, 26H), 3.16 (t, J = 5.7 Hz, 3H), 2.65 (t, J = 6.9 Hz, 3H), 2.58-2.48 (m, 30H), 2.38 (q, J = 1.9 Hz, 1H). 2.02 (d, J = 1.7 Hz, 3H) ppm.

RP-HPLC (5%/95% MeCN/H_2O → 30%/70% MeCN/H_2O in 60 min): t_R = 19.6 min.

ESI-MS calcd. for $C_{65}H_{116}N_{16}O_{26}$ [M+2H]$^{2+}$ 769.4; found 769.4, [M+3H]$^{3+}$ 513.3; found 513.5.

Man(1,5)-5

This structure was synthesized by applying the general coupling protocol five times with

building blocks in the sequence TDS, EDS, EDS, EDS, EDS, TDS. After capping the primary amine, two mannose units were conjugated to the scaffold according to general CuAAC protocol. The product was cleaved from the resin as final step.

^{1}H NMR (400 MHz, D_2O): δ = 8.26 (s. 1H), 4.71 (br. s, 2H), 4.13 (br. s, 2H), 3.97 (br. s, 2H), 3.86 (br. s, 2H), 3.77-3.72 (m, 5H), 3.70-3.56 (m, 37H), 3.48-3.39 (m, 14H), 3.39-3.31 (m, 22H), 3.16-2.96 (m, 11H), 2.85 (br. s, 6H), 2.52 (br. s, 2H), 2.53-2.50 (m, 24H), 1.94 (br. s, 3H) ppm.

RP-HPLC (5%/95% MeCN/H_2O → 30%/70% MeCN/H_2O in 60 min): t_R = 18.3 min.

ESI-MS calcd. for $C_{76}H_{132}N_{20}O_{31}$ [M+2H]$^{2+}$ 911.5; found 911.5 [M+2H]$^{2+}$, [M+3H]$^{3+}$ 608.0 found 608.2, [M+4H]$^{4+}$ 456.2; found 456.4.

<u>Man(1,2)-5</u>

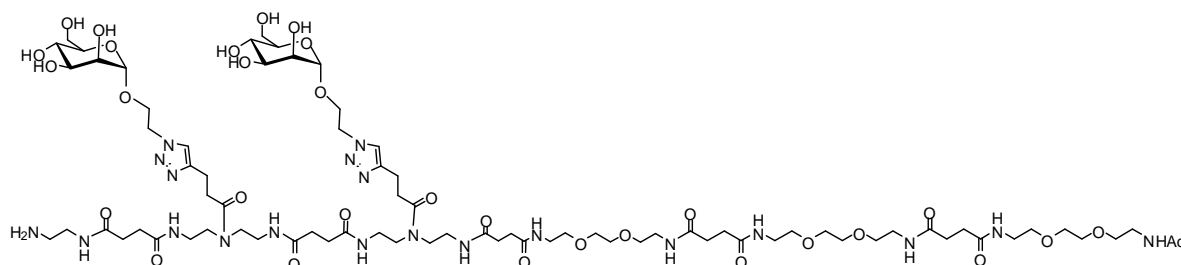This structure was synthesized by applying the general coupling protocol five times with building blocks in the sequence TDS, TDS, EDS, EDS, EDS. After capping the primary amine, two mannose units were conjugated to the scaffold according to general CuAAC protocol. The product was cleaved from the resin as final step.

^{1}H NMR (400 MHz, D_2O): δ = 7.80 (d, J = 6.4 Hz, 2H), 4.54 (br. s, 2H), 4.00-3.96 (m, 2H), 3.83-3.80 (m, 2H), 3.75 (s, 2H), 3.65-3.57 (m, 16H), 3.51 (br. s, 13H), 3.43-3.33 (m, 9H), 3.28 (br. s, 12H), 3.22-3.02 (m, 9H), 2.96-2.86 (m, 5H), 2.69 (br. s, 2H), 2.52 (br. s, 2H), 2.54-2.33 (m, 20H), 1.94 (br. s, 3H) ppm.

RP-HPLC (5%/95% MeCN/H_2O → 30%/70% MeCN/H_2O in 60 min) t_R = 16.4 min.

ESI-MS calcd. for $C_{76}H_{132}N_{20}O_{31}$ [M+2H]$^{2+}$ 911.4; found 911.4, [M+3H]$^{3+}$ 608.0; found 608.1, [M+4H]$^{4+}$ 456.2; found 456.4 [M+5H]$^{5+}$.

5. Experimental Part

Man(1,3,5)-5

This structure was synthesized by applying the general coupling protocol five times with building blocks in the sequence TDS, EDS, TDS, EDS, TDS. After capping the primary amine, three mannose units were conjugated to the scaffold according to general CuAAC protocol. The product was cleaved from the resin as final step.
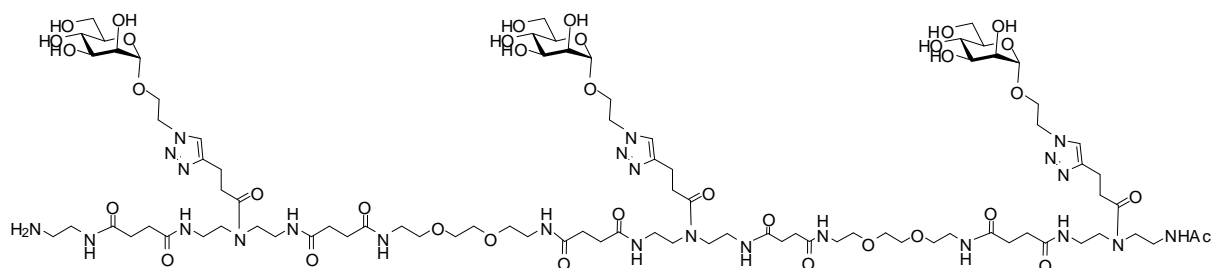
^{1}H NMR (400 MHz, D$_2$O): δ = 7.99 (br. s, 3H), 4.50 (br. s, 10H), 3.96 (br. s, 5H), 3.93 (br. s, 5H), 3.79 (br. s, 4H), 3.70-3.18 (m, 69H), 2.99 (t, J = 6 Hz, 4H), 2.86 (br. s, 12H), 2.50 (br. s, 8H), 2.39-2.32 (m, 22H), 1.77 (d, J = 5 Hz, 3H) ppm.

RP-HPLC (5%/95% MeCN/H$_2$O → 30%/70% MeCN/H$_2$O in 60 min): t$_R$ = 16.6 min.

ESI-MS calcd. for C$_{87}$H$_{148}$N$_{24}$O$_{36}$ [M+2H]$^{2+}$ 1053.5; found 1053.8, [M+3H]$^{3+}$ 702.7; found 702.8, [M+4H]$^{4+}$ 527.3; found 527.5.
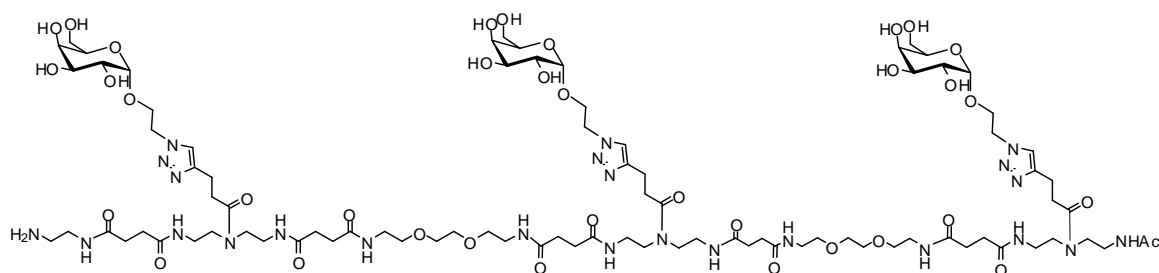
Gal(1,3,5)-5

This structure was synthesized by applying the general coupling protocol five times with building blocks in the sequence TDS, EDS, TDS, EDS, TDS. After capping the primary amine, three galactose units were conjugated to the scaffold according to general CuAAC protocol. The product was cleaved from the resin as final step.

^{1}H NMR (400 MHz, D$_2$O) δ = 8.04 (d, J = 7 Hz, 3H), 4.74 (br. s, 6H). 4.43 (d, J = 8 Hz, 3H), 4.38 – 4.33 (m, 3H), 4.19-4.14 (m, 3H), 3.97 (s, 3H), 3.81-3.79 (m, 7H), 3.72 (s, 10H), 3.65-3.65 (m, 10H), 3.56-3.51 (m, 16H), 3.44-3.39 (m, 18H), 3.20(t, J = 6 Hz, 2H), 3.08 (t, J = 6 Hz, 6H). 2.85 (t, J = 7 Hz, 6H), 2.58-2.50 (m, 20H), 1.99 (d, J = 5 Hz, 3H).
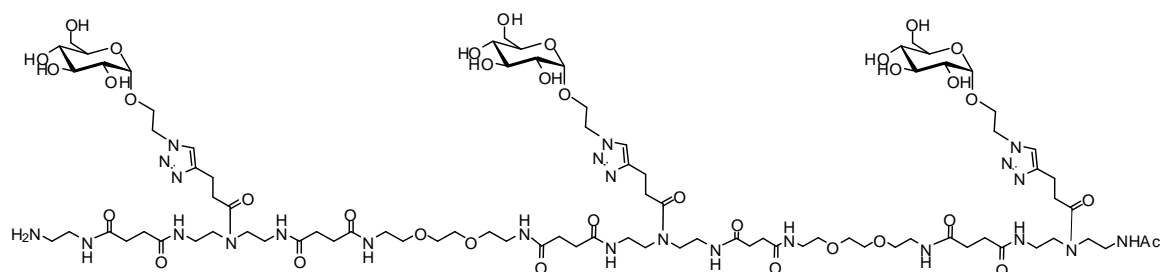
ESI-MS calcd. for $C_{87}H_{148}N_{24}O_{36}$ [M+2H]$^{2+}$ 1053.5; found 1053.8, [M+3H]$^{3+}$ 702.7; found 702.8, [M+4H]$^{4+}$ 527.3; found 527.4, [M+5H]$^{5+}$ 422.0; found 422.2.

RP-HPLC (5 %/95 % MeCN/H$_2$O → 30%/70% MeCN/H$_2$O in 60 min) t_R = 14.1 min
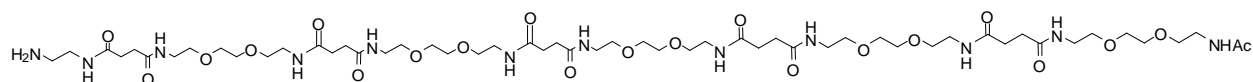
Glc(1,3,5)-5

This structure was synthesized by applying the general coupling protocol five times with building blocks in the sequence TDS, EDS, TDS, EDS, TDS. After capping the primary amine, three glucose units were conjugated to the scaffold according to general CuAAC protocol. The product was cleaved from the resin as final step.

^{1}H NMR (400 MHz, D$_2$O) δ = 8.13 (d, J = 7 Hz, 3H), 4.51 (d, J = 8 Hz, 4H), 4.38-4.35 (m, 4H), 4.19-4.16 (m, 4H), 3.93 (d, J = 12 Hz, 3H), 3.76-3.75 (m, 3H), 3.70 (s, 8H), 3.65 (t, J = 5 Hz, 8H), 3.56-3.45 (m, 19H), 3.43-3.37 (m, 20H), 3.28(t, J = 9 Hz, 4H), 3.19 (t, J = 6 Hz, 2H), 3.10 (br. s, 6H), 2.88 (br. s, 6H), 2.59-2.50 (m, 20H), 1.98 (s, 3H).

ESI-MS calcd. for $C_{87}H_{148}N_{24}O_{36}$ [M+2H]$^{2+}$ calcd. 1053.5; found 1053.6, [M+3H]$^{3+}$ calcd. 702.7; found 702.8, [M+4H]$^{4+}$ calcd. 527.3; found 527.3 [M+5H]$^{5+}$, calcd. 422.01; found 422.3.

RP-HPLC (5%/95% MeCN/H$_2$O → 30%/70% MeCN/H$_2$O in 60 min) t_R = 14.5 min.

EDS-5

This structure was synthesized by applying the general coupling protocol five times with EDS building block. The product was cleaved from the resin as final step.

^{1}H NMR (400 MHz, D$_2$O) δ=3.64 (s, 20 H), 3.58 (t, J=5 Hz, 20 H), 3.47 (t, J=6 Hz, 2 H), 3.35 (t, J=5 Hz, 20 H), 3.11 (t, J=6 Hz, 2 H), 2.51 (t, J=5 Hz, 20 H), 1.96 (s, 3 H).

ESI-MS calcd. for $C_{54}H_{100}N_{12}O_{21}$ [M+H]$^+$ 1253.7; found 1253.5, [M+2H]$^{2+}$ 627.4; found 627.4, [M+3H]$^{3+}$ 418.6; found 418.6.

RP-HPLC (5%/95% MeCN/H$_2$O → 30%/70% MeCN/H$_2$O in 60 min) t_R =20.0 min.

Man(all)-5

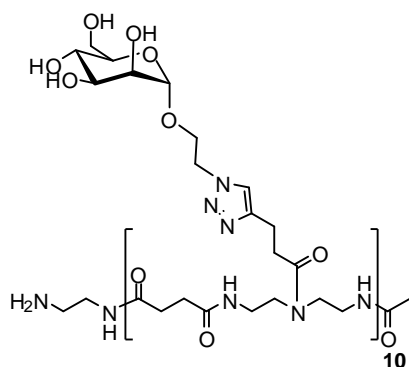This structure was synthesized by applying the general coupling protocol five times with TDS building block. After capping the primary amine, five mannose units were conjugated to the scaffold according to general CuAAC protocol. The product was cleaved from the resin as final step.

Structure was subject to STD-NMR study, therefore the protons could be individually assigned.

^{1}H NMR (600 MHz, D$_2$O) δ = 7.89 (s, 5H, *H9*), 4.63 (br s, 10H, *H8*), 4.10-4.04 (m, 5H, *H7*), 3.92-3.90 (m, 5H, *H7*), 3.85 (s, 5H, *H2*), 3.74-3.66 (m, 10H, *H6*), 3.65-3.62 (m, 5H, *H3*), 3.60-3.54 (m, 5H, *H5*), 3.50-3.49 (m, 2H, *H15*), 3.49-3.40 (m, 20H, *H12+H17*), 3.40-3.28 (m, 20H, *H13+H16*), 3.31 (t, 2H, *J* = 3 Hz, *H16*), 3.05-3.01 (m, 5H, *H4*), 2.99-2.95 (m, 10H, *H10*), 2.81-2.75 (m, 10H, *H11*), 2.62-2.40 (m, 20H, *H14*), 1.92 (d, 3H, *J* = 2 Hz) ppm.

RP-HPLC (5%/95% MeCN/H$_2$O → 30%/70% MeCN/H$_2$O in 60 min) t$_R$ = 8.7 min.

ESI-MS calcd. for C$_{109}$H$_{180}$N$_{32}$O$_{46}$ [M+2 Na]$^{2+}$ 1359.6; found 1359.2, [M+3H]$^{3+}$ 892.15; found 892.3, [M+4H]$^{4+}$ calcd. 669.3; found 669.5, [M+5H]$^{5+}$.

Gal(all)-5

This structure was synthesized by applying the general coupling protocol five times with TDS building block. After capping the primary amine, five galactose units were conjugated to the scaffold according to general CuAAC protocol. The product was cleaved from the resin as final step.

^{1}H-NMR (400 MHz, D$_2$O): δ = 8.07-8.00 (m, 5H), 4.70-4.64 (m, 10H), 4.33 (d, J = 7.8 Hz, 5H), 4.30–4.22 (m, 5H), 4.11–4.03 (m, 5H), 3.88–3.84 (m, 5H), 3.72-3.54 (m, 20H), 3.47-3.36 (m, 25H), 3.36–3.25 (m, 20H), 3.09 (t, J = 6.0 Hz, 2H), 3.00 (t, J = 6.5 Hz, 10H), 2.77 (t, J = 6.2 Hz, 8H), 2.65–2.54 (m, 4H), 2.51-2.36 (m, 20H), 2.00 (d, J = 16.4 Hz, 3H) ppm.

RP-HPLC (5%/95% MeCN/H$_2$O → 30%/70% MeCN/H$_2$O in 60 min): t_R = 10.2 min.

ESI-MS calcd. for C$_{109}$H$_{180}$N$_{32}$O$_{46}$ [M+2H]$^{2+}$ 1337.6; found 1338.0, [M+3H]$^{3+}$ 892.4; found 892.3, [M+4H]$^{4+}$ 669.6; found 669.5.
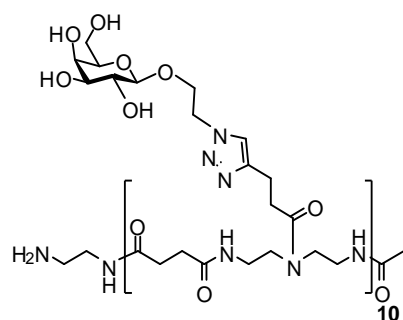

Man(all)-10

This structure was synthesized by applying the general coupling protocol ten times with TDS building block. After capping the primary amine, ten mannose units were conjugated to the scaffold according to general CuAAC protocol. The product was cleaved from the resin as final step.

1H NMR (600 MHz, D2O) δ = 7.96 (s, 10 H), 4.84 (s, 10 H), 4.74-4.66 (m,20 H), 4.17-4.11 (m, 10 H), 3.99-3.96 (m, 10 H), 3.91 (s, 10 H), 3.81-3.76 (m, 10 H), 3.74-3.68 (m, 20 H), 3.66-3.59 (m, 10 H), 3.57 (s, 2 H), 3.55-3.47 (m, 40 H), 3.45-3.32 (m, 40 H), 3.20 (t, 2 H, J = 3 Hz), 3.14-3.08 (m, 10H), 3.08-2.98 (m, 20 H), 2.90-2.79 (m, 20 H), 2.70-2.45 (m, 20 H, H14), 1.99 (d, 3 H, J = 2 Hz) ppm.

RP-HPLC (5%/95% MeCN/H$_2$O → 30%/70% MeCN/H$_2$O in 60 min) t_R = 17.7 min.

ESI-MS calcd. for C$_{214}$H$_{350}$N$_{62}$O$_{91}$ [M+2H+Na]$^{3+}$ 1756.5; found 1757.6, [M+4H]$^{4+}$ 1312.1 found 1312.7, [M+5H]$^{5+}$ 1049.9; found 1050.2.

Gal(all)-10

This structure was synthesized by applying the general coupling protocol ten times with TDS building block. After capping the primary amine, ten galactose units were conjugated to the scaffold according to general CuAAC protocol. The product was cleaved from the resin as final step.

1H-NMR (400 MHz, D2O): δ = 7.89 (s, J = 9.0 Hz, 10H), 4.64-4.58 (m, 20H), 4.33 (d, J = 7.8 Hz, 10H), 4.28-4.21 (m, 10H), 4.09-4.00 (m, 10H), 3.87 (d, J = 3.1 Hz, 10H), 3.73-3.55 (m, 40H), 3.48-3.37 (m, 50H), 3.36-3.23 (m, 40H), 3.13-3.08 (t, J = 5.5 Hz, 2H), 2.94 (t, J = 6.3 Hz, 20H), 2.74 (t, J = 6.3 Hz, 18H), 2.63 – 2.51 (m, 4H), 2.51-2.34 (m, 40H), 1.88 (d, J = 7.7 Hz, 3H) ppm.

RP-HPLC (5%/95% MeCN/H$_2$O → 30%/70% MeCN/H$_2$O in 60 min): t_R = 15.8 min.

ESI-MS calcd. for C$_{214}$H$_{350}$N$_{62}$O$_{91}$ [M+4H]$^{4+}$ 1312.9; found 1312.5, [M+5H]$^{5+}$ 1050.5; found 1050.3, [M+6H]$^{6+}$ 875.6; found 875.3 [M+6H]$^{6+}$.

5.4. Heteromultivalent Structures

Heteromultivalent structures were synthesized by a sequential coupling/CuAAC protocol. For that, one building block was coupled according to the general coupling protocol followed by coupling of one sugar according to the general CuAAC protocol. Then Fmoc was cleaved and followed by another coupling/CuAAC reaction and Fmoc cleavage. These three steps were repeated five times, then the *N*-terminal site was capped. Hydroxyl groups of Glc derivatives (GlcManGlc(1,3,5)-5 and ManGlcMan(1,3,5)-5) were found to be partially acetylated after the capping step as described above. A deacetylation with Zemplén conditions was carried out directly on the resin.

General methanolate protocol:

2.5 ml of a 20 mM solution of sodium methanolate in MeOH was added to the resin and shaken for 30 min.

GalManGal(1,3,5)-5

This structure was synthesized by applying the general coupling protocol for TDS followed by general CuAAC protocol with galactose and coupling of EDS. These three steps were repeated in the sequence TDS/mannose/EDS, TDS/galactose. Then, the primary amine obtained after Fmoc removal was capped with Ac$_2$O.

Structure was subject to STD-NMR study, therefore the protons could be individually assigned. The anomeric proton of Man could not be examined due to interference with the solvent suppression scheme applied during the STD-NMR experiment.
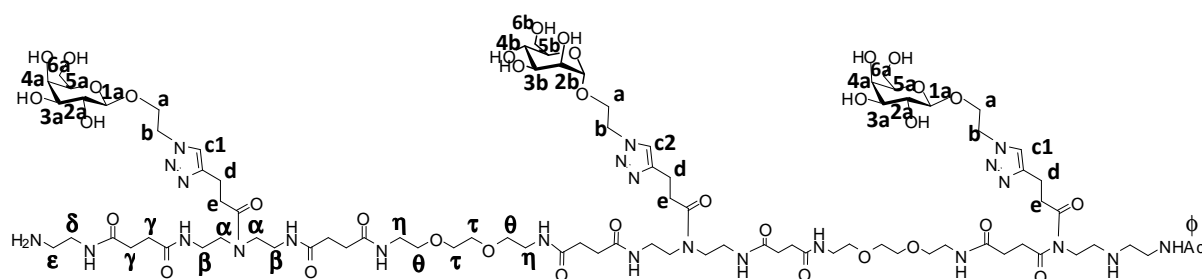
^{1}H NMR (600 MHz, D$_2$O) δ = 7.88 (s, 2H, c1), 7.86 (br. s, 1H, c2), 4.67-4.57 (m, 6H, b), 4.36-4.35 (m, 2H, 1b), 4.28-4.26 (m, 4H, 6b), 4.09-4.07 (m, 4H, a), 3.90 (br. s, 3H, a+4b), 3.84 (s, 1H, 2a), 3.74-3.71 (m, 2H, 6a+3b), 3.65 (br. s, 11H, τ+3a), 3.63-3.58 (m, 10H, 4a, 5a+θ), 3.49-3.45 (m, 16H, α+δ+2b), 3.36 (br. s, 12H, β), 3.32 (br. s, 6H, η), 3.13 (br. s, 2H, δ), 3.05-2.92 (m, 8H, 5b+d), 2.79-2.73 (br. s, 6H, e), 2.55-2.39 (m, 20H, γ), 1.91 (d, 3H, J = 12 Hz, ϕ) ppm.

RP-HPLC (5%/95% MeCN/H$_2$O → 30%/70% MeCN/H$_2$O in 60 min): t_R = 14.6 min.

ESI-MS calcd. for C$_{87}$H$_{148}$N$_{24}$O$_{36}$ [M+2H]$^{2+}$ 1053.5; found 1053.9, [M+3H]$^{3+}$ 702.7; found 702.8, [M+4H]$^{4+}$ 527.3; found 527.5.

ManGalMan(1,3,5)-5

This structure was synthesized by applying the general coupling protocol for TDS followed by general CuAAC protocol with mannose and coupling of EDS. These three steps were repeated in the sequence TDS/galactose/EDS, TDS/mannose. Then, the primary amine obtained after Fmoc removal was capped with Ac$_2$O.

Structure was subject to STD-NMR study, therefore the protons could be individually assigned.

5. Experimental Part

The anomeric proton of Man could not be examined due to interference with the solvent suppression scheme applied during the STD-NMR experiment.
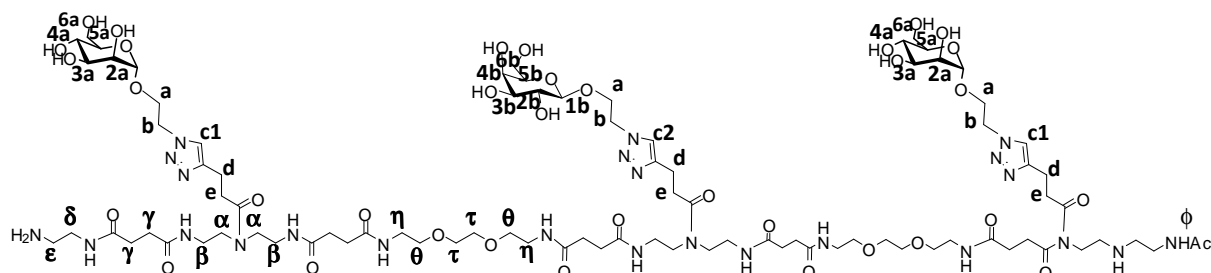

^{1}H NMR (600 MHz, D$_2$O) δ = 7.89 (s, 1H, c2), 7.89 (br. s, 2H, c1), 4.66-4.59 (m, 6H, b), 4.36 (d, J = 7.8 Hz, 1H, 1b), 4.29-4.25 (m, 2H, 6b), 4.09-4.25 (m, 4H, a), 3.92-3.89 (m, 3H, a+4b), 3.85 (br. s, 2H, 2a), 3.74-3.70 (m, 4H, 6a), 3.67-3.64 (m, 11H, τ+3b+3a), 3.63-3.60 (m, 9H, 4a, 5a+θ), 3.49-3.44 (m, 15H, α+δ+2b), 3.37-3.31 (m, 20H, β+ η), 3.13 (t, 2H, J = 6 Hz, ε), 3.01-3.00 (m, 1H, 5b), 2.98 (t, J = 8 Hz, 6H, d), 2.80-2.76 (m, 6H, e), 2.52-2.45 (m, 20H, γ), 1.92 (d, 3H, J = 9 Hz, φ) ppm.

RP-HPLC (5%/95% MeCN/H$_2$O → 30%/70% MeCN/H$_2$O in 60 min): t$_R$ = 14.8 min.

ESI-MS calcd. for C$_{87}$H$_{148}$N$_{24}$O$_{36}$ [M+2H]$^{2+}$ 1053.5; found 1053.7, [M+3H]$^{3+}$ 702.7; found 703.0, [M+4H]$^{4+}$ 527.3; found 527.5, [M+5H]$^{5+}$ 422.0; found 422.3.

ManManGal (1,3,5)-5

This structure was synthesized by applying the general coupling protocol for TDS followed by general CuAAC protocol with mannose and coupling of EDS. These three steps were repeated in the sequence TDS/mannose/EDS, TDS/galactose. Then, the primary amine obtained after Fmoc removal was capped with Ac$_2$O.
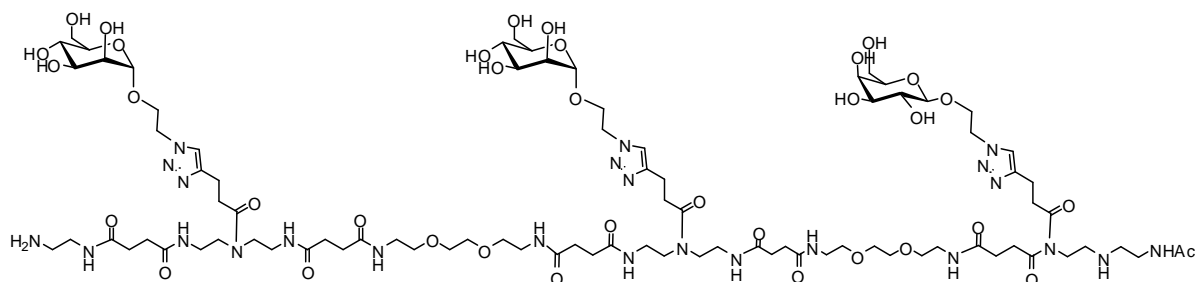
^{1}H NMR (400 MHz, D$_2$O) δ = 8.06 (s, 1H), 7.96 (d, 2H), 4.76 (br. s, 2H), 4.70-4.61 (m, 6H), 4.34 (d, J = 7.8 Hz, 1H), 4.31-4.26 (m, 1H), 4.11-4.04 (m, 3H), 3.92-3.87 (m, 3H), 3.83-3.82 (m, 2H), 3.73-3.70 (m, 4H), 3.67-3.61 (m, 16H), 3.58-3.56 (m, 12H), 3.47-3.41 (m, 16H), 3.35-3.30 (m, 20H),

3.10 (t, 2H, J = 6 Hz, ε), 3.05-2.98 (m, 8H), 2.78 (br. s, 5H), 2.50-2.42 (m, 22), 1.90 (d, 3H, J = 9 Hz) ppm.

RP-HPLC (5%/95% MeCN/H_2O → 30%/70% MeCN/H_2O in 60 min): t_R = 14.2 min.

ESI-MS calcd. for $C_{87}H_{148}N_{24}O_{36}$ $[M+2H]^{2+}$ 1053.5; found 1053.8, $[M+3H]^{3+}$ 702.7; found 702.8, $[M+4H]^{4+}$ 527.3; found 527.4, $[M+5H]^{5+}$ 422.0; found 422.0.

GlcManGlc(1,3,5)-5

This structure was synthesized by applying the general coupling protocol for TDS followed by general CuAAC protocol with glucose and coupling of EDS. These three steps were repeated in the sequence TDS/mannose/EDS, TDS/glucose. Then, the primary amine obtained after Fmoc removal was capped with Ac2O. After applying general methanolate protocol the product was cleaved from the resin.
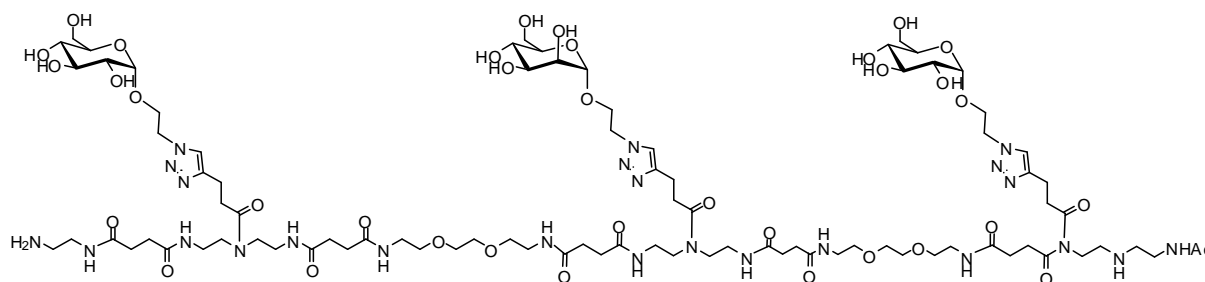
^{1}H NMR (400 MHz, D_2O) δ = 8.12-8.06 (m, 3H), 4.49 (d, J = 8 Hz, 2H), 4.39–4.32 (m, 3H), 4.21-4.13 (m, 4H), 4.02-3.87 (m, 6H), 3.82-3.76 (m, 5H), 3.75-3.69 (m, 13H), 3.66 (t, J = 5 Hz, 8H), 3.56-3.47 (m, 19H), 3.43-3.38 (m, 19H), 3.28 (t, J = 9 Hz, 3H), 3.20 (t, J = 6 Hz, 3H), 3.09 (br. s, 6H), 2.98 (s, 1H), 2.88 (br. s, 7H), 2.62-2.46 (m, 20H), 1.99 (s, 3H).

RP-HPLC (5%/95% MeCN/H_2O → 30%/70% MeCN/H_2O in 60 min) t_R = 14.8 min.

ESI-MS calcd. for $C_{87}H_{148}N_{24}O_{36}$ $[M+3H]^{3+}$ 702.7, found 703.0.

ManGlcMan(1,3,5)-5

This structure was synthesized by applying the general coupling protocol for TDS followed by general CuAAC protocol with mannose and coupling of EDS. These three steps were repeated in the sequence TDS/glucose/EDS, TDS/mannose. Then, the primary amine obtained after Fmoc removal was capped with Ac$_2$O. After applying general methanolate protocol the product was cleaved from the resin.

^{1}H NMR (400 MHz, D$_2$O) δ = 8.10-7.99 (m, 3H), 4.49 (d, J = 8 Hz, 3H), 4.35 (br. s, 3H), 4.16 (m, 5H), 4.00-3.96 (m, 4H), 3.91 (m, 4H), 3.81-3.75 (m, 9H), 3.74-3.69 (m. 13H), 3.57-3.48 (m, 19H), 3.47-3.39 (m, 19H), 3.29 (t, J = 9 Hz, 3H), 3.20 (t, J = 6 Hz, 3H), 3.08 (br. s, 9H), 2.98 (s, 1H), 2.87 (br. s, 8H), 2.61-2.48 (m, 20H), 1.99 (d, J = 4 Hz, 3H).
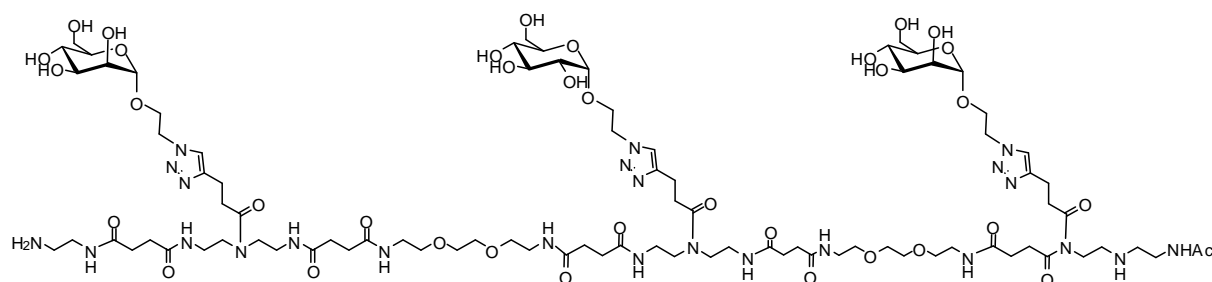
RP-HPLC (5%/95% MeCN/H$_2$O → 30%/70% MeCN/H$_2$O in 60 min) t_R = 15.1 min.

ESI-MS calcd. for C$_{87}$H$_{148}$N$_{24}$O$_{36}$ [M+2H]$^{2+}$ 1053.5; found 1053.6, [M+3H]$^{3+}$ 702.7; found 702.8, [M+4H]$^{4+}$ 527.3; found 527.5.

5.5. Switchable Structures

Cis/trans isomerization by irradiation:

Irradiation of a 2 mM solution of AZO-Gal(1,3)-3 and AZO-Gal(1,3,5)-5 in water was carried out by placing it in a quartz cuvette (1 cm) in the beam of a Xe-lamp equipped with a filter giving light at 360 nm. After one hour the PSS was reached and verified by analytical HPLC. Switching of AZO-Gal(1,3)-3 and AZO-Gal(1,3,5)-5 directly on the Biacore sensor chip was carried out by placing the gold surface in water into the above described beam of light for one hour.

AZO-Gal(1,3)-3
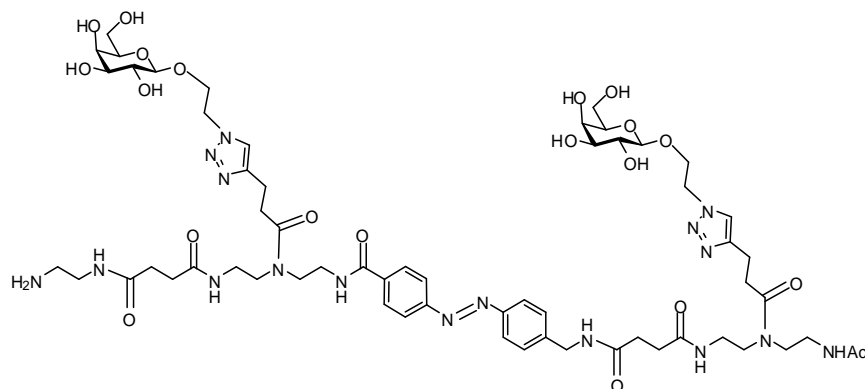
This structure was synthesized by applying the general coupling protocol three times with building blocks in the sequence TDS, AZO, TDS. After capping the primary amine, two galactose

units were conjugated to the scaffold according to general CuAAC protocol. The product was cleaved from the resin as final step.

^{1}H NMR (400 MHz, D$_2$O): δ = 7.84-7.73 (m, 12H), 7.54-7.48 (m, 2H), 4.50-4.42 (m, 9H), 4.29–4.07 (m, 4H), 4.07 (br. s, 2H), 3.78 (s, 4H), 3.67-2.48 (m, 50 H), 1.85 (d, J = 21.0 Hz, 3H) ppm.

RP-HPLC (5%/95% MeCN/H$_2$O → 30%/70% MeCN/H$_2$O in 30 min): t$_R$ = 14.8 min.

ESI-MS calcd. for C$_{60}$H$_{89}$N$_{17}$O$_{20}$ [M+H]$^+$ 1368.6; found 1368.4, [M+2H]$^{2+}$ 684.8; found 684.8, [M+3H]$^{3+}$ 456.9; found 457.0.

5. Experimental Part

AZO-Gal(1,3,5)-5

This structure was synthesized by applying the general coupling protocol three times with building blocks in the sequence TDS, AZO, TDS, AZO, TDS. After capping the primary amine, three galactose units were conjugated to the scaffold according to general CuAAC protocol. The product was cleaved from the resin as final step.

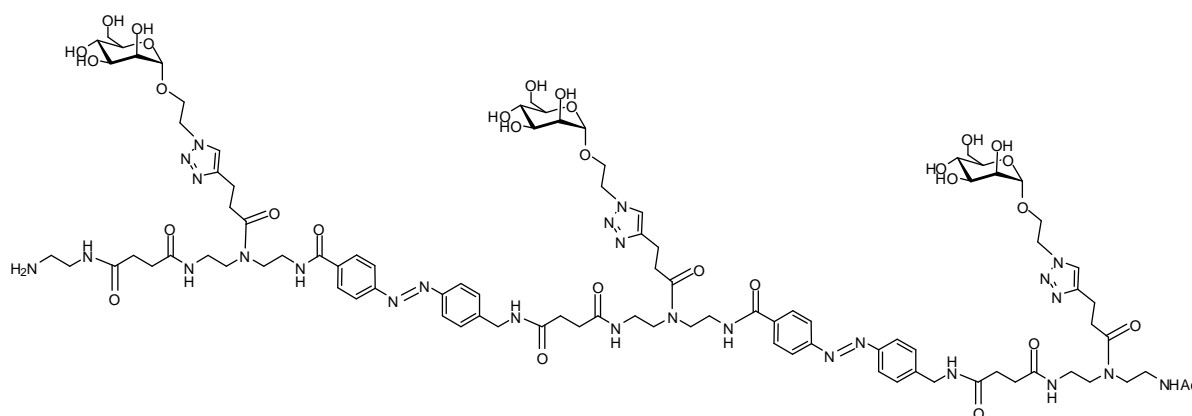^{1}H-NMR (400 MHz, D_2O): δ = 7.73-7.45 (m, 12H), 7.34 (br. s, 3H), 4.48-4.31 (m, 9H), 4.25-4.08 (m, 8H), 3.78-3.66 (m, 8 H), 3.66-3.30 (m, 32H), 3.18 (br. s, 4H), 2.98 (br. s, 3H), 2.98-2.35 (m, 25H), 1.82 (d, *J* = 10.6 Hz, 3H) ppm.

RP-HPLC (5%/95% MeCN/H_2O → 30%/705% MeCN/H_2O in 30 min): t_R = 21.7 min.

ESI-MS calcd. for $C_{95}H_{134}N_{26}O_{30}$ [M+2H]$^{2+}$ 1060.5; found 1060.4, [M+H+Na]$^{2+}$ 1082.9; found 1082.6, [M+3H]$^{3+}$ 707.4; found 707.5$^+$, [M+4H]$^{4+}$ 530.7; found 530.8.
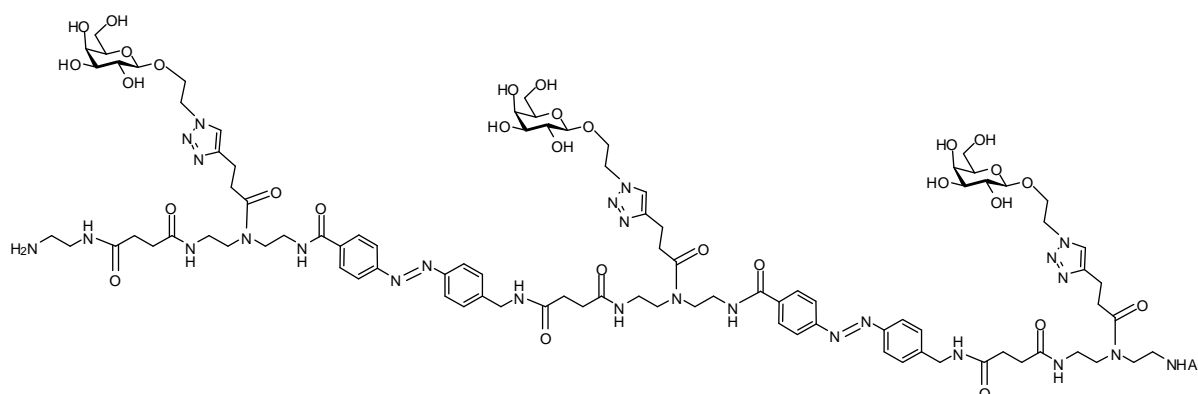
AZO-Man(1,3,5)-5

This structure was synthesized by applying the general coupling protocol three times with building blocks in the sequence TDS, AZO, TDS, AZO, TDS. After capping the primary amine, three mannose units were conjugated to the scaffold according to general CuAAC protocol. The product was cleaved from the resin as final step.
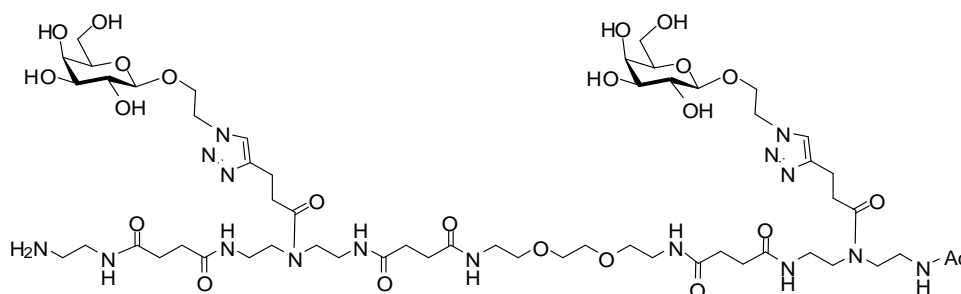
^{1}H NMR (400 MHz, D$_2$O): δ = 7.68-7.48 (m, 12H), 7.32 (br. s, 3H), 4.69-4.58 (m, 3H), 4.41–4.30 (m, 8H), 3.90 (br. s, 2 H), 3.75-3.70 (m, 6H), 3.62–3.08 (m, 48H), 2.86-2.45 (m, 32H), 1.82 (d, J = 8.5 Hz, 3H) ppm.

RP-HPLC (5%/95% MeCN/H$_2$O → 30%/705% MeCN/H$_2$O in 30 min): t_R = 21.7 min.

ESI-MS calcd. for C$_{95}$H$_{134}$N$_{26}$O$_{30}$ [M+H+Na]$^{2+}$ 1082.9; found 1082.8, [M+3H]$^{3+}$ 707.4; found 707.5, [M+4H]$^{4+}$. 530.7; found 530.8.

EDS-Gal(1,3)-3

This structure was synthesized by applying the general coupling protocol three times with building blocks in the sequence TDS, EDS, TDS, EDS, TDS. After capping the primary amine, two galactose units were conjugated to the scaffold according to general CuAAC protocol. The product was cleaved from the resin as final step.

^{1}H NMR (400 MHz, D$_2$O): δ = 8.00 (s, 2H), 4.44 (d, J = 7.8 Hz, 2H), 4.40-4.32 (m, 2H), 4.21-4.12 (m, 2H), 3.99-3.96 (m, 2H), 3.83 – 3.79 (m, 4H), 3.78-3.64 (m, 16H), 3.59-3.50 (m, 12H), 3.43 (t, J = 10.1 Hz, 12H), 3.21 (t, J = 5.8 Hz, 2H), 3.08 (t, J = 7.0 Hz, 4H), 2.86 (t, J = 6.9 Hz, 4H), 2.62-2.52 (m, 12H), 2.00 (d, J = 6.0 Hz, 3H) ppm.

RP-HPLC (5%/95% MeCN/H$_2$O → 30%/70% MeCN/H$_2$O in 60 min): t_R = 12.9 min.

ESI-MS calcd. for C$_{56}$H$_{96}$N$_{16}$O$_{23}$ [M+2H]$^{2+}$ 681.3; found 681.3, [M+3H]$^{3+}$ 454.6; found 454.6.

5.6. Binding Assays

SCP-RICM:

Reflectance Interference Contrast Microscopy (RICM) on an inverted microscope (Olympus IX71, Germany) was used to obtain the contact area between the mannose functionalized microparticles (PEG-Man SCPs) and a Con A functionalized glass surface. For illumination a Hg-vapor lamp was used with a green monochromator (546 nm). A Zeiss Antiflex 63 x NO 1.25 oil-immersion objective, additional polarizers to avoid internal reflections and a Zeiss AxiocamHRm camera were used to image the RICM patterns. To conduct the Johnson-Kendall-Roberts (JKR)

measurements of the adhesion energies, both the contact radius and the particle radius were measured. Image processing and data analysis were done using the image analysis software Image-J and the mathematical software OriginPro. 1 ml of HBS buffer (10 mM Hepes (pH 6), 50 mM NaCl, 1 mM MnCl$_2$ and 1 mM CaCl$_2$) was added to the Con A functionalized surface and PEG-Man SCPs were spread into the solution. After sedimentation of the particles, the contact radius and the particle radius were measured. For inhibition measurements, the glycooligomer inhibitors and α-methyl-D-mannose were dissolved in water with a concentration of 10-25 μM. A known amount of inhibitor solution was added into the solution and the contact and particle radii were measured again. This procedure was repeated stepwise to obtain data points at different concentrations of the inhibitor. To determine the IC$_{50}$ values, the obtained normalized surface energies (derived by JKR plot) were plotted against the concentration of the inhibitor and analyzed in OriginPro using the Hill1 equation. Synthesis of mannose functionalized soft colloidal probe, Concanavalin A (Con A) glass slides, experimental setup and derivation of surface energies from measured contact areas by Johnson-Kendall-Roberts (JKR) theory can be found in Ref [143]
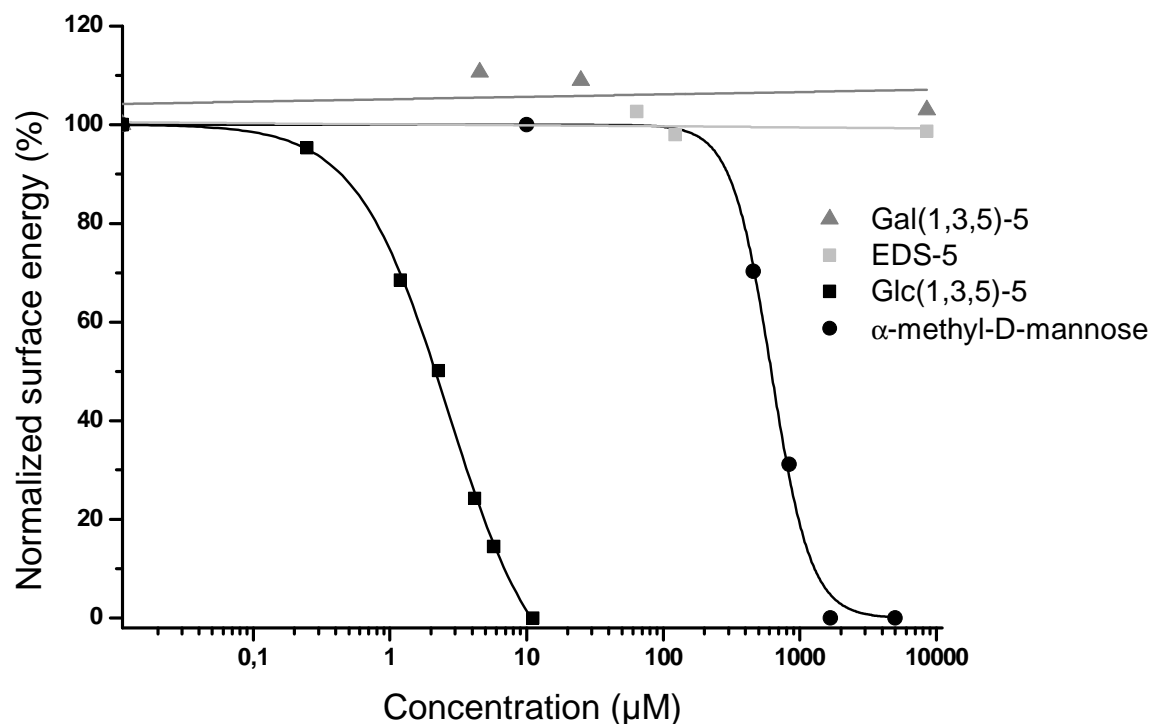
Binding curves of Controls:

Figure 66: Binding curves of control structures determined by SCP-RICM.

127

SPR Con A Inhibition Studies:

Before immobilization, the sensor chip SA pre-immobilized with streptavidin was conditioned with three consecutive injections of 100 µl 1 M NaCl and 50 mM NaOH in a flow rate of 100 µl/min. Biotinylated α-D-mannose-PAA and biotinylated *N*-acetyllactosamine-PAA were diluted to 4.2 µg/ml in HBS-EP buffer and were immobilized with HBS-EP buffer in a flow rate of 5 µl/min on the first lane (~800 response units) and on the second lane of the same chip as a reference (~1050 response units). The *N*-acetyllactosamine-PAA immobilized lane served as reference lane. After immobilization procedure, the chip surface was equilibrated with three consecutive injections (1 min) of running buffer, containing 10 mM Hepes, pH 8.5 and 0.1 mM $CaCl_2$. Binding analyses were carried out with running buffer at a flow rate of 20 µl/min. The Con A binding of the glycooligomers Man(3)-5, Man(1,5)-5, Man(1,3,5)-5 and TDS-5 (as control) and α-methyl mannose was examined. 100 nM Con A was incubated with the specific substance at final concentrations of 300 nM, 1 µM, 3 µM, 10 µM, 30 µM, in running buffer for 18 minutes at room temperature. 35 µl of each sample was injected over both lanes whereas the binding signal on the reference lane (*N*-acetyllactosamine-PAA) was subtracted from the D-mannose-PAA lane during the binding measurement. Each binding cycle consisted of an association phase for 105 s followed by a 180 s dissociation phase. The chip was regenerated after each run (60 s) with regeneration buffer consisting of 100 mM Glycine, pH 2.5 in water. The response values were calculated by subtraction of the report point at the beginning of the sample injections (0 s) from the report point at the end of the dissociation phase (285 s). The binding signal obtained by the 100 nM Con A solution in running buffer without inhibitor was set to 100 % binding. The binding signals of the specific inhibitor was referred to Con A and calculated for relative Con A binding in % of Con A. Each data point represents the mean value (± SEM) of three measurements. IC_{50} values represent the concentration of inhibitor that result from 50 % binding of Con A to α-D-mannose-PAA on the sensor chip.

2fFCS:

For these studies Man(1,3,5)-5, ManGalMan(1,3,5)-5, GalManGal(1,3,5)-5 and ManManGal(1,3,5)-5 were equipped with the fluorescent label Atto 647N. 1.25 mg of glycooligomer was dissolved in 60 µl PBS buffer (pH 8.3) to give a 10 mM solution. 60 µl of a 10 mM solution of Atto 647N dye in DMF was added. The reaction mixture was shaken for one hour. The obtained crude product was purified by preparative HPLC (5/95 MeCN/water → 95/5 MeCN/water in 40 minutes).

2fFCS measurements were performed at room temperature. Con A and the fluorescent labeled glycooligomer samples were dissolved in HBS buffer (10 mM Hepes (pH 7.4), 50 mM NaCl, 1 mM

MnCl$_2$ and 1 mM CaCl$_2$) in 0.5 nM concentration. The exact concentration of Con A was determined by measuring the absorption at 280 nm. The extinction coefficient ε was calculated based on the amount of fluorescent amino acids in the protein with the program ProtParam: ε= 129 720 M^{-1}cm^{-1} (for tetramers). The fluorescent labeled analogues of oligomers Man(1,3,5)-5, ManGalMan(1,3,5)-5, GalManGal(1,3,5)-5 and ManManGal(1,3,5)-5 were kept at a concentration of 0.5 nM and mixed with solutions of Con A, with concentrations ranging between 0.5 μM and 50 μM. All samples were allowed to incubate for 18 min at room temperature before the measurement. The samples were measured in a sandwich of two cover glasses held together with two strips of double-sided adhesive tape, forming a channel with a diameter of less than 1 mm in between, where the sample was inserted by the effect of capillary forces. The labeled oligomers were excited in two foci of light from two 640 nm orthogonally polarized lasers passing a DIC prism. The frequency of the pulsed lasers was chosen so that the fluorescence relaxation time was smaller than the interval between two pulses. In this case, the frequency between two consecutive pulses was 26.7 MHz and the power in each focus was 3 μW. The distance between the foci was determined with a reference sample, Atto655-COOH, whose diffusion coefficient is known.[186] In this setup, the inter-foci distance was 404 nm. The obtained data points for each concentration were plotted with Origin 8.5G and fit with Hill1 equation.

STD-NMR:

Glycooligomers were measured at room temperature in Norell SP5000-7 5 mm tubes in 20 mM deuterated Tris buffer (pH 8.0, uncorrected) on a Varian PremiumCOMPACT 600 MHz spectrometer equipped with a onenmr probe with *d4*-TSP ((3-(trimethylsilyl)-2,2',3,3'-tetradeuteropropionic acid) as internal reference. Prior to STD-NMR studies, proton resonances of compounds GalManGal(1,3,5)-5, ManGalMan(1,3,5)-5, Man(3)-5, Man(1,5)-5, Man(1,3,5)-5 and a TDS backbone without carbohydrates as control (TDS-5) were assigned using standard one-dimensional proton spectra as well as two-dimensional TOCSY, COSY, ^{1}H-^{13}C HSQC, ^{1}H-^{13}C HMBC and ^{1}H-^{13}C H2BC spectra at concentrations varying between 1 and 3.2 mM in D$_2$O. For STD-NMR, samples contained 1 mM ligand and 20 μM Con A. On-resonance irradiation was set to 0.0 ppm, and off-resonance irradiation was set to 30 ppm. A 35 ms T1 spin-lock filter and a W5 WATERGATE for solvent suppression were applied. The saturation pulse train consisted of a series of Gaussian shaped pulses of 50 ms duration and 1 ms interpulse delay with a strength of 10 dB. A total of 1024 scans were recorded. For negative controls (glycooligmomers without Con A and TDS(1,3,5)-5 control with Con A), saturation and relaxation times were set to 4 s, respectively. STD build-up curves were recorded at saturation times of 0.5, 1, 2, 4 and 8 s, adjusting the prescan delay accordingly. Resulting NMR spectra were processed in MestReNova 6.2.0 and data was analyzed in OriginPro8.6G to obtain the binding epitopes according to Meyer

et al.[187] STD-AF(t_{sat}) = STD-AF$_{max}$[1−exp(−$k_{sat}t_{sat}$)] was used as fit function.[188]

SPR PA-IL Inhibition Studies:

A sensor chip SA coated with streptavidin was conditioned with three consecutive injections of 100 µl 1 M NaCl and 50 mM NaOH in a flow rate of 100 µl/min. Then, biotinylated β-D-galactose-PAA (0.1 nM in HBS-EP buffer) was immobilized on flow cell 2 with HBS-EP buffer in a flow rate of 5 µl/min. Biotinylated α-D-mannose-PAA with the same concentration was immobilized as reference on flow cell 1. Binding analyses were carried out with running buffer (HEPES 10 mM, NaCl 150 mM, CaCl$_2$ 10 mM, pH 7.4.) at a flow rate of 20 µl/min. The PA-IL binding of the glycooligomers AZO-Gal(1,3)-3, AZO-Gal(1,3,5)-5, EDS-Gal(1,3)--3, EDS-Gal(1,3,5)-5 and AZO-Man(1,3,5)-5 (as control) was examined. 1 µM Pa-IL was incubated with the specific substance at final concentrations of 400 µM, 100 µM, 50 µM, 25 µM, 10 µM, 1 µM and 0.1 µM, in running buffer for 60 minutes at room temperature. 45 µl of each sample was injected over both lanes whereas the binding signal on the reference cell (α-D-mannose-PAA) was subtracted from the β-D-galactose-PAA flow cell during the binding measurement. Each binding cycle consisted of an injection phase for 80 s followed by a 100 s dissociation phase. The chip was regenerated after each running with 100 mM D-galactose in running buffer. The response values were calculated by subtraction of the report point at the beginning of the sample injections (0 s) from the report point at the end of the dissociation phase (210 s). The binding signal obtained by the 1 µM Pa-IL solution in running buffer without inhibitor was set to 100 % binding. This sample was measured 2 times before and 2 times after each measuring cycle. The binding signals of the specific inhibitor was referred to Pa-IL and calculated for relative PA-Il binding in % of PA-IL. Each data point (concentration) represents the mean value (± SEM) of two measurements. The obtained data points for each concentration were plotted with Origin 8.5G and fit with Hill1 equation. With that, IC$_{50}$ values (the concentration of inhibitor that result from 50 % binding of PA-IL binding to β-D-galactose-PAA on the sensor chip) and its error values were determined.

SPR PA-IL Direct Binding Studies

For direct binding studies, glycooligomers Gal(1,3)-3-trans, Gal(1,3,5)-5-trans, Gal(1,3)-3-PSS and Gal(1,3,5)-5-PSS were immobilized on Biacore CM5 sensor chips. Latter two PSS structures were additionally generated by irradiation of the corresponding trans structure immobilized on the Biacore sensor chip with light at 350 nm (see irradiation section above for details). Immobilisation took place by flowing a solution of 2 mM glycoligand for 5 minutes with 10 µl per minute over one flow cell, after activation of it with 0.4 M EDS in water and 0.1 M NHS in water.

After that, remaining active ester groups were capped by injection of 1 M ethanolamine. HBS-P (0.01 M HEPES pH 7.4, 0.15 M NaCl, 0.005% v/v Surfactant P20 in water) was used as running buffer. A second flow cell was immobilized as blank reference cell. For that, 1 M ethanolamine was flown over the cell after activation with 0.4 M EDS in water and 0.1 M NHS in water. Serial dilutions of PA-IL (25 μM, 10 μM, 5 μM, 1 μM, 0.1 μM and 0 μM) were then flown over the sensor chip at 25°C with Hepes running buffer (HEPES 10 mM, NaCl 150 mM, $CaCl_2$ 10 mM, pH 7.4.). Binding of lectin was evaluated with Biacore T100 evaluation software, determining K_D affinity constants by employing a steady state affinity model.

6. References

[1]   R. A. Dwek, *Ann. Rev. Biochem.* **1988**, *57*, 785–838.

[2]   P. H. Seeberger, W. C. Haase, *Chem. Rev.* **2000**, *100*, 4349–4394.

[3]   C. R. Bertozzi, L. L. Kiessling, *Science* **2001**, *291*, 2357–2364.

[4]   C. R. Bertozzi, *Science* **2001**, *291*, 2357–2364.

[5]   P. H. Seeberger, D. B. Werz, *Nature* **2007**, *446*, 1046–1051.

[6]   H.-J. Gabius, S. André, J. Jiménez-Barbero, A. Romero, D. Solís, *Trends Biochem. Sci.* **2011**, *36*, 298–313.

[7]   Harvey Lodish, A. Berk, L. Zipursky, P. Matsudaira, D. Baltimore, J. Darnell., *Molecular Cell Biology*, W. H. Freeman, **2000**.

[8]   N. Jayaraman, *Chem. Soc. Rev.* **2009**, *38*, 3463–3483.

[9]   H. Lis, N. Sharon, *Chem. Rev.* **1998**, *98*, 637–674.

[10]   A. Varki, R. D. Cummings, J. D. Esko, H. H. Freeze, P. Stanley, J. D. Marth, C. R. Bertozzi, G. W. Hart, M. E. Etzler, *Proteomics* **2009**, *9*, 5398–5399.

[11]   J. H. Naismith, C. Emmerich, J. Habash, S. J. Harrop, J. R. Helliwell, W. N. Hunter, J. Raftery, A. J. Kalb (Gilboa), J. Yariv, *Acta Crystallograp. Sect. D* **1994**, *50*, 847–858.

[12]   J. W. C. Kijne, *Chemtracts Biochem. Mol. Biol.* **1996**, *6*, 180–187.

[13]   N. Sharon, H. Lis, *Science* **1989**, *246*, 227–234.

[14]   J. Hirabayashi, Y. Arata, K. Kasai, *Trends Glycosc. Glycotechnol.* **1997**, *9*, 113–122.

[15]   S. H. Barondes, V. Castronovo, D. N. W. Cooper, R. D. Cummings, K. Drickamer, T. Felzi, M. A. Gitt, J. Hirabayashi, C. Hughes, K. Kasai, et al., *Cell* **1994**, *76*, 597–598.

[16]   H. Leffler, *Trends Glycosc. Glycotechnol.* **1997**, *9*, 9–19.

[17]   G. Barrientos, N. Freitag, I. Tirado-gonza, L. Unverdorben, U. Jeschke, V. L. J. L. Thijssen, S. M. Blois, *Human Reproduction Update* **2013**, *0*, 1–19.

[18]   S. Akahani, H. Inohara, N.-M. Pratima, A. Raz, *Trends Glycosc. Glycotechnol.* **1997**, *9*, 69–75.

[19]   W. I. Weis, K. Drickamer, *Annu. Rev. Biochem.* **1996**, *65*, 441–473.

[20]   G. Ashwell, J. Harford, *Annu. Rev. Biochem.* **1982**, *51*, 531–554.

[21]   R. J. Stockert, *Physiol. Rev.* **1995**, *75*, 591–609.

6. References

[22] M. Spiess, *Biochemistry* **1990**, *29*, 10009–10018.

[23] K. Drickamer, M. E. Taylor, *Annu. Rev. Cell Biol.* **1993**, *9*, 237–264.

[24] S. D. Rosen, *Ann. Rev. Immunol.* **2004**, *22*, 129–156.

[25] L. A. Lasky, *Ann. Rev. Biochem.* **1995**, *64*, 113–140.

[26] J. J. Mccoy, B. J. Mann, *Infect. Immun.* **1994**, *62*, 3045–3050.

[27] I. Ofek, R. J. Doyle, *Bacterial Adhesion to Cells and Tissues*, Chapman And Hall: London, **1994**.

[28] D. C. Wiley, J. J. Skehel, *Annu. Rev. Biochem.* **1987**, *56*, 365–394.

[29] N. K. Sauter, J. E. Hanson, G. D. Glick, J. H. Brown, R. L. Crowther, S. J. Park, J. J. Skehel, D. C. Wiley, *Biochemistry* **1992**, *31*, 9609–9621.

[30] W. Gaastra, A.-M. Svennerholm, *Trends Microbiol.* **1996**, *4*, 444–452.

[31] P. I. Kitov, J. M. Sadowska, G. Mulvey, G. D. Armstrong, H. Ling, N. S. Pannu, R. J. Read, D. R. Bundle, *Nature* **2000**, *403*, 669–672.

[32] A. Mulder, D. N. Reinhoudt, **2004**, 3409–3424.

[33] D. Deniaud, K. Julienne, S. G. Gouin, *Org. Biomol. Chem.* **2011**, *9*, 966–979.

[34] R. J. Pieters, *Org. Biomol. Chem.* **2009**, *7*, 2013–2025.

[35] P. I. Kitov, D. R. Bundle, *J. Am. Chem. Soc.* **2003**, *125*, 16271–16284.

[36] F. Pertici, R. J. Pieters, *Chem. Commun.* **2012**, *48*, 4008–4010.

[37] D. Schwefel, C. Maierhofer, J. G. Beck, S. Seeberger, K. Diederichs, H. M. Möller, W. Welte, V. Wittmann, *J. Am. Chem. Soc.* **2010**, *132*, 8704–8719.

[38] W. Jiang, K. Nowosinski, N. L. Lo, E. V Dzyuba, F. Klautzsch, A. Scha, J. Huuskonen, K. Rissanen, C. A. Schalley, *J. Am. Chem. Soc.* **2012**, *134*, 1860–1868.

[39] S. L. Mangold, M. J. Cloninger, *Org. Biomol. Chem.* **2006**, *4*, 2458–65.

[40] D. Pagé, R. Roy, *Bioorg. Med. Chem. Lett.* **1996**, *6*, 1765–1770.

[41] T. K. Dam, S. Oscarson, R. Roy, S. K. Das, D. Pagé, F. Macaluso, C. F. Brewer, *J. Biol. Chem.* **2005**, *280*, 8640–8646.

[42] R. S. Kane, *Langmuir* **2010**, *26*, 8636–3640.

[43] I. Vrasidas, S. Andre, P. Valentini, C. Bock, M. Lensch, H. Kaltner, R. M. J. Liskamp, H.-J. Gabius, R. J. Pieters, *Org. Biomol. Chem.* **2003**, *1*, 803–810.

[44] T. K. Dam, C. F. Brewer, *Biochemistry* **2008**, *47*, 8470–8476.

[45] J. E. Gestwicki, C. W. Cairo, L. E. Strong, K. A. Oetjen, L. L. Kiessling, *J. Am. Chem. Soc.* **2002**, *124*, 14922–14933.

[46] S. M. Dimick, S. C. Powell, S. A. McMahon, D. N. Moothoo, J. H. Naismith, E. J. Toone, *J. Am. Chem. Soc.* **1999**, *121*, 10286–10296.

[47] S. D. Burke, Q. Zhao, M. C. Schuster, L. L. Kiessling, *J. Am. Chem. Soc.* **2000**, *122*, 4518–4519.

[48] M. Mammen, S.-K. Choi, G. M. Whitesides, *Angew. Chem., Int. Ed.* **1998**, *37*, 2754–2794.

[49] L. L. Kiessling, N. L. Pohl, *Chem. Biol.* **1996**, *3*, 71–77.

[50] C. Clarke, R. J. Woods, J. Gluska, A. Cooper, M. A. Nutley, G.-J. Boons, *J. Am. Chem. Soc.* **2001**, *123*, 12238–12247.

[51] R. U. Lemieux, *Acc. Chem. Res.* **1996**, *29*, 373–380.

[52] R. Kadirvelraj, B. L. Foley, J. D. Dyekjaer, R. J. Woods, *J. Am. Chem. Soc.* **2008**, *130*, 16933–16942.

[53] J. H. Naismith, R. A. Field, *J. Biol. Chem.* **1996**, *271*, 972–976.

[54] D. K. Mandal, N. Kishore, C. F. Brewer, *Biochemistry* **1994**, *33*, 1149–56.

[55] J. M. Rini, *Annu. Rev. Bioph. Biom.* **1995**, *24*, 551–577.

[56] Y. M. Chabre, R. Roy, *Curr. Top. Med.Chem.* **2008**, *8*, 1237–1285.

[57] E. Meinjohanns, M. Meldal, H. Paulsen, R. A. Dwek, K. Bock, *J. Chem. Soc. Perkin Trans 1* **1998**, 549–560.

[58] M. Bejugam, S. L. Flitsch, *Org. Lett.* **2004**, *6*, 4001–4004.

[59] N. Yamamoto, A. Takayanagi, A. Yoshino, T. Sakakibara, Y. Kajihara, *Chem. Eur. J.* **2007**, *13*, 613–625.

[60] I. Papp, J. Dernedde, S. Enders, S. B. Riese, C. Shiao, R. Roy, R. Haag, *ChemBioChem* **2011**, *12*, 1075–1083.

[61] E. K. Woller, M. J. Cloninger, *Org. Lett.* **2002**, *4*, 7–10.

[62] R. Chen, T. J. Tolbert, *J. Am. Chem. Soc.* **2010**, *132*, 3211–6.

[63] C. W. Tornøe, C. Christensen, M. Meldal, *J. Org. Chem.* **2002**, *67*, 3057–3064.

[64] R. S. Loka, C. M. Sadek, N. Romaniuk, C. W. Cairo, *Bioconj. Chem.* **2010**, *21*, 1842–1849.

[65] C. Fasting, C. A. Schalley, M. Weber, O. Seitz, S. Hecht, B. Koksch, J. Dernedde, C. Graf, E.-W. Knapp, R. Haag, *Angew. Chem., Int. Ed.* **2012**, *51*, 10472–10498.

[66] R. T. Lee, P. Lin, Y. C. Lee, *Biochemistry* **1984**, *23*, 4255–4261.

[67]   E. A. Biessen, H. Broxterman, J. H. van Boom, T. J. van Berkel, *J. Med. Chem.* **1995**, *38*, 1846–1852.

[68]   G. Thoma, R. O. Duthaler, J. L. Magnani, J. T. Patton, *J. Am. Chem. Soc.* **2001**, *123*, 10113–10114.

[69]   I. Bossu, M. Šulc, K. Křenek, E. Dufour, J. Garcia, N. Berthet, P. Dumy, V. Křen, O. Renaudet, *Org. Biomol. Chem.* **2011**, *9*, 1948–59.

[70]   J. J. Lundquist, S. D. Debenham, E. J. Toone, *J. Org. Chem.* **2000**, *65*, 8245–8250.

[71]   R. K. Kainthan, J. Janzen, E. Levin, D. V Devine, D. E. Brooks, *Biomacromolecules* **2006**, *7*, 703–709.

[72]   J. Franchini, P. Ferruti, *J. Bioact. Compat. Pol.* **2004**, *19*, 221–236.

[73]   M. J. Cloninger, in *Molecular Recognition and Polymers*, John Wiley & Sons, Inc., **2008**, pp. 335–358.

[74]   I. Papp, J. Dernedde, S. Enders, R. Haag, *Chem. Commun.* **2008**, 5851–5853.

[75]   D. Yi, R. T. Lee, P. Longo, E. T. Boger, Y. C. Lee, W. A. Petri, R. L. Schnaar, *Glycobiology* **1998**, *8*, 1037–1043.

[76]   C. C. M. Appeldoorn, J. A. F. Joosten, F. Ait el Maate, U. Dobrindt, J. Hacker, R. M. J. Liskamp, A. S. Khan, R. J. Pieters, *Tetrahedron-Asymmetr.* **2005**, *16*, 361–372.

[77]   P. R. Ashton, E. F. Hounsell, N. Jayaraman, T. M. Nilsen, N. Spencer, J. F. Stoddart, M. Young, *J. Org. Chem.* **1998**, *63*, 3429–3437.

[78]   E. K. Woller, E. D. Walter, J. R. Morgan, D. J. Singel, M. J. Cloninger, *J. Am. Chem. Soc.* **2003**, *125*, 8820–8826.

[79]   V. Ladmiral, E. Melia, D. M. Haddleton, *Eur. Polym. J.* **2004**, *40*, 431–449.

[80]   V. Ladmiral, G. Mantovani, G. J. Clarkson, S. Cauet, J. L. Irwin, D. M. Haddleton, *J. Am. Chem. Soc.* **2006**, *128*, 4823–4830.

[81]   G. Chen, S. Amajjahe, M. H. Stenzel, *Chem. Commun.* **2009**, 1198–1200.

[82]   S. R. S. Ting, G. Chen, M. H. Stenzel, *Polym. Chem.* **2010**, *1*, 1392–1412.

[83]   M. Okada, *Prog. Polym. Sci.* **2001**, *26*, 67–104.

[84]   A. David, P. Kopečková, A. Rubinstein, J. Kopeček, *Bioconjugate Chem.* **2001**, *12*, 890–899.

[85]   J. Geng, J. Lindqvist, G. Mantovani, G. Chen, C. T. Sayers, G. J. Clarkson, D. M. Haddleton, *QSAR & Combinatorial Science* **2007**, *26*, 1220–1228.

[86]   C. R. Becer, M. I. Gibson, J. Geng, R. Ilyas, R. Wallis, D. a Mitchell, D. M. Haddleton, *J. Am. Chem. Soc.* **2010**, *132*, 15130–15132.

6. References

[87] W. J. Lees, A. Spaltenstein, J. E. Kingery-Wood, G. M. Whitesides, *J. Med. Chem* **1994**, *37*, 3419–3433.

[88] G. B. Sigal, M. Mammen, G. Dahmann, G. M. Whitesides, *J. Am. Chem. Soc.* **1996**, *118*, 3789–3800.

[89] M. Ambrosi, N. R. Cameron, B. G. Davis, S. Stolnik, *Org. Biomol. Chem.* **2005**, *3*, 1476–1480.

[90] T. Hasegawa, S. Kondoh, K. Matsuura, K. Kobayashi, *Macromolecules* **1999**, *32*, 6595–6603.

[91] J.-F. Lutz, *Angew. Chem., Int. Ed.* **2007**, *46*, 1018–1025.

[92] H. C. Kolb, M. G. Finn, K. B. Sharpless, *Angew. Chem., Int. Ed.* **2001**, *40*, 2004–2021.

[93] R. Huisgen, *Angew. Chem., Int. Ed.* **1963**, *2*, 565–598.

[94] H. C. Kolb, K. B. Sharpless, *Drug Discov. Today* **2003**, *8*, 1128–1137.

[95] V. V Rostovtsev, L. G. Green, V. V Fokin, K. B. Sharpless, *Angew. Chem., Int. Ed.* **2002**, *41*, 2596–2599.

[96] V. D. Bock, H. Hiemstra, J. H. van Maarseveen, *Eur. J. Org. Chem.* **2006**, *2006*, 51–68.

[97] B. T. Worrell, J. A. Malik, V. V Fokin, *Science* **2013**, *340*, 457–460.

[98] R. Alvarez, S. Velazquez, A. San-Felix, S. Aquaro, E. De Clercq, C.-F. Perno, A. Karlsson, J. Balzarini, M. J. Camarasa, *J. Med. Chem.* **1994**, *37*, 4185–4194.

[99] M. J. Genin, D. A. Allwine, D. J. Anderson, M. R. Barbachyn, D. E. Emmert, S. A. Garmon, D. R. Graber, K. C. Grega, J. B. Hester, D. K. Hutchinson, et al., *J. Med. Chem.* **2000**, *43*, 953–970.

[100] D. R. Buckle, C. J. M. Rockell, *J. Chem. Soc. Perkin Trans 1* **1982**, 627–630.

[101] J. E. Moses, A. D. Moorhouse, *Chem. Soc. Rev.* **2007**, *36*, 1249–1262.

[102] M. Meldal, C. W. Tornøe, *Chem. Rev.* **2008**, *108*, 2952–3015.

[103] M. R. B, *J. Am. Chem. Soc* **1963**, *85*, 2149–2154.

[104] W. C. Chan, P. D. White, *Fmoc Solid Phase Peptide Synthesis: A Practical Approach*, Oxford University Press, **2004**.

[105] B. Castro, J.-R. Dormoy, B. Dourtoglou, G. Evin, C. Selve, J.-C. Ziegler, *Synthesis* **1976**, *1976*, 751–752.

[106] C. A. G. N. Montalbetti, V. Falque, M. Park, A. Ox, *Tetrahedron* **2005**, *61*, 10827–10852.

[107] V. Dourtoglou, J.-C. Ziegler, B. Gross, *Tetrahedron Lett.* **1978**, *19*, 1269–1272.

[108] A. Czarnik, *Biotechnol. Bioeng.* **1998**, *61*, 77–79.

[109] A. R. Vaino, K. D. Janda, *J. Comb. Chem.* **2000**, *2*, 579–596.

[110] C. K. Stover, X. Q. Pham, A. L. Erwin, S. D. Mizoguchi, P. Warrener, M. J. Hickey, F. S. L. Brinkman, W. O. Hufnagle, D. J. Kowalik, M. Lagrou, et al., *Nature* **2000**, *406*, 959–964.

[111] P. Seneci, *Solid-Phase Synthesis and Combinatorial Technologies*, Wiley Interscience, **2002**.

[112] W. Bannwarth, *Helv. Chim. Acta* **1988**, *71*, 1517–1527.

[113] P. H. H. Hermkens, H. C. J. Ottenheijm, D. Rees, *Science* **1996**, *52*, 4527–4554.

[114] J. M. Frechet, C. Schuerch, *J. Am. Chem. Soc.* **1972**, *94*, 604–609.

[115] O. J. Plante, E. R. Palmacci, P. H. Seeberger, *Science* **2001**, *291*, 1523–1527.

[116] P. H. Seeberger, *Chem. Soc. Rev.* **2008**, *37*, 19–28.

[117] P. Stallforth, B. Lepenies, A. Adibekian, P. H. Seeberger, *J. Med. Chem.* **2009**, *52*, 5561–5577.

[118] L. Hartmann, E. Krause, M. Antonietti, H. G. Börner, *Biomacromolecules* **2006**, *7*, 1239–1244.

[119] L. Hartmann, *Synthese Monodisperser, Multifunktionaler Poly(amidoamine) Und Ihre Anwendung Als Nicht-virale Vektoren Für Die Gentherapie*, Dissertation, Universität Potsdam, **2007**.

[120] A. Varki, *Glycobiology* **1993**, *3*, 97–130.

[121] P. Sears, C. Wong, *Angew. Chem., Int. Ed.* **1999**, *38*, 2300–2324.

[122] L. Kiessling, *Curr. Opin. Chem. Biol.* **2000**, *4*, 696–703.

[123] R. J. Pieters, *Med. Res. Rev.* **2007**, *27*, 796–816.

[124] A. Bernardi, J. Jiménez-Barbero, A. Casnati, C. De Castro, T. Darbre, F. Fieschi, J. Finne, H. Funken, K.-E. Jaeger, M. Lahmann, et al., *Chem. Soc. Rev.* **2012**.

[125] L. Hartmann, S. Häfele, R. Peschka-Süss, M. Antonietti, H. G. Börner, *Chem. Eur. J.* **2008**, *14*, 2025–2033.

[126] D. Xu, K. Prasad, O. Repic, T. J. Blacklock, *Tetrahedron Lett.* **1995**, *36*, 7357–7360.

[127] J. C. Verheijen, B. A. L. M. Deiman, E. Yeheskiely, G. A. Van Der Marel, J. H. Van Boom, *Angew. Chem., Int. Ed.* **2000**, *39*, 369–372.

[128] A. Song, X. Wang, J. Zhang, J. Marik, C. B. Lebrilla, K. S. Lam, *Bioorg. Med. Chem. Lett.* **2004**, *14*, 161–165.

[129] B. Priewisch, K. Rück-Braun, *J. Org. Chem.* **2005**, *70*, 2350–2352.

[130] L. Ulysse, J. Chmielewski, *Bioorg. Med. Chem. Lett.* **1994**, *4*, 2145–2146.

[131] C. E. Hoyle, C. N. Bowman, *Angew. Chem., Int. Ed.* **2010**, *49*, 1540–1573.

6. References

[132] S. S. van Berkel, M. B. van Eldijk, J. C. M. van Hest, *Angew. Chem., Int. Ed.* **2011**, *50*, 8806–8827.

[133] P. E. Dawson, T. W. Muir, I. Clark-Lewis, S. B. Kent, *Science* **1994**, *266* , 776–779.

[134] R. Quarrell, T. D. W. Claridge, G. W. Weaver, G. Lowe, *Mol. Diversity* **1995**, *1*, 223–232.

[135] V. D. Bock, H. Hiemstra, J. H. van Maarseveen, *Eur. J. Org. Chem.* **2006**, *2006*, 51–68.

[136] M. I. Shar G. A Bhanger, *Jour. Chem. Soc. Pak.* **2002**, *24*, 185–189.

[137] J. L. Jiménez Blanco, C. Ortiz Mellet, J. M. García Fernández, *Chem. Soc. Rev.* **2013**, *42*, 4518–4531.

[138] C. W. Cairo, J. E. Gestwicki, M. Kanai, L. L. Kiessling, *J. Am. Chem. Soc.* **2002**, *124*, 1615–1619.

[139] Z. Derewenda, J. Yariv, J. R. Helliwell, A. J. Kalb, E. J. Dodson, M. Z. Papiz, T. Wan, J. Campbell, *EMBO* **1989**, *8*, 2189–2193.

[140] D. K. Mandal, C. F. Brewer, *Biochemistry* **1993**, *32*, 5116–5120.

[141] C. R. Becer, *Macromol. Rapid Comm.* **2012**, *33*, 742–52.

[142] L. Limozin, K. Sengupta, *ChemPhysChem* **2009**, *10*, 2752–2768.

[143] D. Pussak, D. Ponader, S. Mosca, S. V. Ruiz, L. Hartmann, S. Schmidt, *Angew. Chem., Int. Ed.* **2013**, *52*, 6084–6087.

[144] K. H. Schlick, M. J. Cloninger, *Tetrahedron* **2010**, *66*, 5305–5310.

[145] J. B. Corbell, J. J. Lundquist, E. J. Toone, *Tetrahedron: Asymmetr.* **2000**, *11*, 95–111.

[146] O. Ramström, S. Lohmann, T. Bunyapaiboonsri, J.-M. Lehn, *Chem. Eur. J.* **2004**, *10*, 1711–1715.

[147] Z. Pei, H. Anderson, T. Aastrup, O. Ramström, *Biosens. Bioelectron.* **2005**, *21*, 60–66.

[148] A. Schierholt, M. Hartmann, K. Schwekendiek, T. K. Lindhorst, *Eur. J. Org. Chem.* **2010**, *2010*, 3120–3128.

[149] E. Fan, Z. Zhang, W. E. Minke, Z. Hou, C. L. M. J. Verlinde, W. G. J. Hol, *J. Am. Chem. Soc* **2000**, *122*, 2663–2664.

[150] E. M. Munoz, J. Correa, E. Fernandez-Megia, R. Riguera, *J. Am. Chem. Soc.* **2009**, *131*, 17765–17767.

[151] O. Ramström, J. M. Lehn, *ChemBioChem* **2000**, *1*, 41–48.

[152] T. Dertinger, V. Pacheco, I. von der Hocht, R. Hartmann, I. Gregor, J. Enderlein, *ChemPhysChem* **2007**, *8*, 433–443.

6. References

[153] P. Maffre, K. Nienhaus, F. Amin, W. J. Parak, G. U. Nienhaus, *Beilstein J. Nanotech.* **2011**, *2*, 374–383.

[154] G. U. Nienhaus, P. Maffre, K. Nienhaus, *Methods Enzymol.* **2013**, *519*, 115–137.

[155] E. Ahmad, A. Naeem, S. Javed, S. Yadav, R. H. Khan, *J. Biochem.* **2007**, *142*, 307–315.

[156] H. Kato, N. Kaneta, S. Nii, K. Kobayashi, N. Fukui, H. Shinohara, Y. Nishida, *Chem. Biodiversity* **2005**, *2*, 1232–1241.

[157] R. Loris, D. Maes, F. Poortmans, L. Wyns, J. Bouckaert, *J. Biol. Chem.* **1996**, *271*, 30614–30618.

[158] C. P. Swaminathan, N. Surolia, A. Surolia, *J. Am. Chem. Soc.* **1998**, *120*, 5153–5159.

[159] M. Mammen, G. Dahmann, G. M. Whitesides, *J. Med. Chem.* **1995**, *38*, 4179–4190.

[160] M. Ortega-Muñoz, F. Perez-Balderas, J. Morales-Sanfrutos, F. Hernandez-Mateo, J. Isac-García, F. Santoyo-Gonzalez, *Eur. J. Org. Chem.* **2009**, *2009*, 2454–2473.

[161] M. Gómez-García, J. M. Benito, R. Gutiérrez-Gallego, A. Maestre, C. O. Mellet, J. M. G. Fernández, J. L. J. Blanco, *Org. Biomol. Chem.* **2010**, *8*, 1849–1860.

[162] Y. Gou, J. Geng, S.-J. Richards, J. Burns, C. Remzi Becer, D. M. Haddleton, *J. Polym. Sci., Part A: Polym. Chem.* **2013**, *51*, 2588–2597.

[163] M. Mayer, B. Meyer, *J. Am. Chem. Soc.* **2001**, *123*, 6108–17.

[164] M. Mayer, B. Meyer, *Angew. Chem., Int. Ed.* **1999**, *35*, 1784–1788.

[165] N. Sharon, *Biochim. Biophys. Acta* **2006**, *1760*, 527–537.

[166] S. P. Diggle, R. E. Stacey, C. Dodd, M. Cámara, P. Williams, K. Winzer, *Environ. Microbiol.* **2006**, *8*, 1095–1104.

[167] N. G.-G. D. Avichezer, D. J. Katcoff, N. C. Garber, *J. Biol. Chem.* **1992**, *267*, 23023–23027.

[168] S. Cecioni, S. Faure, U. Darbost, I. Bonnamour, H. Parrot-Lopez, O. Roy, C. Taillefumier, M. Wimmerova, J.-P. Praly, A. Imberty, et al., *Chem. Eur. J.* **2011**, *17*, 2146–2159.

[169] S. Cecioni, R. Lalor, B. Blanchard, J.-P. Praly, A. Imberty, S. E. Matthews, S. Vidal, *Chem. Eur. J.* **2009**, *15*, 13232–13240.

[170] J. Wu, M. H. Nantz, M. A. Zern, *Front. Biosci.* **2002**, *7*, 717–725.

[171] R. U. Kadam, M. Bergmann, M. Hurley, D. Garg, M. Cacciarini, M. a Swiderska, C. Nativi, M. Sattler, A. R. Smyth, P. Williams, et al., *Angew. Chem., Int. Ed.* **2011**, *50*, 10631–10635.

[172] S. Cecioni, V. Oerthel, J. Iehl, M. Holler, D. Goyard, J.-P. Praly, A. Imberty, J.-F. Nierengarten, S. Vidal, *Chem. Eur. J.* **2011**, *17*, 3252–3261.

[173] Z. H. Soomro, S. Cecioni, H. Blanchard, J.-P. Praly, A. Imberty, S. Vidal, S. E. Matthews, *Org. Biomol. Chem.* **2011**, *9*, 6587–6597.

[174] S. Cecioni, J.-P. Praly, S. E. Matthews, M. Wimmerová, A. Imberty, S. Vidal, *Chem. Eur. J.* **2012**, *18*, 6250–6263.

[175] Y. M. Chabre, D. Giguère, B. Blanchard, J. Rodrigue, S. Rocheleau, M. Neault, S. Rauthu, A. Papadopoulos, A. A. Arnold, A. Imberty, et al., *Chem. Eur. J.* **2011**, *17*, 6545–6562.

[176] A. Noble, *Justus Liebigs Ann. Chem.* **1856**, *98*, 253–256.

[177] A. A. Beharry, G. A. Woolley, *Chem. Soc. Rev.* **2011**, *40*, 4422–4437.

[178] H. Fliegl, A. Köhn, C. Hättig, R. Ahlrichs, *J. Am. Chem. Soc.* **2003**, *125*, 9821–9827.

[179] C. Renner, R. Behrendt, S. Spörlein, J. Wachtveitl, L. Moroder, *Biopolymers* **2000**, *54*, 489–500.

[180] L. Ulysse, J. Cubillos, J. Chmielewski, *J. Am. Chem. Soc.* **1995**, *117*, 8466–8467.

[181] K. Rück-Braun, S. Kempa, B. Priewisch, A. Richter, S. Seedorf, L. Wallach, *Synthesis* **2009**, *24*, 4256–4267.

[182] V. Chandrasekaran, T. K. Lindhorst, *Chem. Commun.* **2012**, *48*, 7519–7521.

[183] V. Chandrasekaran, K. Kolbe, F. Beiroth, T. K. Lindhorst, *Beilstein J. Org. Chem.* **2013**, *9*, 223–233.

[184] O. Srinivas, N. Mitra, A. Surolia, N. Jayaraman, *J. Am. Chem. Soc.* **2002**, *124*, 2124–2125.

[185] O. Srinivas, N. Mitra, A. Surolia, N. Jayaraman, *Glycobiology* **2005**, *15*, 861–873.

[186] "http://www.picoquant.com/images/uploads/page/files/7353/appnote_diffusioncoeffi cients.pdf," **n.d.**

[187] B. Meyer, T. Peters, *Angew. Chem., Int. Ed.* **2003**, *42*, 864–890.

[188] J. Angulo, P. M. Enríquez-Navas, P. M. Nieto, *Chem. Eur. J.* **2010**, *16*, 7803–7812.

7. Appendix

7.1. Acknowledgements

7.2. List of Abbreviations

2fFCS	Dual focus fluorescence correlation spectroscopy
α-Me-Man	Methyl α-D-mannopyranoside
Abs	Absorbance
Ac	Acetyl-
Ac$_2$O	Acetic anhydride
calcd	Calculated
Con A	Concanavalin A lectin
CuAAC	Copper-Catalyzed Azide-Alkyne Cycloaddition
DCM	Dichloromethane
DCC	*N,N'*-Dicyclohexylcarbodiimide
DIC	*N,N'*-Diisopropylcarbodiimide
DIPEA	*N,N*-Diisopropyethylamine
DMF	Dimethylformamide
EDA	Ethylene diamine
EDC	*N*-Ethyl-*N'*-(3-dimethylaminopropyl)-carbodiimide
ELLA	Enzyme linked lectin assay
EtOAc	Ethyl acetate
Et$_2$O	Diethyl ether
EtOH	Ethanol
ESI-MS	Electron spray ionisation mass spectrometry
Fmoc	Flourenylmethoxycarbonyl
Gal	Galactose
Glc	Glucose
HOBT	1-Hydroxybenzotriazol
RP-HPLC	Reverse phase high pressure liquid chromatography
IR	Infrared spectroscopy

NEt$_3$	Triethylamine
NMR	Nuclear magnetic resonance spectroscopy
Man	Mannose
MeCN	Acetonitrile
MeOH	Methanol
TLC	Thin layer chromatography
PAA	poly[*N*-(2-hydroxyethyl)acrylamide
PA-IL	Lectin from Pseudomonas aeruginos
PEG	Poly(ethylene glycol)
Ph	Phenyl-
PyBOP	(Benzotriazol-1-yloxy)tripyrrolidinophosphonium hexafluorophosphate
Quant	Quantitative
SCP-RICM	Soft colloidal probe reflection interference contrast microscopy
SPS	Solid phase synthesis
SPPS	Solid phase peptide synthesis
SPR	Surface plasmon resonance
STD-NMR	Saturation transfer difference NMR
Suc	Succinyl-
TFA	Trifluoroacetic acid
TES	Triethylsilane
THF	Tetrahydrofurane
TSP	Trimethylsilyl propanoic acid
Trt	Trityl-, Triphenylmethyl-
UV-VIS	Ultraviolet visible